PERFORMANCE OF A PARTIALLY STRATIFIED-CHARGE GASOLINE ENGINE

By

Greg Brown

B.Sc., University of Calgary, Calgary, Alberta, Canada, 2000

A THESIS SUBMITTED IN PARTIAL FULFILLMENT OF

THE REQUIREMENTS FOR THE DEGREE OF

MASTER OF APPLIED SCIENCE

In

THE FACULTY OF GRADUATE STUDIES

DEPARTMENT OF MECHANICAL ENGINEERING

We accept this thesis as conforming

to the required standard

THE UNIVERSITY OF BRITISH COLUMBIA

April 2003

In presenting this thesis in partial fulfilment of the requirements for an advanced degree at the University of British Columbia, I agree that the Library shall make it freely available for reference and study. I further agree that permission for extensive copying of this thesis for scholarly purposes may be granted by the head of my department or by his or her representatives. It is understood that copying or publication of this thesis for financial gain shall not be allowed without my written permission.

Department of Mechanical Engineering

The University of British Columbia
Vancouver, Canada

Date April 23 2007

DE-6 (2/88)

Abstract

Stratified-charge lean burn engines have shown promise in their ability to reduce certain emissions and improve fuel economy while still providing acceptable driveability and performance. A local charge stratification process, the Partially Stratified-Charge (PSC) concept, has been developed at the University of British Columbia in an attempt to further improve lean burn operation. In the PSC engine, a lean homogeneous mixture is inducted into the combustion chamber and is compressed during the compression stroke. Just prior to the spark, a small amount of fuel is injected into the combustion chamber in the vicinity of the spark plug. This produces a rich pocket that can be ignited more easily and facilitates the combustion of the remaining lean homogeneous mixture. The main objective of the research presented here was to implement a PSC system on a gasoline engine and examine the performance of the PSC system relative to its homogeneous fuelled counterpart. Two different PSC systems were tested. The first system was based on a natural gas PSC system developed during previous work while the second system was a new gasoline PSC system developed specifically for this research.

Analysis of the performance and emissions results for the natural gas PSC studies showed significant advantages over conventional lean burn and stoichiometric homogeneous-charge operation. The most notable improvement was up to a 15% extension in the relative air-to-fuel ratio (λ). Through this extension of the lean limit, the useable range of brake mean effective pressure was expanded, by up to 20%, when using PSC. A reduction in nitrogen oxide emissions and an increase in total unburned hydrocarbons also accompanied this extension of the lean limit. In-cylinder pressure data analysis demonstrated significantly higher peak in-cylinder pressures and shorter ignition delays

with PSC. Throttled tests with the natural gas PSC system revealed the potential to reduce nitrogen oxide emissions, carbon monoxide emissions and brake specific fuel consumption over stoichiometric homogeneous charge operation. Improvements in PSC volumetric efficiency of up to 15% and 5% were realised compared to stoichiometric homogeneous and conventional lean burn operation, respectively.

Extensive experiments were also undertaken with a gasoline PSC system, however, performance improvements, though expected, were not observed. Examinations of the gasoline PSC system suggested that there were some challenges in achieving local charge stratification in the vicinity of the ignition source. These results implied that further optimisation, and perhaps a redesign of the gasoline PSC system, would be required to fully realise the performance benefits demonstrated with the natural gas PSC system.

Table of Contents

List of Tables

List of Figures

Nomenclature

Symbols

ϕ	Relative Humidity
γ	Specific heat ratio
η	Thermal Efficiency
η_m	Mechanical Efficiency
η_v	Volumetric Efficiency
λ	Relative Air-Fuel Ratio
θ	Crank Angle
ρ	Density
σ	Standard Deviation
τ	Torque
ω	Uncertainty
B	Barometric Pressure
H	Specific Humidity
K	Dry to Wet Emission Correction Factor
KH	NOx Humidity Correction Factor
M	Molecular Mass
$\dot{m}$	Mass Flow Rate
n	Number of Samples
N	Engine Speed
P	In-Cylinder Pressure
P_{H20}	Water Vapor Pressure

r_c	Compression Ratio
r	Ratio of Connection Rod Length to Crank Radius
R	Operational Parameter (Dependent Variable)
Ri	Ratio IMEP to Reference IMEP
T	Temperature
V	Cylinder Volume
V_c	Clearance Volume
V_d	Volumetric Displacement
Q	Heat Release
y	Hydrogen to Carbon Ratio
x_i	Sample Values
x_m	Mean Value
z_i	Independent Variables

Subscripts

a	Air
d	Dry
Exh	Exhaust
f	Fuel
fe	Gasoline Energy Equivalent Fuel
gas	Gasoline
$gasMAIN$	Main Gasoline Fuel System, (i.e. the port injection system)
$gasPSC$	Gasoline PSC Fuel System

i	Indices, (i.e. 1,2....)
ng	Natural Gas
ngPSC	Natural Gas PSC Fuel System
w	Wet

Abbreviations

ABDC	After Bottom Dead Center
ATDC	After Top Dead Center
BBDC	Before Bottom Dead Center
BC	British Columbia
BDC	Bottom Dead Center
BMEP	Brake Mean Effective Pressure
BSFC	Brake Specific Fuel Consumption
BSCO	Brake Specific Carbon Monoxide
BSEm	Brake Specific Emissions
BSHC	Brake Specific Hydrocarbons
BSNOx	Brake Specific Nitrogen Oxides
BTDC	Before Top Dead Center
CA	Crank Angle
CO	Carbon Monoxide
CO_2	Carbon Dioxide
COV	Coefficient of Variation
DC	Direct Current
Em	Emissions, i.e. CO, HC, NOx

GIMEP	Gross Indicated Mean Effective Pressure
FS	Full Scale
FT	Full Throttle
GDI	Gasoline Direct Injection
H_2	Hydrogen
HC	Hydrocarbons
HPS	(Gasoline) High-Pressure Fuel System
IMEP	Indicated Mean Effective Pressure
LL	Lean Limit
LML	Lean Misfire Limit
MBT	Minimum Spark Advance for Best Torque
NG	Natural Gas
NOx	Nitrogen Oxides
OCP™	Orbital Engine Corporations' Combustion Process
PMAX	Maximum In-Cylinder Pressure
PSC	Partially Stratified-Charge
PT	Part Throttle
SC	Stratified-Charge
SPI™	Saabs' Spark Plug Injector
TCP/IP	Transmission Control Protocol – Internet Protocol
TDC	Top Dead Center
THC	Total Hydrocarbons

Acknowledgements

Firstly, I would like to thank my supervisor, Dr. Robert L. Evans, for the opportunity to study at the University of British Columbia and to do something, that up until now, I had only dreamed of.

I would also like to thank Conor Reynolds as well as the rest of the alternative fuels group including Gord McTaggart-Cowan and Richard Vandolder, who have provided me with invaluable advice, guidance and assistance through out my work.

I greatly appreciate all of the contributions of the faculty and staff at UBC during my studies, in particular, those of Doug Yuen, Gordon Wright, Perry Yabuno and Barb Murray. I am also grateful to all my colleagues and students who have made my graduate experience fun and memorable.

I would like to recognize and thank my friends and family. My best friends back home, Dawn Mok, Jared Featherstone and Kari Bretz. My best friend Qi Meng and her family, who have helped me in innumerable ways from the beginning of my studies and have welcomed me into their family. Alice and Roy Hutchinson who helped me adjust to my new surroundings and gave me a warm and friendly shoulder whenever it was needed. Patty White, whose love, friendship and support have made this journey possible. Without her, I would never have survived even the first week away from home! Lastly, my mom, dad, sister, and grandma. You have been there for me from the very start. You have nurtured me, protected me and guided me through all the challenges in life. You have taught me to always strive to be the best that I can be and you have helped shape me into the person that I am today. This is my way of saying thanks. Thank you for everything.

Chapter 1
Introduction

1.1 Introduction

Motor vehicles are recognized as a major source of air pollution on the earth (National Research Council, 2001). Motor vehicles are believed to be responsible for up to 50 percent of hydrocarbon emissions, 50 percent of nitrogen oxide emissions and 90 percent of carbon monoxide emissions in urban areas (Heywood, 1998). Although most of us are aware of air pollution and its harmful effects, very few of us are willing to give up the convenience that our automobiles provide. In fact, recent consumer trends have been towards larger, less efficient vehicles, especially throughout North America. For example in the United States of America, vans, pickups and sport utility vehicles accounted for 47.5 percent of vehicle sales in 2000 versus 30 percent in 1990 (United States Environmental Protection Agency, 2001). This trend, along with growing environmental concern and dwindling fuel resources, has forced governments to establish stringent engine performance targets for motor vehicles. The quest for a solution to these issues has fallen on the shoulders of automotive manufacturers. The dilemma they face is how to reduce engine emissions and fuel consumption while still maintaining vehicle driveability, performance and economics. As in the past, new technologies have paved the way to solving these issues.

One technology that has shown considerable promise is the lean burn spark ignition engine (Germane, Wood, & Hess, 1983). In a lean burn engine, power output can be controlled by varying the air-fuel ratio of the inducted homogeneous mixture. Traditionally, spark ignition engines use throttling to accomplish load control, however

the resulting intake airflow restrictions reduce engine efficiency. This is especially noticeable at part load where most driving is done. In addition to the efficiency advantages due to reduced throttling, leaner mixtures have lower heat transfer and dissociation losses due to lower combustion temperatures and higher specific heat ratios (γ). A first law thermodynamic analysis of the ideal Otto gas cycle using constant specific heats, see Figure 1.1, results in the following relationship between the engine's thermal efficiency (ηt), compression ratio (r), and the specific heat ratio.

$$\eta_t = 1 - \frac{1}{r^{\gamma-1}} \qquad (1.1)$$

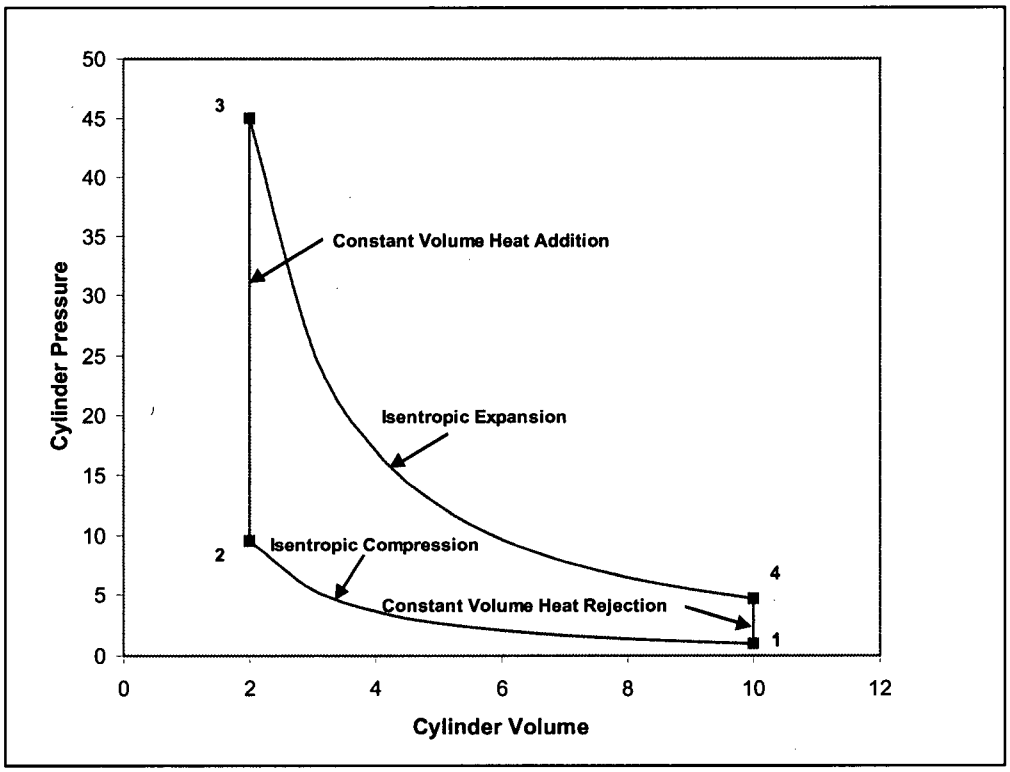

Figure 1.1: Air Standard Otto Cycle

Although this equation oversimplifies the variables involved in a real engine, it serves to demonstrate the effect of the specific heat ratio of the working gas on engine

efficiency. As mentioned, leaner mixtures have a higher specific heat ratio. This is a result of lower flame temperatures and the fact that air has a higher specific heat ratio than most fuels. For the purposes of gas cycle analysis Ferguson and Kirkpatrick, 2001, suggests the following for γ as a function of the relative air-fuel ratio (λ):

$$\gamma = 1.4 - \frac{0.16}{\lambda} \qquad (1.2)$$

$$\lambda = \left(\frac{\dot{m}_{air}}{\dot{m}_{fuel}}\right)_{actual} / \left(\frac{\dot{m}_{air}}{\dot{m}_{fuel}}\right)_{stoichiometric} \qquad (1.3)$$

The use of homogeneous lean burn technology in engines has not only produced efficiency improvements, but also reductions of some key emissions. Of particular concern are carbon monoxide (CO), hydrocarbons (HC) and nitrogen oxides (NOx). CO and HC are a direct result of incomplete oxidation of the fuel from incomplete combustion, while NOx results from the oxidation of nitrogen from the atmosphere at the high temperatures encountered during the combustion process. Carbon monoxide is poisonous to humans as it prevents the blood from absorbing oxygen. Hydrocarbons on the other hand can contribute to ground level ozone, which is also poisonous. Some hydrocarbon emissions are also known carcinogens. The combination of HC, NOx and ultra-violet light results in the formation of photochemical smog, which is known to cause breathing related issues in urban areas. Nitrogen oxides can also combine with water to form nitrous acid, a constituent of acid rain, which can cause severe environmental damage.

Figure 1.2 demonstrates the trade off of these emissions as a function of λ. It is clear from Figure 1.2 that by running an engine lean we can achieve a significant reduction in CO and NOx emissions compared to stoichiometric operation. Carbon monoxide is reduced due to the lower carbon and increased oxygen content of lean mixtures, while NOx decreases due to the reduced combustion temperatures of lean mixtures. However, leaner mixtures also result in higher hydrocarbon emissions due to the onset of misfire and partial burning of the air-fuel mixture. In homogeneous lean burn engines careful attention must be paid to mixture formation and ignition to reduce HC emissions. Germane et al. (1983), give a complete review of homogeneous lean burn engines.

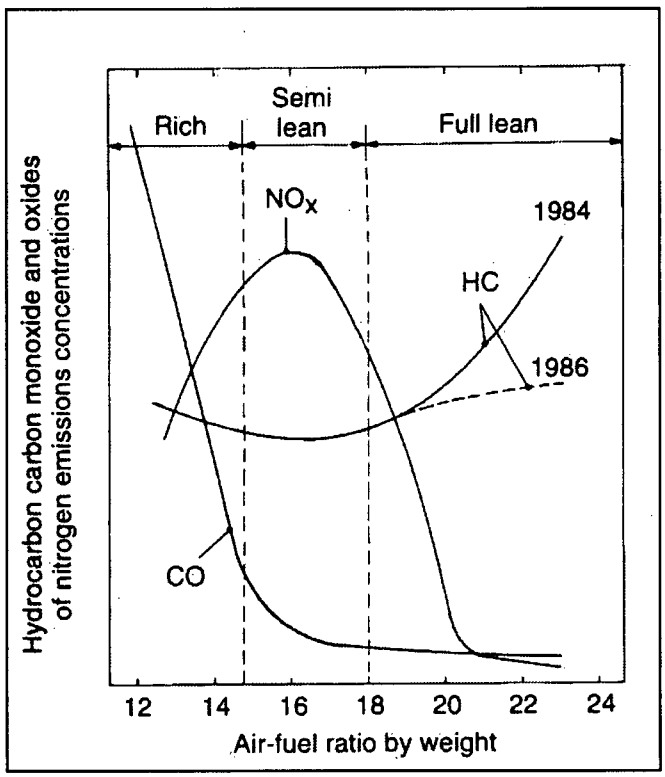

Figure 1.2: Effect of Air-Fuel Ratio on Emissions
Source: (Heisler, 1995)

The stratified-charge (SC) engine concept was conceived as early as Otto, and Ricardo performed his first experiments in 1915. A historical overview of stratified charge engines can be found in Abata (1987). The stratified-charge concept is seen as a promising solution to the issues presented by poor mixture formation and ignition in homogeneous charge lean burn engines. In a SC engine, the in-cylinder mixture, which is composed of air, re-circulated gases and fuel, is non-uniformly distributed. The engine is usually designed in a manner that promotes ignition of the overall lean mixture, i.e. richer mixtures are located in the region of the spark. The result is reduced cycle-to-cycle variation and an extension of the lean limit.

A large number of stratified-charged engine concepts have been developed over the past half a century and a few of these have made their way into production vehicles. Everything from carbureted engines with separate valves for rich and lean mixtures, to axially stratified multi-port fuel injected engines have been tried. Although many of these engines shared promise to improved engine efficiencies, few performed well in practice. This was due to difficulties in ensuring that the rich mixture reached the vicinity of the ignition source over the range of loads and speeds encountered during normal engine operation. In general, lower CO and NOx emissions could be realized due to the excess oxygen and lower temperatures, respectively, of lean mixtures. Hydrocarbon emissions were still high, however, due to incomplete combustion of the lean portion of the mixture and the presence of an overly rich mixture around the ignition source (Abata, 1987, Frank & Heywood, 1990). With the development of more sophisticated engine management systems and high-pressure injectors, the recent focus of stratified-charge gasoline engines has been towards the Gasoline Direct Injection (GDI) engine. Fraidl, Piock, & Wirth

(1996), Lake, Stokes, Whitaker, & Crump (1998) and Spicer, Kolmel, Kubach, & Topfer (2000) provide a good introduction to some of the more popular GDI designs and related issues. A few of these engines have reached mass production, (Iwamoto, Noma, Nakayame, Yamauhi, & Ando , 1997, Kamura & Takada, 1998) and have been shown to improve engine efficiency and emissions compared to conventional homogeneous fuelled engines.

A local charge stratification process, the Partially Stratified-Charge (PSC) concept, has been developed at the University of British Columbia in an attempt to improve lean burn engine performance (Evans, 1999 and Reynolds, 2001). In the PSC engine, an overall lean mixture is inducted or formed in the combustion chamber and is compressed during the compression stroke. Just prior to the spark, a small amount of fuel, comprising up to 10% of the total fuel mass, is injected into the combustion chamber in the vicinity of the spark plug. This produces a rich pocket that can be ignited more easily and facilitates the combustion of the remaining lean mixture. See Figure 1.3.

The local charge stratification process is unique in that only a small portion of the total fuel injected is used for stratification. This compares to most other SC system in which bulk stratification of the entire air-fuel mixture is utilised (Abata, 1987). Some research on local charge stratification in lean burn engines has been performed over the past decade with good results. Early developmental work was performed by Green and Zavier (1992), and used a modified spark plug with a hypodermic injection tube to directly inject natural gas into homogeneous-charge gasoline and natural gas engines. Green and Zavier reported an extension of the lean limit and a significant improvement in

fuel consumption at lean air-fuel ratios. Carbon monoxide emissions remained constant or slightly lower than homogeneous operation, while unburned hydrocarbon emissions increased. This increase was attributed to the injected fuel burning at the rich flammability limit and potential quenching of the fuel in the spark plug and hypodermic tube.

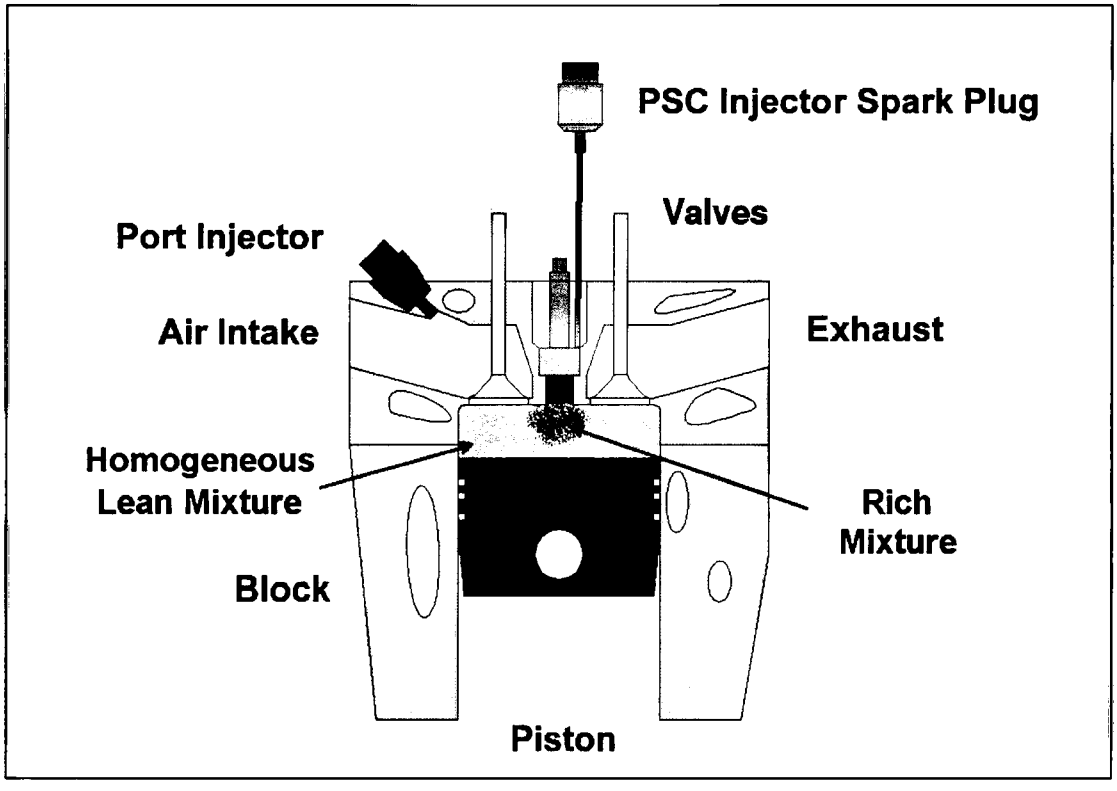

Figure 1.3: The Partially Stratified Concept

Arcoumanis, Hull, & Whitelaw (1994) examined local charge stratification with propane / air mixtures in a constant volume combustion chamber. A lean homogeneous mixture was first created and injected into the cylindrical combustion chamber with rotational velocities typical of modern engines. Subsequently, a small amount of a rich premixed propane mixture was injected towards the spark plug from a gas injector located perpendicular to the spark plug to create the local charge stratification. The

investigation included the effects of spark plug positioning and bulk flow velocities as well as positioning, duration and equivalence ratio of the local injected mixture. Using an optimised set-up, they were able to extend the lean limit in the constant volume chamber from λ=1.5 to λ = 2.6. Using pressure analysis and shadowgraph visualization techniques, the researchers were able to confirm faster burn rates and higher peak pressures at a given relative air-fuel ratio when using the local charge stratification process. The successes of this system led the researchers to try a similar system on a single cylinder research engine (Arcoumanis, Hull, & Whitelaw, 1997). The tests were performed at low load and speed using propane fuelling. The researchers investigated both the effects of the locally generated flow and turbulence from the in-cylinder injection, as well as the air-fuel ratio of the injected mixture. Local injection of mixtures with the same relative air-fuel ratio as the main mixture resulted in peak pressure improvements of up to 55% for lean mixtures. The lean limit was also extended from λ = 1.45 to λ = 1.55 (where the criterion for acceptable engine operation was a coefficient of variation (COV) of indicated mean effective pressure (IMEP) of less than 10%). With the injection of a slightly rich mixture (λ = 0.91), making up approximately 3.5% of the total fuel flow, greater performance improvements were realised. The lean limit was extended to λ = 1.80 and peak pressure increases of up to 65% were achieved. Tests with approximately 2% stratified fuel flow resulted in similar trends with a slight reduction in peak pressures and the lean limit of operation.

Reynolds (2001), using a natural gas fuelled single cylinder engine at the University of British Columbia, investigated a system similar to Green and Zavier (1992), utilising the Partially Stratified-Charge concept. Pure natural gas was injected through the

spark plug to create the local charge stratification at the ignition source. Reynolds reported improved performance in terms of reduced fuel consumption, emissions, cyclic-to-cycle variability, ignition delay and combustion duration in the region of the homogeneous lean limit. More specifically, tests at full load and 2500 rpm indicated improved brake specific fuel consumption beyond $\lambda = 1.5$, up to a maximum of 7% at $\lambda = 1.65$. This was also accompanied by a 7% increase in brake mean effective pressure at $\lambda = 1.65$ and an extension of the lean limit from $\lambda = 1.6$ to $\lambda = 1.7$. Beyond $\lambda = 1.5$ the mass fraction burned calculations indicated that the 0% – 5% and 5% - 95% burn duration dropped consistently when using PSC. Decreases of 7 degrees and 4 degrees in ignition delay and combustion duration, respectively, were observed at $\lambda = 1.65$. There were noticeable reductions in CO emissions for mixtures leaner than $\lambda = 1.4$ with a 25% decrease at $\lambda = 1.65$ (Note that emissions were reported on a brake specific basis). Hydrocarbon emissions remained constant, except for mixtures beyond the homogeneous lean limit where there was a slight reduction. At a given air-fuel ratio, nitrogen oxide emissions were higher when using PSC. However, the extension of the lean limit when using PSC meant lower NOx emissions were achievable with the PSC system.

The research presented in this thesis follows from the successful application of local charge stratification in lean burn engines by previous researchers. The research presented here will focus on the development, implementation and investigation of a partially stratified-charge gasoline engine. The research objectives were as follows:

1. Implement the current natural gas PSC system on a gasoline fuelled single cylinder Ricardo Hydra research engine and compare the performance of the PSC engine relative to its homogeneous fuelled counterpart.

2. Design and implement a gasoline PSC system for the above-mentioned engine and compare gasoline PSC performance relative to its homogeneous fuelled counterpart.

3. Make recommendations on future PSC system development and testing. Comment on the potential of the PSC system.

Based on previous work by Reynolds (2000), is believed that the implementation of the PSC system on a gasoline fuelled engine will provide more stable engine operation under lean conditions over conventional homogeneous charge engine operation. The result of this improved lean burn performance under very lean conditions will potentially be realised as a reduction in fuel consumption and engine emissions. Should this be achieved, it would be an important step towards reducing the burden that internal combustion engines place on our natural resources and the environment.

Chapter 2
Experiment

2.1 Introduction

This chapter introduces the experimental apparatus and experimental methodology used throughout this research. The first section will start off by discussing the mechanical, partially stratified-charge, and data acquisition systems in some detail. This is followed by an examination of the experimental procedures used as well as the reasoning behind the tests performed.

2.2 Apparatus

All the data presented in this thesis was acquired using a Ricardo Hydra single cylinder research engine. The testing was performed between November and December, 2003 in the Department of Mechanical Engineering at the University of British Columbia. Mechanically, the Ricardo Hydra was set up in a conventional gasoline fuelled engine configuration with the only major additions being the gasoline and natural gas partially stratified-charge systems. The engine was thoroughly instrumented, allowing measurements of in-cylinder pressure, torque output, air-fuel ratio and exhaust emissions. A custom-built control system provided control of ignition and injection parameters in addition to the basic controls provided by the original Ricardo control system. The data from the instrumentation and control systems was remotely acquired using a custom data acquisition system and displayed through a Labview based interface.

2.2.1 Mechanical systems

The Ricardo Hydra used for testing, serial number 31, is a purpose built research engine from Ricardo PLC Company in the United Kingdom (see Figure 2.1). The compact, modular design of this engine allows for quick optimization of the mechanical components to suit research requirements. The Hydra can, for instance, operate as either a spark ignition or compression ignition engine and can burn a wide variety of liquid and gaseous fuels with only minor modifications.

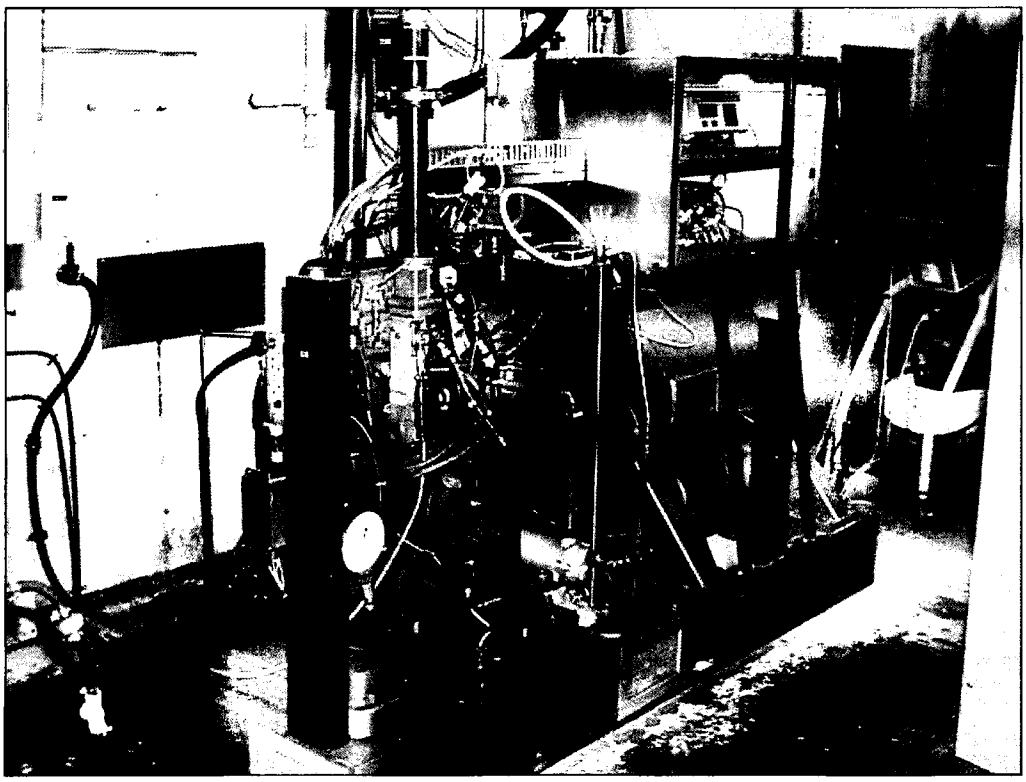

Figure 2.1: Ricardo Hydra Research Engine

For all of the tests the cylinder head was composed of 2 separate components; a two-valve, single overhead cam, flat cylinder head, shown in Figure 2.2, and the PSC injector plate. The latter consisted of a thick steel plate with a large volume removed to accommodate the intake valve, exhaust valve, spark plug and in-cylinder pressure

transducer located in the flat cylinder head. As shown in Figure 2.3, the combination of the flat cylinder head and PSC injector plate provided a clearance volume similar to a conventional gasoline spark ignition engine. The final clearance volume was calculated to be 60 cm^3. An oversized Ford Cortina flat top piston was used which, with the engine's 88.2 mm, stroke resulted in a displaced volume of 463 cm^3 and a calculated compression ratio of 8.7:1. Cast iron piston rings were used to ensure quick seating and valve seals installed to reduce oil usage. The valve clearance and timings were set according to Ricardo's specifications. Before any testing commenced the engine was also run-in for 16 hours. Table 2.1 below shows a complete list of engine specifications.

Table 2.1 : Engine Specifications

Specification	Measurement	Specification	Measurement
Bore (mm)	81.5	Oil Pressure (bar)	5.3
Stroke (mm)	88.9	Oil Temperature (°C)	98 – 103
Connecting Rod Length (mm)	158.0	Coolant Temperature (°C)	92 – 97
Clearance Volume (cm^3)	60.0	Port Injection Pressure (bar)	2.0
Volumetric Displacement (cm^3)	463.3	Port Injection Start Timing (°)	145 BTDC
Compression Ratio	8.7	Spark plug gap (mm)	1.65
Rated Speed (rpm)	5400	Intake Valve Clearance (mm)	0.15
Rated Power (kW)	15	Exhaust Valve Clearance (mm)	0.4
Intake Valve Open (°)	12 BTDC	Exhaust Valve Open (°)	56 BBDC
Intake Valve Close (°)	56 ABDC	Exhaust Valve Close (°)	12 ATDC

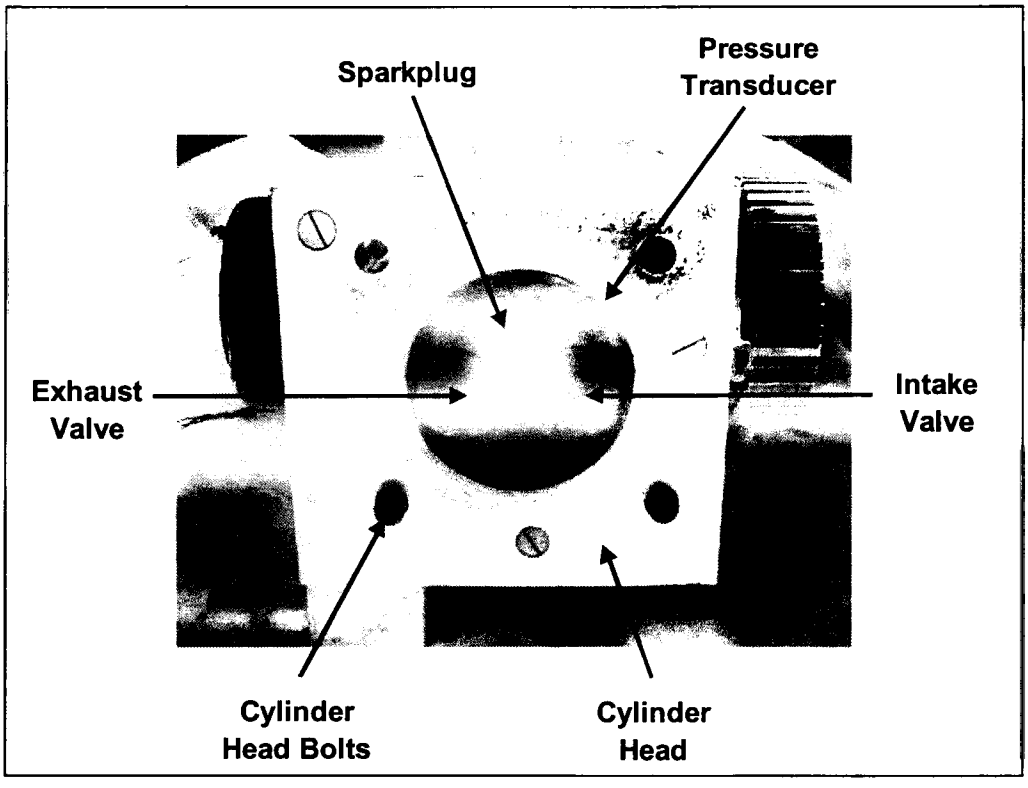

Figure 2.2: Ricardo Hydra, 2-Valve, Flat Cylinder Head

The intake system for the Ricardo Hydra consisted of an air filter, laminar flow element air flow meter, plenum chamber, throttle body and intake manifold. The air inlet for the engine was moved outside the test cell into an adjacent laboratory in an attempt to mitigate inlet temperature variations and ensure a clean air supply to the engine. A large 38 L plenum chamber, consisting of a high density ployethylene storage container and a metal baffle, was implemented to reduce pulsations travelling upstream from the intake valve to the laminar flow element test section. 1.5" tubing was utilized throughout the entire intake system. The exhaust system was composed of 1.25" diameter, 90°- bend, exhaust manifold that terminated into a 3" diameter free-floating steel pipe that served as a condensate trap and oxygen sensor location as well as the exhaust gas sample point. The exhaust pipe was routed, by way of flexible tubing, to the ceiling and exhausts through a muffler on the roof of the test cell.

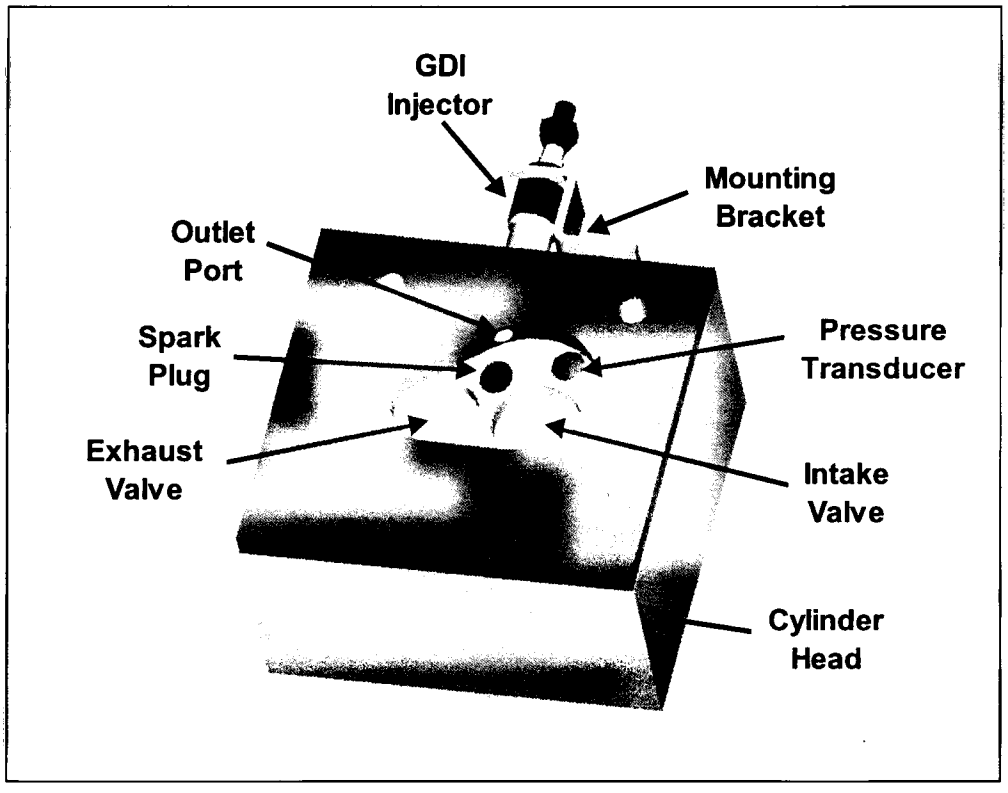

Figure 2.3: Flat Cylinder Head and PSC Plate

The main fueling for the engine was accomplished using a standard port injection system with a few adaptations for fuel consumption measurement, safety and maintenance. A schematic of the fuel system is given Figure A.1 in Appendix A. Fuel is gravity fed from a fuel tank in the test cell, through a filter to a gravimetric fuel balance. The fuel balance supplies fuel to the fuel injection system, which includes an electric fuel pump, fuel injector manifold, fuel injector, fuel lines and a back pressure regulator. In addition to this basic hardware, the fuel injection system contains a set of shut off valves for easy maintenance, a safety shut off solenoid for emergencies and an appropriate control system. There are no facilities for heating or cooling the fuel. Note that the fuel pressure is kept constant at 1.6 bar as per the manufacturers recommendations. Typical

fuel consumption rates over the range of tests conducted here are in the range of 0.5 – 2.0 kg/hr.

2.2.2 PSC Systems

Two different PSC systems were used during testing. The first system was based on the previous natural gas PSC system developed by Reynolds (2001). This system was primarily used to determine whether there were any advantages to using the PSC concept on a gasoline engine. The second system was a purpose built gasoline PSC system designed to examine the performance characteristics of a mono-fuel gasoline PSC engine.

Natural Gas PSC

The major components of the natural gas PSC system can be seen in Appendix A, Figure A.2. High-pressure natural gas is provided from a bank of natural gas cylinders located adjacent to the test cell. These cylinders are recharged, using a series of compressors, from the local BC natural gas lines and the gas regulated to 27 bar for use in the natural gas PSC system. This pressure, the highest achievable with the current natural gas PSC regulator, was chosen, to minimize the amount of combustion gases that may enter the PSC system, diluting the incoming PSC charge. From the natural gas PSC regulator the natural gas passes through a thermal mass flow meter and a fast response solenoid that serves as the fuel injector. A stainless steel capillary tube with a 0.5 mm orifice runs from the block mounted solenoid to the custom PSC spark plug, (shown in Figures 2.4 and 2.5).

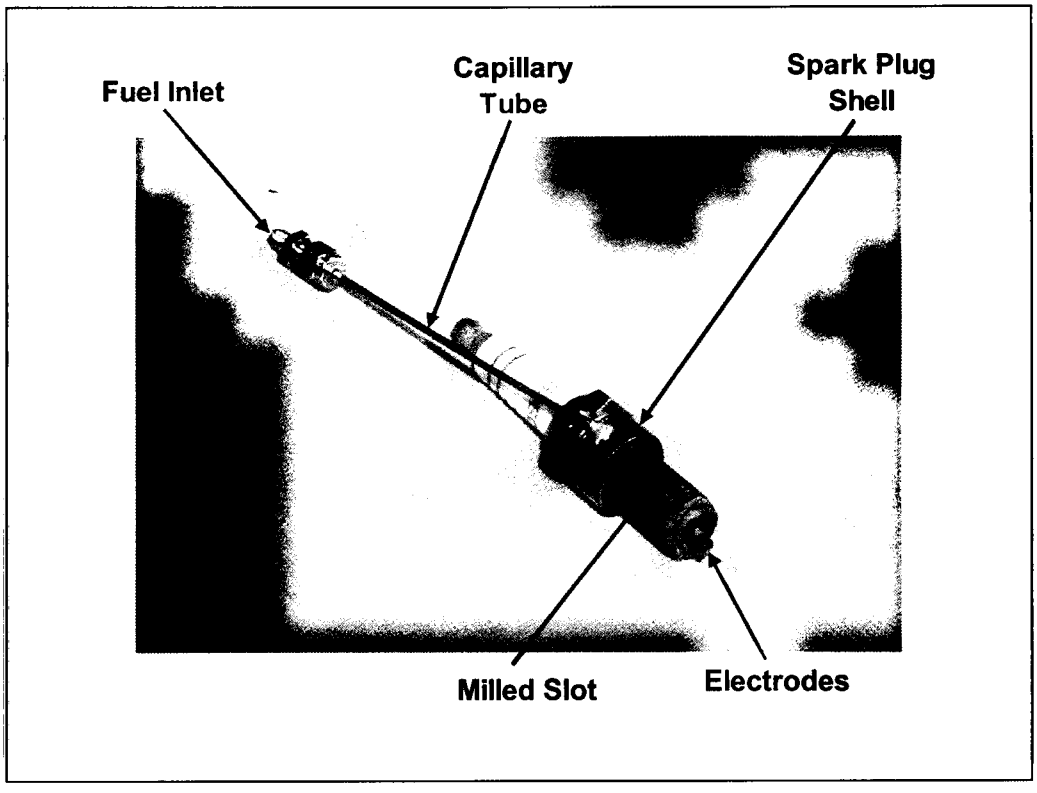

Figure 2.4: Natural Gas PSC Plug
Source: (Reynolds, 2001)

The PSC plug is a modified Bosch XR4CS spark plug. A hole is drilled through shoulder of the spark plug shell and intersects a slot that is milled along the spark plug threads. A small tube is welded to the hole on the outside of the shell and provides a point to connect the outlet of the solenoid. The milled slot is 1-2 threads less than the total plug thread reach. This allows a second small hole to be drilled towards the center electrode of the plug so that when gas is injected through the plug a small jet is ejected and surrounds the spark plug electrodes.

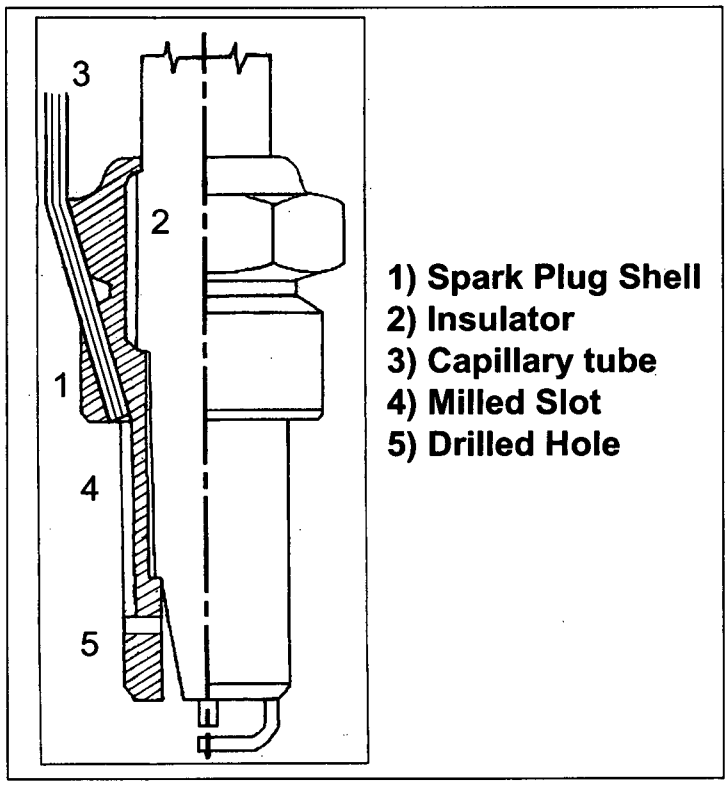

Figure 2.5: Cutaway View of the Natural Gas PSC Plug
Source: (Reynolds, 2001)

Gasoline PSC

Originally it was hoped that a spark plug injector, similar to that used for the natural gas system, could be utilized for the gasoline PSC system. Early designs integrated a gasoline direct injection (GDI) injector into the spark plug shell. The goal was to take advantage of the injector's spray pattern, minimize wall wetting and ensure good mixing. This design required too much space, even when a custom spark plug was used, however. It was decided that the GDI injector could be integrated into a steel plate. This plate would then be sandwiched between a flat cylinder head and the current cylinder block and thus form an integral part of the clearance volume. The completed

design is shown in Figure 2.6 and detailed drawings in Figure A.3 and A.4 in Appendix A.

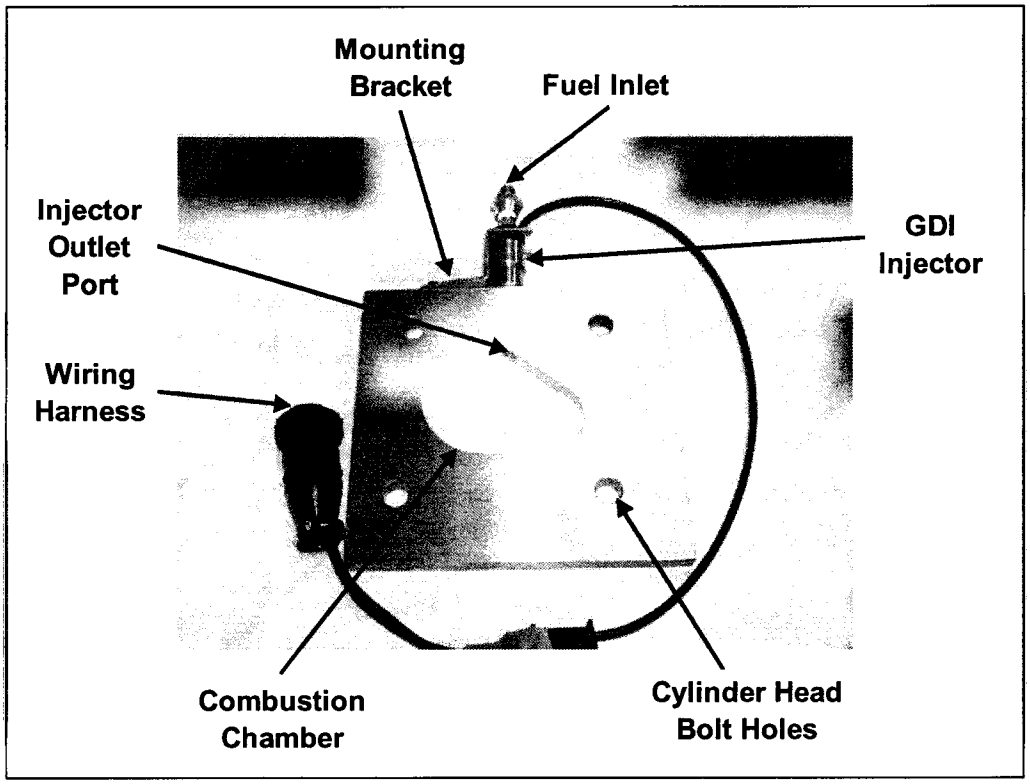

Figure 2.6: Gasoline PSC Plate

The size of the cylinder head and the diameter of the GDI injector nozzle dictated the outer dimensions of the gasoline PSC plate. A plate thickness of approximately 11mm was required to ensure sufficient wall thickness between the outer plate surfaces and the injector nozzle. The shape and size of the clearance volume in the center of the plate was dictated by the need to allow sufficient clearance for the valves, spark plug and in-cylinder pressure transducer while minimizing the clearance volume to achieve the highest possible compression ratio. The GDI injector was positioned directly in-line with the spark plug to minimize the injection distance and improve the probability of local charge stratification in the region of the ignition source. The injector was mounted to the

edge of the plate with a simple "Z"-shaped bracket. A Teflon seal on the injector provided a tight seal between the injector nozzle and the PSC plate. Soft, thin copper gaskets were chosen to improve heat transfer away from the plate to the cylinder head and block, as the plate had no facilities for water-cooling.

The other main component of the gasoline PSC system was the high-pressure fuel system (HPS) needed to inject the liquid fuel directly into the combustion chamber, (refer to Figure 2.7). The layout of the HPS is shown in Appendix A, Figure A.5. In the HPS, fuel is manually pumped at low pressure through a check valve and into a bladder accumulator. A nitrogen cylinder is then used to slowly pressurize the gas side of the accumulator to approximately 80 bar. The liquid fuel, now at 80 bar, passes through a regulator, which maintains the fuel pressure at up to 50 bar. From here the fuel passes through a fine filter and a safety relief valve that protects the thermal mass flow meter and GDI injector downstream from over-pressure. Multiple bleed valves throughout the system are used to remove air from the system and facilitate system maintenance. With a one-litre storage capacity, the HPS can provide up to seven hours of PSC operation at flow rates nearing 100 g/h. Short durations of full GDI operation are also possible.

2.2.3 Data Acquisition, Instrumentation and Control

A wide variety of engine parameters including temperatures, pressures, flow rates, and emissions are measured during testing. These parameters are not only used for analysis purposes but also to control and ensure safe operation of the engine. The systems that are used to acquire and manipulate these variables can be divided in to three categories, namely Data Acquisition, Instrumentation and Control.

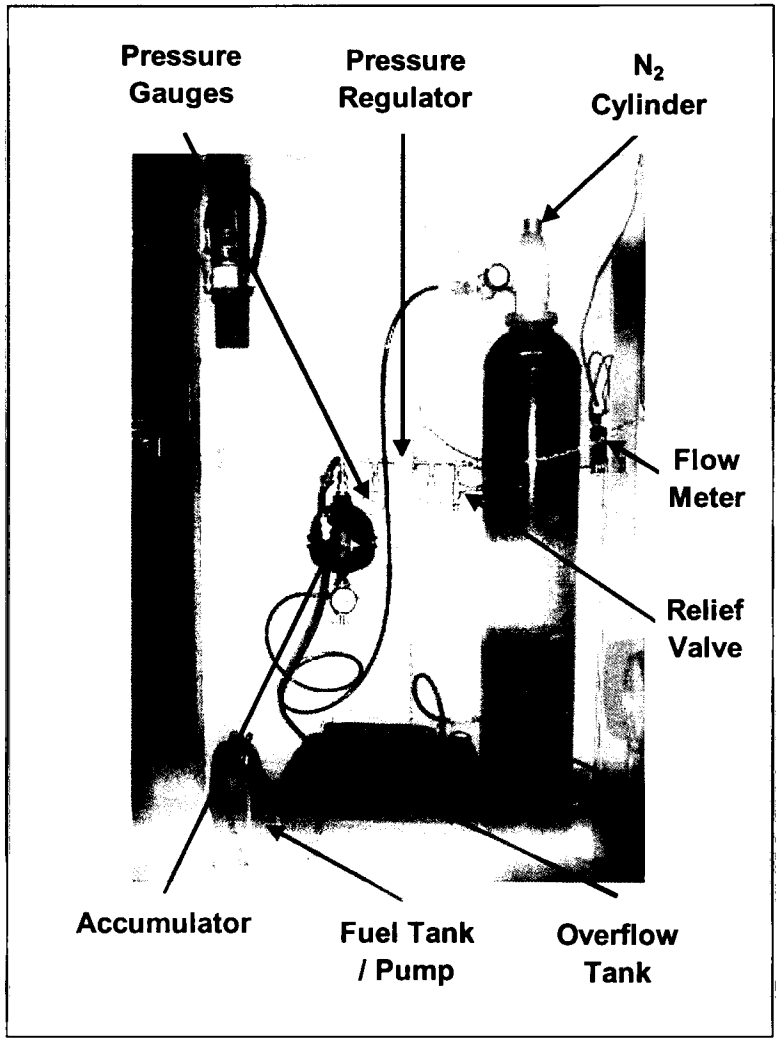

Figure 2.7: High Pressure Gasoline Fuel System

Data Acquisition

The Data Acquisition system is responsible for acquiring sensor outputs, performing signal conditioning, running pre-data analysis, as well as providing an interface for viewing, formatting and saving data. The Data Acquisition system for the Ricardo Hydra is made up of five signal conditioning boards, a data acquisition board and two computers, (see Table 2.2). A schematic of the system is given in Figure A.6 in Appendix A. Signals from the various instruments are sent to their respective signal

conditioning boards where the signals are filtered and gains / offsets applied. From here the signals are sent to the data acquisition board, which samples the individual channels. These measured values are moved to a server in the test cell running a Labview application, the DynoServer. This application performs gain and offset corrections to get engineering units and serves this data to a remote computer in an adjacent room via the TCP/IP protocol. The remote computer grabs this data from the network and displays it through a second Labview application, the DynoClient. The DynoClient also serves as an interface to enter manually recorded data and save test results to disk.

During sampling the data acquisition board uses multiplexing to sample all of the fifty-three available channels. This is performed two hundred and fifty times at a sampling rate of 1 KHz per channel and the data is averaged using the DynoServer application before it is sent to the DynoClient. Subsequently, one cycle each of intake manifold pressure and in-cylinder pressure data is acquired at 0.5^{o} crankangle increments. Between the intake and compression strokes the DynoServer application uses the average intake manifold pressure at BDC +/- 10^{o} to peg the average in-cylinder pressure from BDC +/- 5^{o}. The resulting waveform is then sent to a PressureClient application for display on the remote computer. The entire data sweep takes approximately 1 second and for most tests a minimum of 100 sweeps are made. The saved output from the DynoClient is in comma delimited text format.

Table 2.2: Data Acquisition Components

Component	Manufacturer	Model
Low Pass Filter and Amplifier Card	IOtech	DBK-18
Programmable Low- & High-Gain Analog Input Modules	IOtech	DBK-53
High-Accuracy Thermocouple Input Module	IOtech	DBK-52
Data Acquisition Board (16bit, 200 kHz)	IOtech	DAQBOARD 2000
Counter / Timer Board	National Instruments	PCI-6601

Although the in-cylinder pressure data is displayed using the above-mentioned procedures, the saved data from the PressureClient is generated differently. The pegging procedure is the same except that only 1 cycle of intake manifold pressure data is used to peg each of 100 consecutive in-cylinder pressure cycles. The saved data from the PressureClient then consists of 100 cycles of in-cylinder pressure data at 0.5° crankangle increments, again in comma delimited text format.

Instrumentation

Table 2.3, presents a list of general specifications for the major instruments used throughout this research. The data in the table was referenced from manufacturer's user manuals.

Airflow measurements were made using a Meriam laminar flow element that produces a pressure differential proportional to the volumetric flow rate. A differential pressure transducer is used to measure this pressure drop and by utilizing the atmospheric test conditions, i.e. pressure, temperature and humidity, this volumetric flow rate can be converted to a mass airflow.

All temperature measurements are performed using K-Type thermocouples. An Iotech thermocouple input module is used to provide linearization and cold junction compensation. Barometric pressure and humidity measurements were made manually using a mercury barometer and a hygrometer gauge in the lab.

Two different devices were used to measure fuel flow rates. The main gasoline flow rate was measured using an AVL gravimetric fuel balance while both the gasoline and natural gas PSC flow rates were measured by thermal mass flow meters.

Engine torque is measured using a strain gauge load cell, which is located on a torque arm mounted to the side of the dynamometer. The strain gauge is of the electrical-resistance type and is bonded to the torque arm. A charge amplifier is used for signal conditioning before the torque signal reaches the data acquisition system. A plate on the opposite side of the dynamometer is used to counterbalances the torque arm. A 20 Nm weight can be attached to the torque arm for static calibration purposes.

Table 2.3: Instrument Specifications

Measurement	Manufacturer	Model	Range	Uncertainty
Intake Air Flow Rate	Meriam	50MW 20 – 1.5	0 – 30 scfm	0.3 scfm
Intake Air and Exhaust Temperature	Omega	1/8" K-Type	-200 – 1250°C	± 2.2 °C
Intake Manifold Pressure	Sensym	LX1803AZ	0 – 30 Psia	± 0.6 Psi
Differential Pressure Transducer (Intake Air Flow Rate)	AutoTran	600 D-014	0 – 20" H_2O	± 0.2" H_2O
Gasoline Main Fuel Flow Rate	AVL	Dynamic Fuel Balance 7030	0 – 50 kg/h	$\pm 10 < \dot{m} < \pm 20$ g/h
Exhaust Relative Air-Fuel Ratio	ECM	AFRecorder 2400G	$\lambda = 0.4 - 10.0$	± 0.006 ($\lambda = 1.0$) ± 0.008 ($0.8 < \lambda < 1.2$) ± 0.009 (elsewhere)
In-Cylinder Pressure Transducer	AVL	QC33C	0 – 200 bar	± 0.4 bar
Gasoline PSC Fuel Flow Rate	Horiba	LF-410	0 – 120 g/h	± 2.4 g/h
Natural Gas PSC Fuel Flow Rate	MKS Instruments	179A-24-S3BM	0 – 20 slm	± 0.12 slm
Engine Crank Angle / Speed	US Digital	H1-360-IE	0 – 10,000 rpm	± 0.5° ± 2.5 rpm
Engine Torque	n/a	n/a	0 – 50 Nm	± 0.5 Nm
Carbon Dioxide Emissions	Beckman	880	0 – 20%	± 0.2%
Hydrocarbon Emissions	Ratfisch	RS-55	0 – 10,000 ppm	± 100 ppm
Carbon Monoxide Emissions	Siemens	Ultramat 21P	0 – 10,000 ppm	± 100 ppm
Nitrogen Oxide Emissions	API	200AH	0 – 4500 ppm	± 50 ppm

A variety of instruments are used for emissions measurement. The exhaust sample in all cases originates from the large free-floating exhaust pipe approximately 1 m downstream of the exhaust port. From here the sample passes through a heated sample line and into the emissions bench. Once inside the emissions bench, the sample is pumped through heated filters using a heated sample pump. A portion of the sample is passed into the flame ionization detector total hydrocarbon analyzer. The remaining portion of the sample is pumped through a chiller where water is removed and then through the remaining carbon monoxide, carbon dioxide, and nitrogen oxide analyzers. Both the carbon monoxide and carbon dioxide emissions are measured using non-dispersive infrared analyzers. Nitrogen oxide emissions are measured using a chemiluninescent analyzer with an integrated nitrogen dioxide to nitrogen oxide converter. Flow rate control to the instruments is achieved using a set of rotameters.

In-cylinder pressure measurements are made using a piezo-electric water-cooled AVL pressure transducer. A charge amplifier serves as the primary signal filter and amplification device. The amplified signal is passed to the data acquisition system. One major advantage of the water-cooled pressure transducer is that it reduces the occurrence of thermal shock and sensor drift. This is a result of the temperature extremes encountered during engine operation and can significantly affect the in-cylinder pressure measurements. Figure 2.8 shows some typical homogeneous lean burn and partially stratified-charge log P – log V curves. This particular plot is useful for troubleshooting problems with in-cylinder pressure transducer measurements. Other than some small perturbations due to injector noise during the compression stroke, there are no significant signs of thermal shock, mechanical vibration or pegging problems in the pressure signal.

The slope of the log P – log V curve during the intake and exhaust strokes are quite linear with corresponding polytropic indices (slopes) in the range of 1.30 +/- 0.05, with the lower values occurring for the expansion process and richer mixtures. An absolute pressure transducer is used to peg the in-cylinder pressure to the pressure in the intake manifold at BDC during the intake stroke.

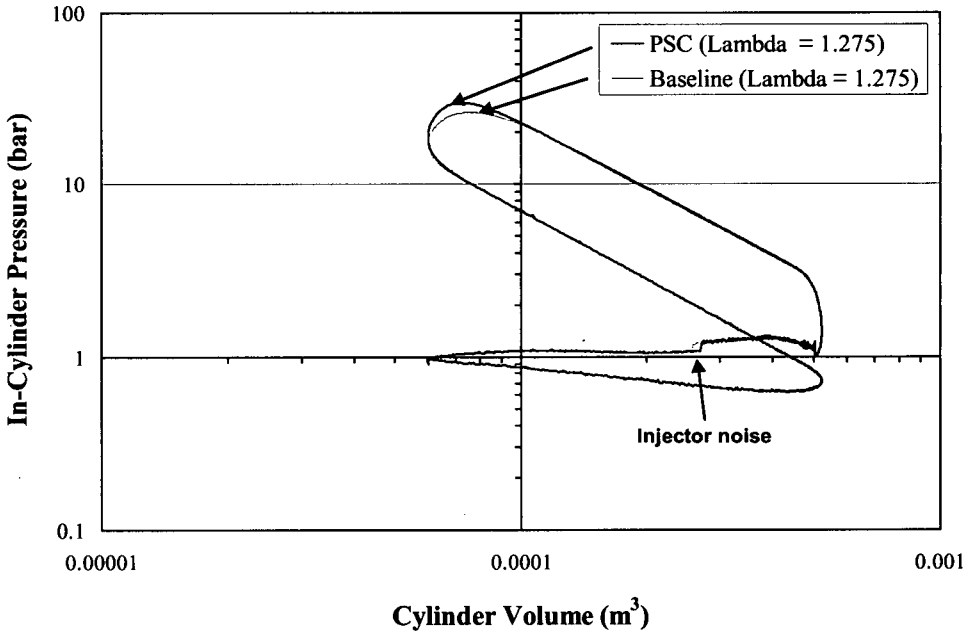

Figure 2.8: Log P - Log V Diagram, Part Throttle

A universal exhaust gas oxygen sensor is utilized to acquire and set relative air-fuel ratios. This special exhaust gas sensor allows measurements over a much wider range of air-fuel ratios than conventional sensors. The oxygen sensor measurements provided a simple way to set test points in a repeatable manner. Furthermore, instantaneous mass flow measurements were unavailable to determine air-fuel ratios during testing. Air-fuel ratio measurements, however, were verified using mass air flow

and fuel flow measurements during the data processing stage. The oxygen sensor and mass flow air-fuel ratio measurements agreed within $\lambda = 0.01$ at full throttle and stoichiometric conditions. In regions of poorer combustion, for example at the lean limit, the mass flow based air-fuel ratio calculations were within $\lambda = 0.06$. For accurate air-fuel ratio measurements the oxygen sensor requires knowledge of the hydrogen to carbon ratio of the fuel as well as knowledge of combustion completeness. The hydrogen to carbon ratio of the gasoline ad natural gas were determined to be 1.824 and 3.907 respectively, through a gas chromatograph analysis. The incomplete combustion coefficients were unknown and typical coefficients were implemented. What is important, however, is that in all but the throttled baseline tests, the mass flow calculations indicated leaner mixtures than those recorded by the oxygen sensor. This means that in the worst case scenario, the oxygen sensor readings are a conservative measurement of the actual air-fuel ratio. Throughout this work the air-fuel ratio measured by the oxygen sensor will be reported.

Speed and crank angle measurements are performed using a rotary shaft optical encoder. The U.S. Digital model used on the Hydra has three separate tracks, two of which are have markings every degree and one which has a single marking. The provides a TDC reference while the other two, which are a quarter-degree out of phase, can be used to achieve quarter degree accuracy. A second optical sensor was used to peg the crankshaft sensor to the correct part of the cycle.

Control

Engine load and speed control is carried out using a DC dynamometer that is directly coupled to the Ricardo Hydra. The dynamometer is rated at a maximum of 30 kW and a speed of 100 rev/s and may be used to either provide or absorb power. Closed loop speed control is provided by a KTK thrysistor converter unit that references a tachogenerator on the dyno's output shaft. Engine speed and throttle are set using multiturn dials on the control console. The throttle setting is relayed to a servomotor, which opens and closes the butterfly throttle valve. A safety trip system, the Automatic Control Unit, is integrated into the control console to prevent engine damage should a failure occur. This safety device monitors critical parameters such as engine oil pressure and dynamometer temperatures.

A custom built timing system was utilized to control the injection and ignition parameters. This included instantaneous control of signal timing and duration for the natural gas PSC, gasoline PSC, gasoline port injection and ignition systems, (see Figure A.7 in Appendix A). The desired control settings are entered into a Labview application, the TimingControl, running on the Data Acquisition server. These settings are then relayed to a counter/timer card located in the server. The counter/timer card references the angular position of the camshaft and crankshaft and generates the appropriate control response based on the desired control settings. This output signal is then used as input to a driver box, which contains the drivers for the ignition and various injection systems. Sample outputs from the driver box are given in Figures 2.9 through 2.11. The encoder signal in these figures is in half-degree increments. As illustrated by these figures, a peak and hold signal, accomplished through gated current control of the power source, is

generated for all of the injectors to ensure faster opening and closing. To further improve injector response times, a high voltage source, approximately 315 V for the GDI/port injectors and 450 V for the natural gas injector, is used in combination with a resistance in series with the injectors (this reduces the charging and discharging time constants). In the case of the ignition system, the 450 V source is input directly into the primary windings of a high-energy ignition coil. This results in up to 45,000 V being available at the spark gap.

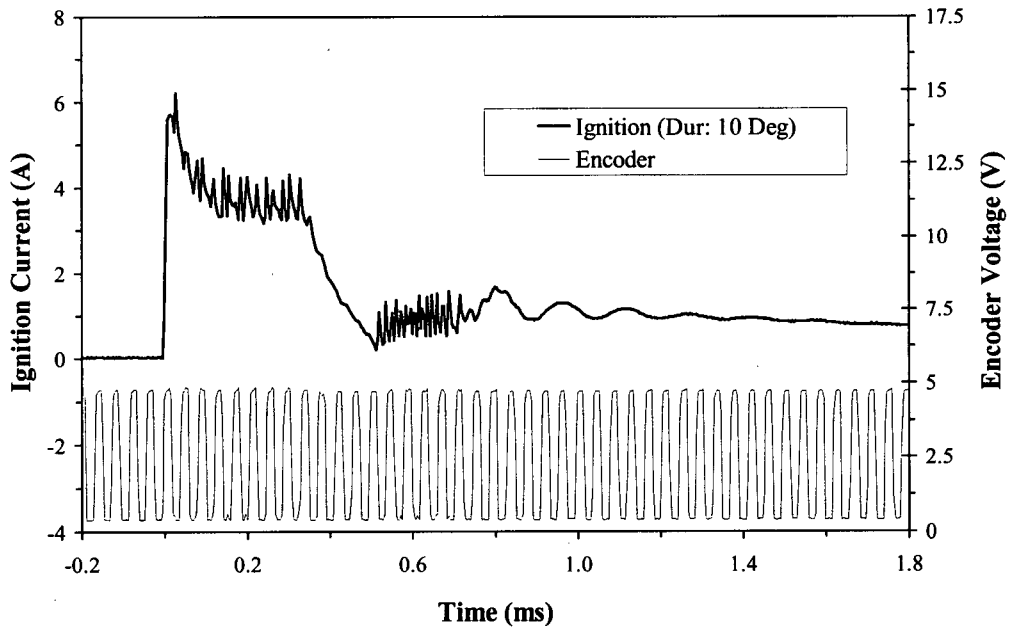

Figure 2.9: Ignition System Current Signal

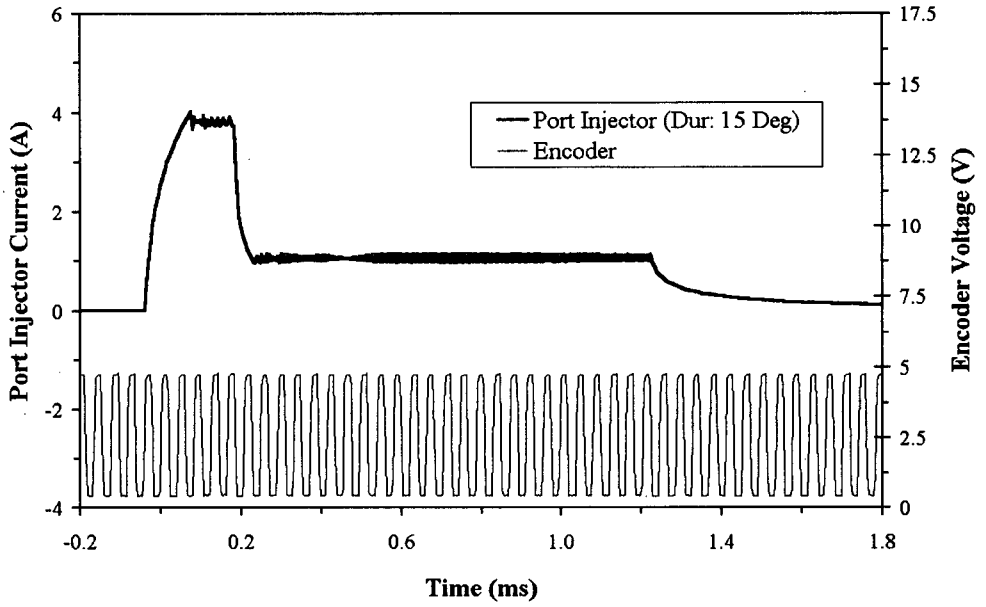

Figure 2.10: Port Injection System Current Signal

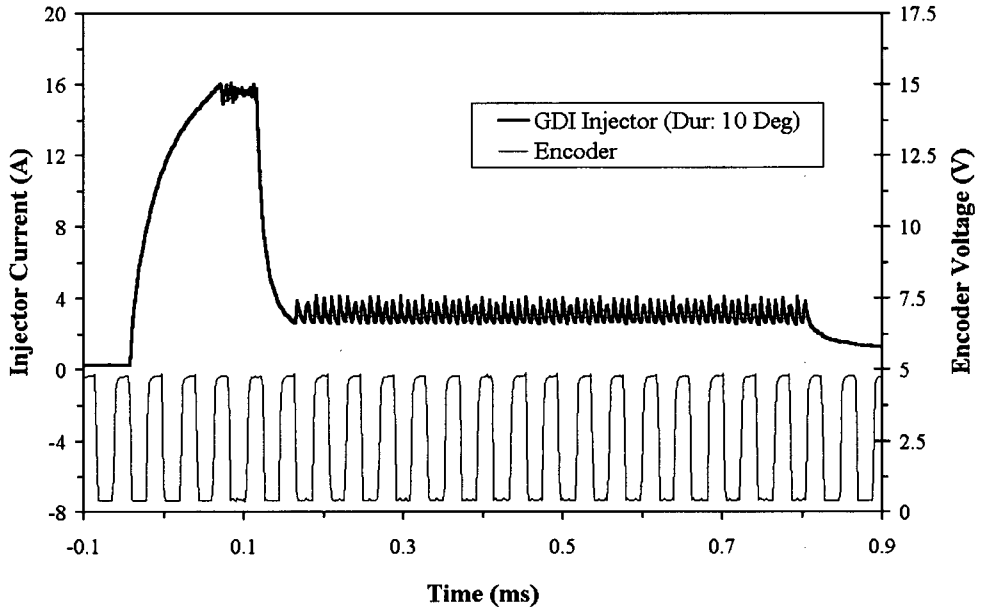

Figure 2.11: Gasoline PSC System Current Signal

2.3 Methodology

The research for this thesis was subdivided into two parts, corresponding to the natural gas and gasoline PSC tests respectively. The following indicators of improved engine performance were used to evaluate if PSC operation improved engine operation.

1. Increased brake mean effective pressure and reduced brake specific fuel consumption.

2. Extension of the lean misfire limit and reduced cycle-to-cycle variation under lean conditions.

3. Reduced ignition delay and burn duration.

4. Increased combustion pressures and heat release rates.

5. Reduced power-specific emissions in particular CO, HC and NOx.

All tests were performed at 2000 rpm, which is indicative of mid speed operating conditions for light or medium duty engines. This speed choice was driven by concerns with knock at lower engine speeds and issues with the PSC injection timing control at higher speeds. Load conditions varied according to test objectives. Start-up and set-up procedures for the engine and PSC systems are given in Appendices B and C.

2.3.1 Natural Gas PSC

The natural gas PSC tests were carried out to examine the feasibility of PSC on a primarily-gasoline-fuelled engine. The testing included examining the performance of the PSC system under lean and throttled conditions that would be encountered during normal

engine operation. Optimisation of the system was minimal and in most cases stemmed from the earlier research work performed on a pure natural gas engine by Reynolds (2001). For instance, the previous work indicated that injection timing around 10 degrees before the spark and PSC flow rates 20 g/h or greater, showed the best performance. A PSC injection pressure of 27 bar was chosen. In all cases the minimum advance for best torque (MBT) spark timing was used. This was carried out by advancing the spark beyond MBT and then gradually retarding it until a drop in torque was noticed. MBT spark timing would then be 0.5 to 1 degree earlier.

For the lean baseline tests the throttle was fixed and the engine gradually leaned out by reducing the main fuel flow, and test points taken incrementally until the lean limit was reached. These tests were performed both at full and part throttle conditions. In the case of the part throttle tests, the throttle was set so that 75% of the load at full throttle was achieved under stoichiometric conditions. This throttle position was then maintained for the remaining tests. For the throttled baseline tests, the air-fuel mixture was stoichiometric and the throttle position altered instead. Note that the throttle position does not correlate directly with engine load. The natural gas PSC tests followed the same procedures with the added complexity of changing the PSC injection parameters being investigated. Furthermore, only mixtures at or leaner than the homogeneous lean limit were tested with PSC, as previous work showed little improvement with richer mixtures. A test summary is given in Table 2.4.

Table 2.4: Natural Gas PSC Test Summary

Test Day	Type of Tests Performed	Throttle Position (%)	Relative Air-Fuel Ratio	PSC Injection Flow Rate (g/h)	PSC Injection Lead Timing (° Before Spark)
1	Lean baseline	100	0.95 – 1.35	-	-
	Lean PSC	100	1.3 – 1.45	49 – 59	5
	Lean PSC	100	1.3 – 1.45	50 – 62	10
2	Lean Baseline	100	1, 1.25 – 1.325	-	-
3	Lean Baseline	100	1	-	-
	Lean Baseline	53.5	1, 1.2 – 1.275	-	-
	Lean PSC	53.5	1.3 – 1.475	55 – 70	5
	Lean PSC	53.5	1.3 – 1.475	52 – 63	10
4	Throttled Baseline	20 – 100	1	-	-
	Lean PSC	100	1.275 – 1. 375	67 - 68	10
	Throttled PSC	40 – 100	1.375	72 - 77	10
5	Lean Baseline	100	1 – 1.3	-	-
	Dual Fuel Baseline	100	1.2 – 1.3	-	-
6	Lean Baseline	100	1	-	-
	Lean Baseline	53.5	1, 1.2 – 1.3	-	-
	Lean PSC	53.5	1.275 – 1.6	29 – 39	10

2.3.2 Gasoline PSC

The gasoline PSC tests were performed in much more detail and focused on a particular regime of operation. As there was some difficulty in optimising the gasoline PSC system, tests focussed on achieving a performance improvement around the homogeneous lean limit, where previous work had shown the greatest potential for combustion enhancement. A variety of injection parameters were changed including injection pressure, flow rate and timing to try and improve engine performance. The effect of spark plug reach was also investigated. The range of values attempted were limited by system design or resulted from the previous natural gas PSC tests. For instance, injection pressure was limited to a range of 21 – 41 bar by the GDI injector's design and the maximum pressure the flow metering device could withstand. The PSC flow rates on the other hand were based on the earlier natural gas PSC results. Unlike the

natural gas PSC tests, a spectrum of ignition timings around the lean homogeneous timing were studied while the injection timing was optimised to achieve best torque. This was done by first fixing the spark timing and advancing the injection timing significantly. The injection timing was then retarded until a peak torque value was achieved. This procedure was used, as there was some concern that the formation of the local charge stratification would be very sensitive to injection timing given the gasoline PSC system's design. All the gasoline PSC tests were done at full throttle. The lean baseline test points were performed in the same manor as the natural gas tests. A test summary is given in Table 2.5.

Table 2.5: Gasoline PSC Test Summary

Test Day	Type of Tests Performed	Ignition Timing (°BTDC)	Relative Air-Fuel Ratio	PSC Injection Flow Rate (g/h)	PSC Injection Pressure (bar)
1	Lean baseline	MBT	1, 1.3 – 1.375	-	-
	PSC	35 – 52.5	1.3	75	31
2	Lean Baseline	MBT	1, 1.3 – 1.35	-	-
	PSC	39 – 55	1.3	75	21, 31, 41
3	Lean Baseline	MBT	1, 1.275 – 1.35	-	-
	PSC	39 – 51	1.3	50, 90	21
4	Lean Baseline	MBT	1, 1.275 – 1.35	-	-
	PSC	39 – 51	1.3	50, 75	21
5	Lean Baseline*	MBT	1, 1.275 – 1.35	-	-
	PSC*	39 – 51	1.3	75	21, 31, 41

* - Used recessed plug.

Chapter 3
Analysis

3.1 Introduction

This chapter has been divided into two sections. The first section presents the procedures and calculations that were used for data analysis during this research. An analysis and discussion of experimental errors then follows with a particular focus on the operational parameters used to examine engine performance.

3.2 Analysis

Analysis of the raw data obtained from the Dyno and Pressure Clients is performed using a combination of spreadsheets that have been developed specifically for the task. These spreadsheets calculate a variety of key engine operational parameters and are used to plot and compare test results. The raw data is corrected for instrument calibration and environmental conditions. Definitions of the critical operational parameters used for analyzing engine performance follows. Unless otherwise stated, these definitions and the various equations used in this section are referenced from Heywood (1998).

3.2.1 Performance Analysis

The performance analysis is performed on the data acquired by the DynoClient. One hundred averaged measurements of engine speed, torque, air / fuel flow rates, temperatures and pressures were recorded at approximately one second intervals. This data is averaged and then used to calculate the relevant performance parameters relating to power output, fuel consumption and emissions.

The net mean effective pressure (MEP) is a measure of the work output of an engine normalized by its volumetric displacement. It is the average pressure, over which the complete engine cycle would result in the same net work output. Brake mean effective pressure (BMEP) is a measure of the useful work output from an engine measured from the crankshaft and thus includes friction losses. BMEP is calculated using the following equation:

$$BMEP = \frac{4\pi\tau}{V_d} \quad (3.1)$$

where V_d and τ represent the volumetric displacement and engine torque, respectively. In addition, BMEP is corrected for environmental conditions using the following equations (Taylor, 1985):

$$\frac{BMEP_2}{BMEP_1} = 1 + \frac{R_i - 1}{\eta_m} \quad (3.2)$$

$$R_i = \left(\frac{B_2 - \phi_2 P_{2H_20}}{B_1 - \phi_1 P_{1H_20}}\right)\left(\frac{T_1}{T_2}\right)^{\frac{1}{2}} \quad (3.3)$$

where "*1*" and "*2*" refer to the test conditions and corrected conditions, respectively. B_i and T_i refer to the barometric pressure and ambient temperatures, while ϕ and P_{iH20} are the relative humidity and saturated water vapor pressure. The mechanical efficiency (η_m) will be introduced in the section 3.2.2.

The brake specific fuel consumption (BSFC) is the mass flow rate of fuel used by the engine normalized by engine power output. BSFC is thus a measure of engine efficiency rather than just fuel consumption. As some of the tests performed used both natural gas and gasoline simultaneously, the fuel consumption is converted to a gasoline energy equivalent basis. The relevant equations are:

$$BSFC = \frac{\dot{m}_{fe}}{\dot{W}} = \frac{\dot{m}_{fe}}{2\pi\tau N} \qquad (3.4)$$

$$\dot{m}_{fe} = \dot{m}_{gasMAIN} + \dot{m}_{gasPSC} + \frac{q_{ng}}{q_{gas}}\dot{m}_{ngPSC} \qquad (3.5)$$

where $\dot{m}_{fe}$ is the gasoline equivalent fuel flow rate, q is the lower heating value of the fuel and N is engine speed.

Volumetric efficiency (η_v) is used to indicate the effectiveness by which air can be inducted into an engine and may be calculated as follows:

$$\eta_v = \frac{2\dot{m}_a}{\rho_a V_d N} \qquad (3.6)$$

where $\dot{m}_a$ is the mass flow rate of air and ρ_a the corresponding air density.

Exhaust gas emissions (Em), i.e. hydrocarbon (HC), carbon monoxide (CO) and nitrogen oxide (NOx), were calculated using SAE Recommended Practice J1088. All

emission molar concentrations were converted to a wet basis using the correction factor K where necessary. The significant equations are shown below:

$$[H_2\%_d] = \frac{0.5y[CO\%_d]([CO\%_d]+[CO_2\%_d])}{[CO\%_d]+3[CO_2\%_d]} \quad (3.7)$$

$$K = \frac{1}{1+0.005([CO\%_d]+[CO_2\%_d])y - 0.01[H_2\%_d]} \quad (3.8)$$

$$[Em\%_w] = K[Em\%_d] \quad (3.9)$$

In these equations H_2 and CO_2 are hydrogen and carbon dioxide, respectively. The hydrogen to carbon ratio of the fuel, y, is 1.824 for gasoline and 3.907 for natural gas. For the natural gas PSC tests an equivalent hydrogen to carbon ratio was determined by considering the hydrogen to carbon ratio contributions of each component on a percentage of total fuel mass basis. These values were then added to calculate the overall hydrogen to carbon ratio.

Once the wet emissions concentrations were established, Equation 3.10 was used to determine the mass flow rates $\dot{m}_{Em_w}$:

$$\dot{m}_{Em_w} = \frac{M_{Em}}{M_f}\frac{\dot{m}_f}{[CO\%_w]+[CO_2\%_w]+[HC\%_w]}[Em\%_w] \quad (3.10)$$

where M_{Em} is the molecular mass of the emission in question and M_f is the molecular mass of the fuel. In the case of HC emissions the molecular mass is assumed to be the

same as the molecular mass of the fuel and can be determined using Equation 3.11. The actual fuel flow rate corresponds to $\dot{m}_f$.

$$M_f = 12.011 + 1.008 * y \quad (3.11)$$

For nitrogen oxide emissions, a further correction factor KH was applied to Equation 3.10 to compensate for the effect of humidity. Using the specific humidity, *H,* the following equation resulted:

$$KH = \frac{1}{(1 - 0.0329(H - 10.71))} \quad (3.12)$$

As the final step, the individual exhaust emission mass flow rates, i.e. $\dot{m}_{CO_w}$, $\dot{m}_{HC_w}$, and $\dot{m}_{NOx_w}$, were inserted into Equation 3.13 to calculate the exhaust emissions on a brake specific basis (BSEm).

$$BSEm = \frac{\dot{m}_{Em_w}}{2\pi\tau N} \quad (3.13)$$

The major advantage of reporting on a brake specific basis and using mean effective pressures is that the resulting parameters are independent of power output and engine size, respectively. This allows engines of different size, design, etc. to be compared on an equal basis.

3.2.2 Combustion Analysis

The combustion analysis for this research is based on in-cylinder pressure and crank angle measurements recorded by the PressureClient application. One hundred cycles of pressure data at half-degree crank angle increments are obtained for each test point and are averaged to produce an average pressure cycle. Using Equation 3.14 the total in-cylinder volume V can be determined from the crank angle θ. Pressure-Volume and log Pressure-log Volume plots can then be created and compared to ideal and motoring cases.

$$V = V_c(1 + \tfrac{1}{2}(r_c - 1)(r + 1 - \cos\theta - (R^2 - \sin^2\theta)^{\frac{1}{2}})) \qquad (3.14)$$

Here V_c is the clearance volume, r_c the compression ratio, and r the ratio of connecting rod length to crank radius. Note that the slope of the compression and expansion processes on the log Pressure – log Volume plot also results in the polytropic indices for those processes.

The gross indicated mean effective pressure (GIMEP), a measure of the work transfer from the combustion gases to the piston during the compression and expansion processes only, can be calculated by integrating the Pressure-Volume diagram and normalizing it by the volumetric displacement.

$$GIMEP = \frac{\oint PdV}{V_d} \qquad (3.15)$$

The gross indicated mean effective pressure is related to the brake mean effective pressure as follows:

$$GIMEP = BMEP + FMEP \quad (3.16)$$

where *FMEP* is the friction mean effective pressure and is attributed to the work resulting from engine friction and pumping losses. The ratio of BMEP to GIMEP is referred to as the mechanical efficiency (η_m).

The chemical energy release during combustion (Q) can be approximated using the following equation resulting from a simple first law analysis:

$$\frac{dQ}{d\theta} = \frac{\gamma}{\gamma - 1} P \frac{dV}{d\theta} + \frac{1}{\gamma - 1} V \frac{dP}{d\theta} \quad (3.17)$$

As before, θ is the crank angle while γ is the specific heat ratio of the air-fuel mixture just prior to combustion. P and V are the in-cylinder pressure and total volume respectively. Note that this equation does not explicitly include heat transfer to the cylinder walls or crevice effects, i.e. it represents the net heat release rate. In addition, constant specific heats and ideal gas behavior are assumed. Integration of Equation (3.17) with respect to the crank angle results in the integrated heat release. When normalized by the total heat release from the combustion process, this produces a curve that indicates burn duration. Throughout this research the terms ignition delay and combustion duration are used to indicate the 0-5% and 5-95% total heat release, respectively.

The coefficient of variation (COV) of GIMEP, maximum in-cylinder pressure (PMAX) and the crank angle at which the maximum pressure occurs, (CA PMAX) can be found from a statistical analysis of the raw pressure data. The maximum pressure and corresponding crank angle are determined for each individual cycle and subsequently averaged to determine the overall PMAX and CA PMAX. In the case of the COV of GIMEP, Equation (3.15) is used to find the GIMEP for each cycle before the coefficient of variation is calculated. The key equations are listed below (Holman, 2001):

$$x_m = \frac{\sum_{i=1}^{n} x_i}{n} \qquad (3.18)$$

$$\sigma = \left[\frac{\sum_{i=1}^{n} (x_i - x_m)^2}{n-1} \right]^{\frac{1}{2}} \qquad (3.19)$$

$$COV = \frac{\sigma}{x_m} \qquad (3.20)$$

A COV of GIMEP of 5% was choosen to represent the lean limit (LL) based on qualitative observations, i.e. the onset of rough running, of the Ricardo Hydra's performance. For homogeneous lean mixtures this value worked out very well as the COV of GIMEP increased dramatically after this point, (refer to Figure 3.1). Traditionally a COV of GIMEP of 10% is used (Heywood, 1988). Note that this definition of the lean limit differs from the commonly used lean misfire limit, which is defined as the limit at which a certain number or frequency of misfires first occurs.

3.3 Error Analysis

There are two main issues concerning experimental error in measurements, namely, their accuracy and precision. Accuracy is defined as the deviation between a known value and the value indicated by an instrument. Precision on the other hand describes the ability of an instrument to consistently reproduce a reading within a given accuracy (Holman, 2001).

The performance of an engine is dependent on a large number of variables, many of which can only be controlled within a certain precision and may be changing during testing. Of particular concern here are the day-to-day changes in environmental conditions which not only affect engine performance but also the measuring devices themselves.

3.3.1 Accuracy

The data collected for a given sensor during each test actually consists of thousands of averaged data points. As a result, a high level of confidence can be placed in the output being the value actually seen by the instrument. This does not say that this value is accurate however. A true understanding of the accuracy of the measurement would require a though analysis of all the errors, i.e. sensing errors, systematic errors, random errors and so forth, that could potential affect it. As a first step, a simple uncertainty analysis can be performed using the uncertainty in instrument accuracy reported by manufacturers. Here, uncertainty is defined as the range in which the true value of a measurement in known to lie (Plint et. al, 1995). It is important to keep in mind that this is an ideal case, for instance, it does not take into account the change in

instrument calibration over time or even if the instrument is sensing the right quantity to begin with.

A mathematical procedure can be used to calculate the over uncertainty of a given operational parameter based on the uncertainty of the individual variables. The resulting equation is given in Equation 3.21 (Holman, 2001).

$$\omega_R = \left\{ \sum_{i=1}^{n} \left[\left(\frac{\partial R}{\partial z_i} \right) \omega_i \right]^2 \right\}^{\frac{1}{2}} \qquad (3.21)$$

In this formula, R, the operational parameter, is a function of independent variables $z_1, z_2, \ldots z_n$. Furthermore, ω_R and ω_i represent the uncertainty in the function R and of the independent variables, respectively. Using the brake mean effective pressure as an example, refer to Equation 3.1, the following relation can be derived for the uncertainty in BMEP (ω_{BMEP}):

$$\omega_{BMEP} = \left[\left(\frac{4\pi}{V_d} \omega_\tau \right)^2 + \left(\frac{4\pi\tau}{V_d^2} \omega_{V_d} \right)^2 \right]^{\frac{1}{2}} \qquad (3.22)$$

where ω_τ and ω_{Vd} is the uncertainty in the torque and the volumetric displacements. Uncertainties for the important operational parameters were calculated in this way and the results are given in Table 3.1 through 3.3. Table 3.1 includes results for homogeneous operation at $\lambda = 1$, $\lambda = 1.25$ and $\lambda = 1.3$ for both full and part throttle operating conditions. $\lambda = 1$ is indicative of a very stable and repeatable operational point,

while $\lambda = 1.3$ is at the lean limit of operation where cycle-to-cycle variation starts to become a concern. Table 3.2 contains uncertainty data for the operational parameters near the PSC lean limit ($\lambda = 1.45$). Uncertainties for the PSC tests would be expected to lye between these values and the corresponding value at $\lambda = 1.25$ during homogeneous operation. Table 3.3 shows uncertainty results for the throttled baseline tests. The calculated uncertainties for stoichiometric operation at 30% throttle were the highest encountered for all operational parameters, except BMEP.

For measurements of BMEP and BSFC the uncertainty in engine torque had the greatest effect on their overall uncertainty. In the case of the emissions parameters a combination of airflow measurements and emissions instrument uncertainty had the largest effect.

Table 3.1: Uncertainty – Lean Baseline Tests

	Uncertainty					
	Full Throttle			Part Throttle		
Operational Parameter	**$\lambda = 1$**	**$\lambda = 1.25$**	**$\lambda = 1.3$**	**$\lambda = 1$**	**$\lambda = 1.25$**	**$\lambda = 1.3$**
BMEP (bar)	0.15	0.14	0.14	0.14	0.14	0.14
BSFC (g/kWh)	4.9	5.9	6.2	6.6	8.2	9.4
BSCO (g/kWh)	0.6	0.5	0.5	0.6	0.5	0.6
BSHC (g/kWh)	0.2	0.3	0.3	0.2	0.3	0.5
BNOx (g/kWh)	na	1.6	1.3	na	1.2	1.0

Table 3.2: Uncertainty – PSC Tests

	Uncertainty	
	Full Throttle	**Part Throttle**
Operational Parameter	**λ = 1.45**	**λ = 1.45**
BMEP (bar)	0.14	0.14
BSFC (g/kWh)	6.7	10.1
BSCO (g/kWh)	0.5	0.6
BSHC (g/kWh)	0.4	0.5
BNOx (g/kWh)	0.5	0.9

Table 3.3: Uncertainty – Throttled Baseline Tests

	Uncertainty		
	100 % Throttle	**60 % Throttle**	**30 % Throttle**
Operational Parameter	**λ = 1**	**λ = 1**	**λ = 1**
BMEP (bar)	0.15	0.14	0.14
BSFC (g/kWh)	4.9	5.8	18.0
BSCO (g/kWh)	0.6	0.5	1.3
BSHC (g/kWh)	0.2	0.2	0.4
BNOx (g/kWh)	na	1.3	1.1

3.3.2 Repeatability

As mentioned previously, repeatability is of great importance to the work presented here as test data was acquired over a period of weeks. If baseline engine operation can be shown to be repeatable with in a certain range then any deviation occurring outside of this with the implementation of the PSC system is the result of the technology change. This allows an indication of performance benefits and disadvantages regardless of how accurate the operational parameters are.

Figures 3.1 through 3.6 contain data for COV of GIMEP, BMEP, BSFC, BSCO, BSHC and BSNOx, from the lean baseline tests performed during the natural gas PSC studies of this research. A qualitative inspection of these plots shows that the operational parameters, except perhaps BSNOx, are reasonably repeatable from day-to-day. (It is believed that an error was made in recording the fuel flow rate for the point at $\lambda = 1.2$ and 260 g/kWh on the BSFC plot). Table 3.4 and 3.5 display a statistical analysis of the lean baseline data at different relative air-fuel ratios. $\lambda = 1$ and $\lambda = 1.25$ represent test points which are easily reproduced, while $\lambda = 1.3$ on the other hand correspond to the lean limit of operation and larger variability may be expected. This statistical analysis not only includes errors associated with instrument precision but calibration, procedural and random errors of the entire measurement system as well. Furthermore, it would include the effect of some uncontrolled variables that change on a day-to-day basis. Error bars originating from the statistical analysis presented in Table 3.4 and 3.5 are included on Figures 3.1 through 3.6.

Table 3.4: Repeatability Analysis for $\lambda = 1$ and $\lambda = 1.25$

		$\lambda = 1$			$\lambda = 1.25$	
Statistic	**COV of GIMEP (%)**	**BMEP (bar)**	**BSFC (g/kWh)**	**BSHC (g/kWh)**	**BSCO (g/kWh)**	**BSNOx (g/kWh)**
Number of Test Points	8	8	8	8	4	4
Average	0.8	8.47	259.6	4.0	3.9	21.2
Standard Deviation	0.1	0.05	2.3	0.3	0.2	3.8
95% Confidence Interval	0.2	0.09	4.5	0.6	0.4	7.4

Table 3.5: Repeatability Analysis for $\lambda = 1.3$

	$\lambda = 1.3$					
Statistic	**COV of GIMEP (%)**	**BMEP (bar)**	**BSFC (g/kWh)**	**BSHC (g/kWh)**	**BSCO (g/kWh)**	**BSNOx (g/kWh)**
Number of Test Points	4	4	4	4	4	4
Average	5.2	6.78	252.8	5.2	4.0	16.6
Standard Deviation	4.1	0.06	2.2	1.1	0.4	2.4
95% Confidence Interval	8.1	0.11	4.3	2.2	0.8	4.7

3.3.3 Discussion

It is expected that the repeatability of any given test condition will be similar to those conditions presented here. Furthermore, the calculated uncertainties should give an indication of the accuracy of the various operational parameters over the range of test conditions. The only area of any concern would be the repeatability of the NOx measurements, which was poorer than expected. This was true, although the uncertainty analysis suggested that the measurements should be reasonably accurate. This may indicate that the reported NOx values are correct and that the large variations in NOx emissions may be a result of day-to-day changes in engine performance. The steep slope of the NOx data in Figure 3.6 illustrates that NOx is sensitive to the air-fuel ratio. Deviations in the air-fuel ratio set point could thus have a large impact on NOx emissions. Furthermore, NOx emissions are very sensitive to ignition timing, which itself is sensitive to environmental conditions (Heywood, 1988). The location of MBT during the homogeneous baseline tests were seen to vary as much as three degrees from day-to-day for a given test point.

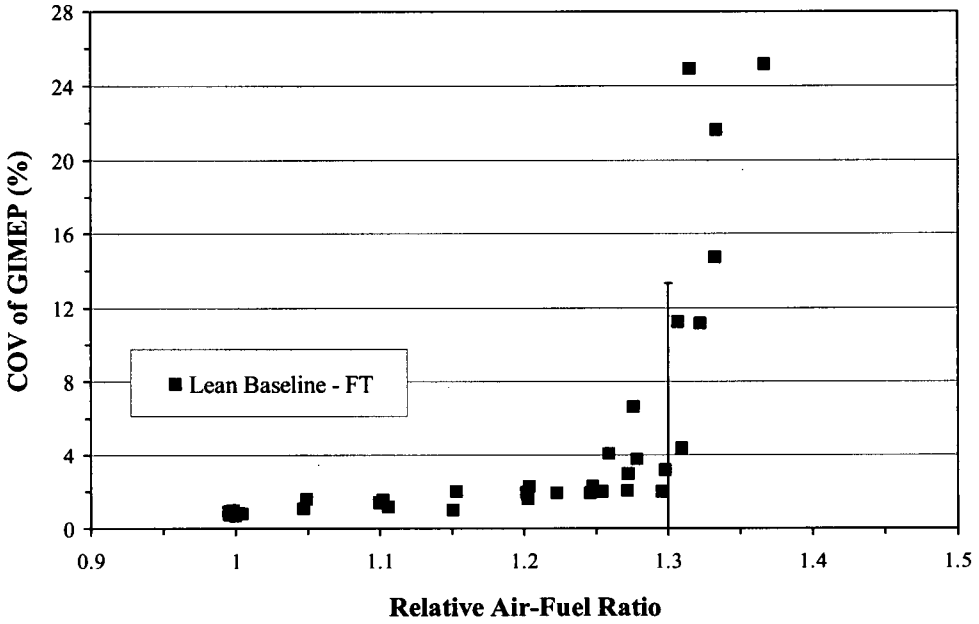

Figure 3.1: Coefficient of Variation of Indicated Mean Effective Pressure, Repeatability Study

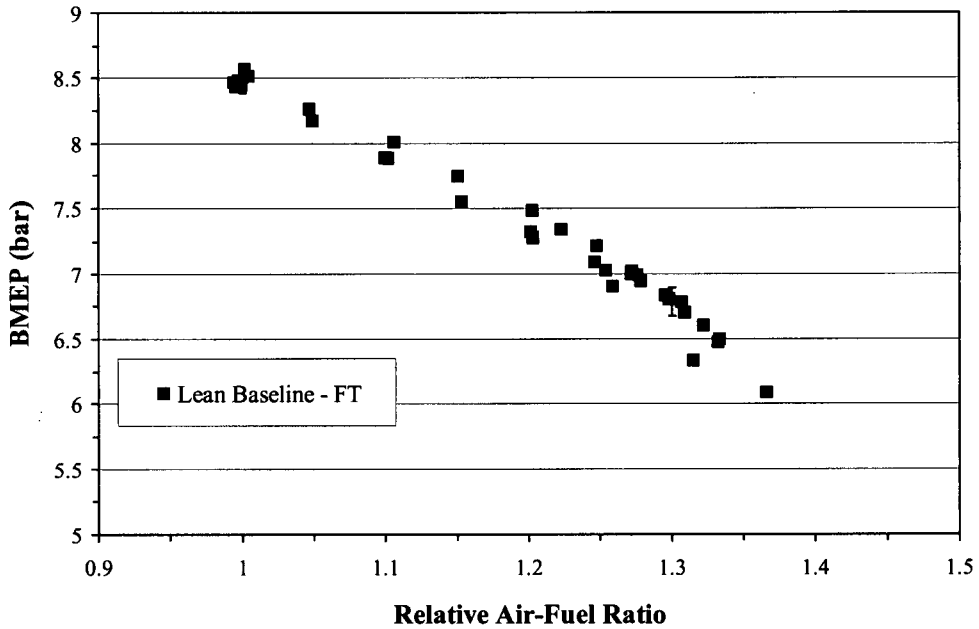

Figure 3.2: Brake Mean Effective Pressure, Repeatability Study

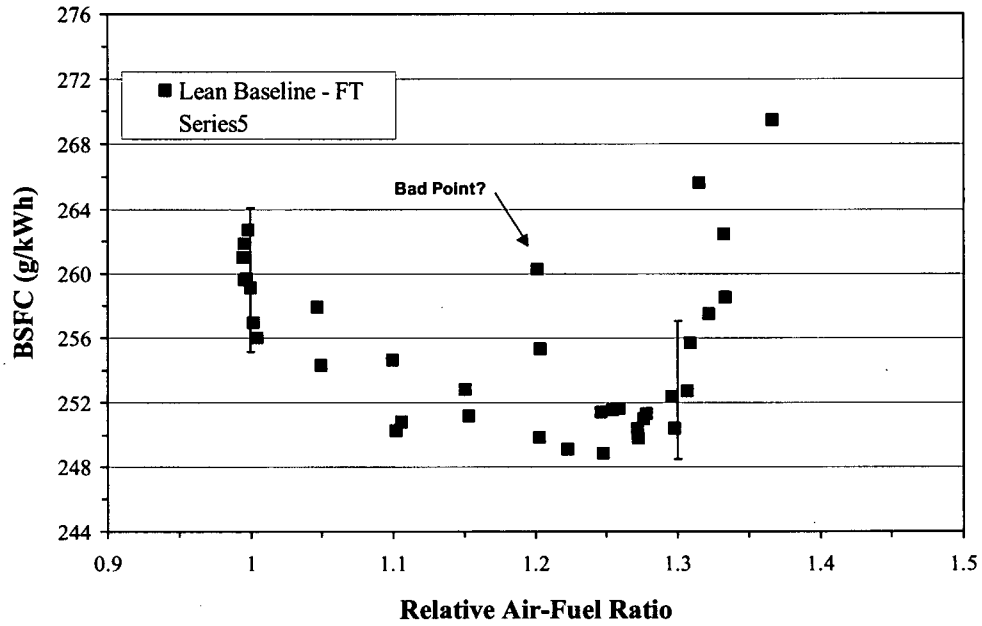

Figure 3.3: Brake Specific Fuel Consumption, Repeatability Study

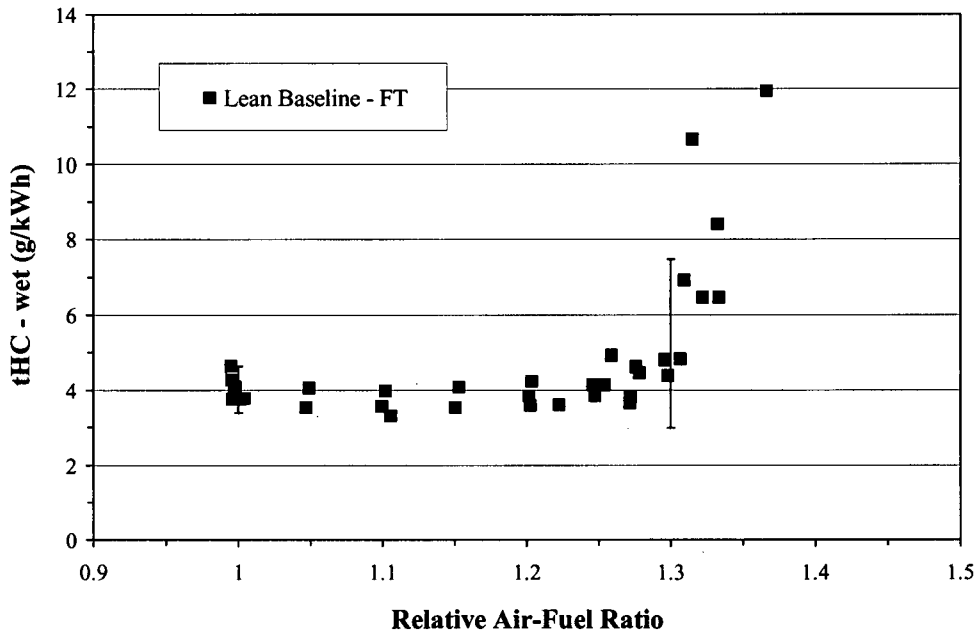

Figure 3.4: Brake Specific Hydrocarbon Emissions, Repeatability Study

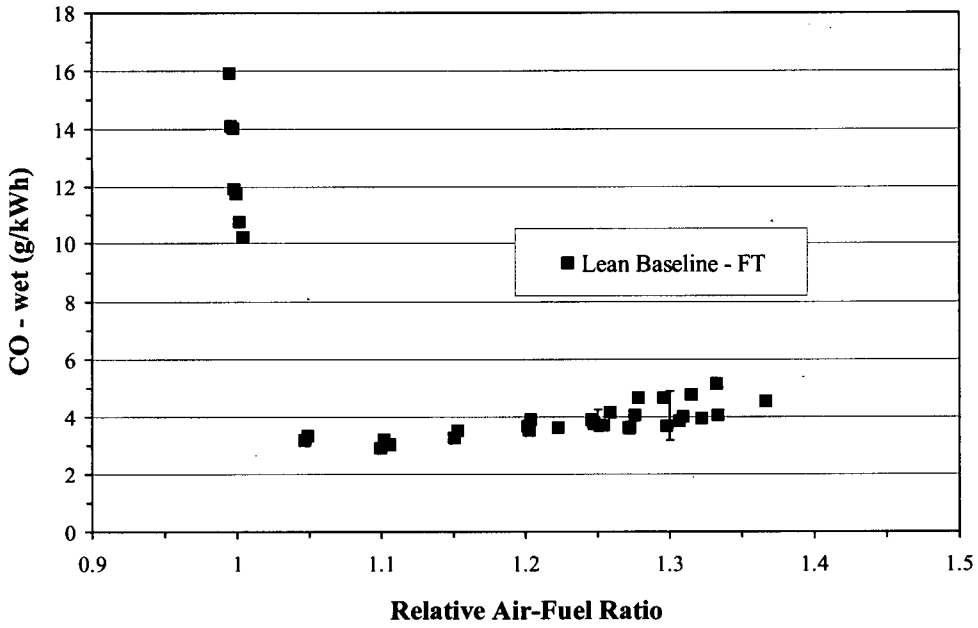

Figure 3.5: Brake Specific Carbon Monoxide Emissions, Repeatability Study

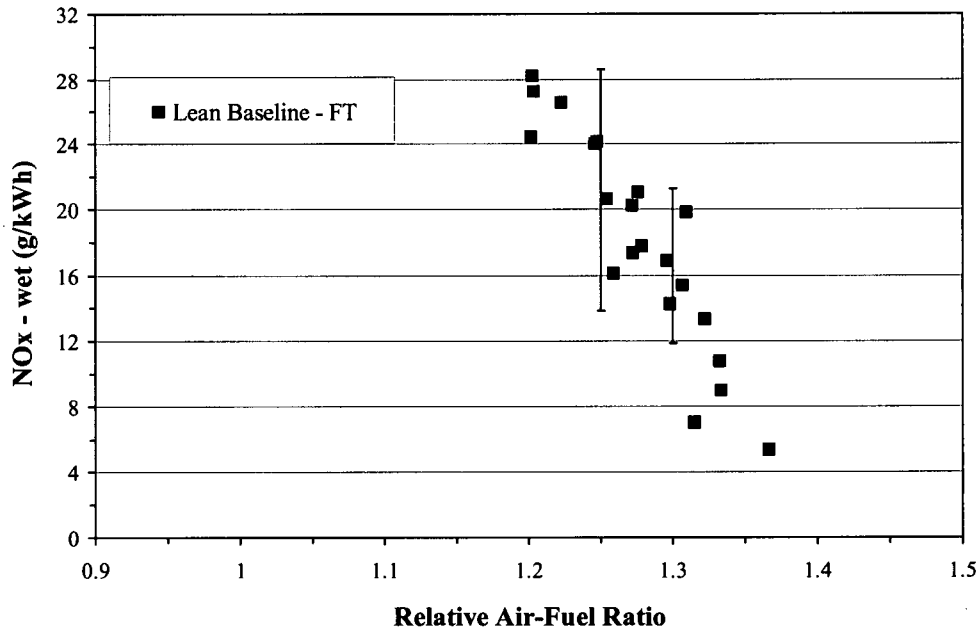

Figure 3.6: Brake Specific Nitrogen Oxide Emissions, Repeatability Study

Chapter 4
Results and Discussion

4.1 Introduction

The following section presents the detailed results of the partially stratified-charge tests previously outlined. For clarity, the results and discussion have been divided into two sections corresponding to the results of the natural gas and gasoline PSC tests respectively.

4.2 Natural Gas PSC Results

The natural gas PSC tests, with gasoline main fueling, were performed at 2000 rpm using a variety of load conditions. The majority of the tests were completed by gradually leaning out the overall air-fuel ratio, while maintaining a fixed throttle position. These tests were run with and without PSC to determine what effect the PSC system had on engine performance. A few different PSC flow rates and injection timings were also attempted to see what effect, if any, they had. A small number of tests, with and without PSC, were also performed by fixing the overall air-fuel ratio and throttling the engine instead. This procedure is analogous to current engine practice and would most likely be used in a commercial application of the PSC system.

4.2.1 Fixed Throttle Results

The implementation of the natural gas partially stratified-charge system resulted in a significant extension of the lean limit. This was further accompanied by a reduction in fuel consumption and an increase in power output for mixtures leaner than the homogeneous lean limit. Reductions in NOx emissions were achieved at the expense of

an increase in HC emissions with negligible changes in CO. Analysis of in-cylinder pressure data revealed an improvement in ignition delay, combustion duration, peak pressures and the COV of GIMEP when using PSC.

Two sets of tests were performed at full and part throttle, i.e. not fixed load, respectively. The throttle position for the part throttle tests was set so that it resulted in approximately 75% of the peak power output at 2000 rpm and $\lambda = 1$. For the natural gas PSC series the following nomenclature is used in the accompanying plots, PSC – *x* g/h – *y* Deg – PT/FT. Where *x* is the PSC flow rate, *y* is the injection lead-time relative to the spark and PT/FT represent part throttle of full throttle tests respectively. A range of PSC flow rates are given as there was limited incremental control of the flow rates from one test point to the next. The flow rate at any one-test point, however, was stable to within ± 2 g/h.

Using a COV of GIMEP of 5% as the cut off point, the lean limit (LL) was extended by approximately 15% (see Figure 4.1 and 4.11). For full throttle operation this corresponded to a LL extension from $\lambda = 1.275$ to at least $\lambda = 1.45$. Similarly, the LL was extended from $\lambda = 1.275$ to $\lambda = 1.475$ for part throttle operation. In addition to this extension, there was a drop in the COV of GIMEP for lean mixtures around the homogeneous lean limit. In the PSC case, the COV of GIMEP increased much more gradually as the lean limit was approached than in the homogeneous case. For example if a COV of GIMEP of 10% is chosen as the cut off point, the part- throttle lean limit is extended by 23% to $\lambda = 1.575$ for PSC operation. However, no change in the

homogeneous lean limit is observed with the change in the cutoff point. The effect of the PSC injection timing and flow rate on the COV of GIMEP was negligible.

As illustrated by Figure 4.2 and Figure 4.12, PSC operation results in similar or slightly greater BMEP compared to homogeneous lean operation. This is especially true beyond the homogeneous lean limit, where BMEP during homogeneous operation drops off due to increasing misfires and partial burning of the air-fuel mixture. BMEP appears to drop off almost linearly with the relative air-fuel ratio right out to the LL and beyond when using PSC. Once again, it appears that the PSC injection timing and flow rate has little or no effect on BMEP, at least in the bounds tested. The most significant observation here is that through the extension of the LL we are able to achieve much lower power outputs without further throttling. For the part throttle tests the LL extension resulted in a 1 bar decrease in BMEP. A similar reduction was also observed under wide open throttle conditions.

Changes in BSFC were apparent for mixtures beyond the homogeneous lean limit, (refer to Figure 4.3 and 4.13). These improvements may be a result of shorter burn durations and reduced cycle-to-cycle variability. Trends indicated that BSFC remained more or less constant for PSC operation up to some critical point after which it gradually increased. This critical point appeared to be around $\lambda = 1.35$ and $\lambda = 1.425$ for the part and full throttle tests, respectively, and may be a result of longer burn durations and an increasing number of non-optimum cycles. A non-optimum cycle, here, refers to a cycle whose ideal MBT timing is removed somewhat from the timing set for the average engine cycle. Non-optimum cycles will thus result in an IMEP loss. Lighter loads are

known to result in closer to stoichiometric critical points due to increased residual gas fraction and poorer combustion with increased dilution and reduced turbulence (Heywood, 1988).

As indicated by Figure 4.4 and 4.14, changes in CO emissions were negligible, although there was a slight drop when using PSC at the homogeneous lean limit. In general, CO emissions were shown to increase gradually with an increase in the relative air-fuel ratio. Slightly higher rates of increase are noticeable after the PSC lean limit. Carbon monoxide emissions tend to be very low under lean conditions due to the excess oxygen, which promotes oxidation. As very lean mixtures are approached and combustion deteriorates it is possible that unburned hydrocarbons in crevices as well as from oil layers and deposits are only partially oxidized (Heywood, 1988). This potentially explains the gradual increase in CO emissions observed with further leaning of the air-fuel mixture.

Hydrocarbon emissions increased somewhat with the use of local charge stratification as mixtures were made leaner. Usually, HC emissions are lowest for slightly lean mixtures, due to relatively high temperatures and excess oxygen, and increase rapidly for very lean mixtures, due to increasing cycle-to-cycle variability and partial burning (Heywood, 1988). The implementation of PSC results in an increase in HC emissions, even though cycle-to-cycle variability is reduced. This trend is shown in Figure 4.5 and 4.15. The source of the HC emissions may be attributed to locally rich combustion, a leaner homogeneous mixture, and low-pressure fuel from the PSC system entering the combustion chamber late in the expansion or during the exhaust process. For

the part throttle tests, higher PSC flow rates and reduced injection-ignition delay times led to higher HC emissions. This was most likely a result of more fuel burning rich and a reduction in mixing time.

NOx production is highly dependent on peak combustion temperatures and peak NOx concentrations occur for slightly lean mixtures where excess oxygen is available (Heywood, 1988). In the case of very lean mixtures, the excess air acting as a heat sink serves to lower peak combustion temperatures. While NOx emissions are similar for both PSC and homogeneous lean operation at a given air-fuel ratio, the ability to run leaner means PSC can reduce nitrogen oxides significantly. Figure 4.6 shows that during full throttle operation NOx can be reduced by nearly two-thirds from $\lambda = 1.275$ to $\lambda = 1.45$ with higher PSC flow rates. For part throttle operation a similar reduction in NOx, approaching 75% over the LL extension, is apparent for the higher PSC flow rates (see Figure 4.16). As fuel is removed from the main charge to achieve higher PSC flow rates it is believed that the leaner homogeneous charge is responsible for lowering combustion temperatures and thus lowering NOx emissions.

The results of the combustion analysis are given in Figures 4.7 through 4.10 for the full throttle tests and Figures 4.17 through 4.23 for the part throttle tests. Higher in-cylinder pressures are apparent with PSC operation. At $\lambda = 1.275$ peak pressures for part throttle operation are at least 5% higher with the PSC system and this value increases dramatically for leaner mixtures, (see Figure 4.17). More rapid combustion, closer to that of ideal constant volume combustion, is apparent in the P-V plot for PSC operation at $\lambda = 1.275$. Figures 4.7 and 4.18 reveal that maximum in-cylinder pressures are higher

with PSC in the vicinity of the LL. Furthermore, the peak pressure at the PSC lean limit is comparable to that at the homogeneous lean limit. Both Figures 4.8 and 4.19 illustrate that CA PMAX approaches TDC for PSC operation beyond the homogeneous lean limit. In contrast, CA PMAX appears to move slightly away from TDC with increasing air-fuel ratios for the homogeneous lean burn case.

As shown in Figures 4.20 and 4.21, higher heat release rates can be realized with PSC operation. At $\lambda = 1.275$, for instance, the peak heat release rate is approximately 20% greater for PSC at part throttle. In addition, heat release occurs earlier when pressures and temperatures are higher meaning more useful work can be extracted. Interestingly, the ignition delay with PSC at $\lambda = 1.475$ is less than that for homogeneous operation at $\lambda = 1.275$. Although this is true, the slope of the 5 – 95% heat release region is not as steep for PSC operation at $\lambda = 1.475$ as it is for homogeneous operation at $\lambda = 1.275$, indicating longer burn durations at this point. These observations are verified by Figures 4.22 and 4.23, which are plots of the 0% - 5% and 5% - 95% heat release, ignition delay and burn duration respectively, against the relative air-fuel ratio. At $\lambda = 1.275$ there is approximately a 12^{o} improvement in ignition delay and 5^{o} improvement in burn duration with PSC. As shown in Figures 4.9 and 4.10 this improvement is less pronounced under wide open throttle conditions where ignition delay and burn duration at the LL were up to 7^{o} and 4^{o} shorter, respectively. In general the combustion analysis performed supports the performance improvements observed with PSC operation.

4.2.2 Variable Throttle Results

Ideally, in a lean burn engine, it would be possible to control engine load without the use of throttling. In practice, however, the range of speeds and loads required of an engine makes this difficult to achieve. In most applications, manufacturers are interested in improving engine efficiency and emissions at a given load rather than a given air-fuel ratio. Throttled tests using PSC demonstrated the potential to reduce fuel consumption and NOx emissions at fixed loads when compared to both throttled stoichiometric and throttled homogeneous lean burn operation.

The throttled PSC test points were generated by first leaning out the air-fuel mixture under wide-open throttle conditions from $\lambda = 1.275$ to $\lambda = 1.375$. From here, the air-fuel ratio was fixed and the throttle gradually closed. A relative air-fuel ratio of $\lambda = 1.375$ was chosen because it represented about 50% of the total possible extension when using PSC and thus ensured low cycle-to-cycle variation, good emissions performance, and low fuel consumption. The air-fuel ratio and throttle position could be optimized further to meet specific targets if desired.

Figure 4.24 shows a plot of COV of GIMEP versus BMEP. (Note that throughout the variable throttle results the uncorrected BMEP is utilized). For all but the lowest load conditions PSC is able to maintain a COV of GIMEP below the 5% cut of point. For all cases PSC shows cycle-to-cycle variability equal to or lower than that achieved by throttled homogeneous lean operation but in general higher than that for throttled stoichiometric operation. Test points with a COV of GIMEP greater than 5% have been removed from the remaining plots for clarity.

The lower cycle-to-cycle variation of throttled stoichiometric operation comes at a great price when BSFC is considered, (refer to Figure 4.25). For a given BMEP, lean burn operation, with or without PSC, improves BSFC significantly. Reductions of 20 g/kWh can be seen under intermediate load conditions. There is also some indication that PSC shows a slight improvement in BSFC over lean stoichiometric operation under higher load conditions. As these points are at constant load, the improvement is strictly a result of reduced fuel consumption. Part of the reason for this efficiency improvement is the reduced throttling losses that accompany lean burn operation. This is illustrated in Figure 4.26 with a plot of volumetric efficiency versus BMEP. PSC operation leads to improvements of up to 15% and 5% in volumetric efficiency versus throttled stoichiometric and throttled lean homogeneous operation, respectively.

Perhaps the most important changes are in the engine emissions, (refer to Figures 4.27 through 4.29). Through lean burn operation, there is a drop of up to 75% in CO emissions at a fixed BMEP, although differences with and without PSC are small. In addition, the use of PSC and its leaner mixtures results in a decrease in NOx emissions over both its homogeneous lean and throttled stoichiometric counterparts. Between 4 and 6.5 bar BMEP, NOx emissions are at least 10 g/kWh less than that of throttled stoichiometric operation and about 5 g/kWh less than homogeneous lean operation. HC emissions are shown to increase for PSC operation. While this increase is negligible at higher loads, it is much more significant at lower loads and by 4 bar BMEP, there is an increase of about 50% over throttled stoichiometric operation.

4.2.3 Discussion

The PSC system allows for improved power output, driveability, and fuel consumption at fixed air-fuel ratios in the region of the homogeneous lean limit. In addition, a significant extension of the lean limit was observed. The improved engine performance was verified by combustion analysis of the in-cylinder pressure, which revealed shorter ignition delay and combustion duration. There were also higher in-cylinder pressures and reductions in cycle-to-cycle variability. These results indicate that the local stratification produced by PSC allows for more reliable ignition under lean operating conditions. Work by Arcoumanis et al. (1997) showed that the performance improvement of local stratification was a result of both changes in local flow characteristics and mixture properties from the local injection. This is also believed to be the case for PSC. Arcoumanis et al. (1997) found that the jet produced by their local injection help to convect and stretch the flame throughout the combustion chamber, increase local turbulence, as well as to provide a more ignitable mixture in the vicinity of the spark plug.

A separate issue is the homogeneity of the lean homogeneous mixture, which can suffer greatly from variability in mixture formation and in-cylinder flow conditions from cycle-to-cycle. In reality, homogeneous engines are heterogeneous, as full mixing does not occur. Depending on the degree of mixing it is possible to achieve slightly richer or leaner pockets throughout the combustion chamber. If one of these pockets is in the region of the ignition source it can serve to either promote or hinder the early stages of combustion. Work by Quader (1974,1976), showed a significant extension of the LL could be achieved by solely improving the homogeneity of the air-fuel mixture in a

homogeneous lean burn engine. This is an important fact to remember as the homogenous lean burn performance of the Ricardo Hydra could change dramatically with changes to its external mixture preparation.

A major focus of the research undertaken here has been on the extension of the LL. As mixtures are made leaner, flame speeds drop and combustion occurs more slowly. Eventually, partial burning occurs as flames are extinguished prematurely, due to dropping temperatures and pressures late in the expansion cycle. In some cases, no ignition occurs resulting in a misfire. In the tests performed here, there are indications that the lean air-fuel mixture is still burning effectively and that the homogenous LL is a limitation of flame initiation, not propagation, (refer to Figure 4.30 and 4.31). For homogeneous lean operation the first signs of misfire occur at $\lambda = 1.3$ which is shown by the two motored cycles around top dead center (TDC) in Figure 4.30. The onset of misfire occurs exactly with the homogeneous LL of $\lambda = 1.275$. Figure 4.31 demonstrates that in the case of PSC operation, the first signs of misfire do not occur until well after the LL at $\lambda = 1.6$. This is an indication that flame propagation is becoming the limiting factor for PSC operation. Flame propagation and flame initiation are related. However, there will be a point where the mixtures are too lean for a flame to propagate, no matter how much the PSC system and flame initiation are optimized.

The injection properties of the PSC system are also expected to have a significant effect on engine performance. The properties of interest here are the injection pressures, flow rates, timing, and air-fuel ratio of the injected mixture. When the PSC injection parameters were changed, only small changes in performance were observed. The

injection pressure used for testing was held constant at the highest possible with the current system (27 bar). High injection pressure was favored to ensure PSC flow at more retarded injection timings, i.e. when in-cylinder pressures are higher, and to prevent combustion gases from entering the PSC plug. High pressures could result in better jet penetration and mixing, but perhaps at the cost of more sensitive timing. In addition, higher pressures resulted in less flow variation as injection timing was changed. This may be attributed to the compressibility of the natural gas. Low pressures could result in much of the PSC charge entering the combustion chamber too late and being exhausted without being completely burned.

The flow rates that were used were based on previous work by Reynolds (2001), who found that flow rates below about 20 g/h of natural gas produced little or no performance improvement. Extremely high flow rates could result in large increases in THC and CO due to incomplete combustion and would remove more and more fuel from the main charge. Higher flow rates during testing, up to 70 g/h, appeared to improve NOx performance and there was some indication of improved BSFC. The PSC flow rate was limited to 4 stable increments below 70 g/h.

The effect of injection timing relative to spark timing appeared to be negligible for the few test cases investigated. It is certainly possible that changing the injection timing, within a reasonable range, would not affect PSC performance. Enough time must be allowed for injection and mixing of the fuel to take place, but not so much that the local stratification moves away from the ignition source. In some qualitative tests, PSC

appeared to work for injection timings as early as 15 degrees before the spark and as late as 10 degrees after.

In all the tests performed, the locally stratified mixture was pure fuel. It is assumed that this fuel burned under rich conditions, potentially resulting in the higher HC emissions found during testing. Using a premixed stoichiometric or slightly rich mixture may actually serve to reduce emissions and improve combustion compared to the injection of pure fuel. Further work will be required to fully examine and optimize all the PSC injection parameters and thus maximize the performance of the PSC system.

The effect of injecting natural gas rather than gasoline into the engine needs to be addressed. The two fuels are different in many respects and there are potential advantages for each. Gasoline, unlike natural gas, is a liquid fuel and must be first atomized and then vaporized before proper mixing and combustion can occur. Natural gas diffuses at a much faster rate than vaporized gasoline and a greater degree of homogeneity may thus be expected. Adjustments for mixture preparation in the cylinder and to the PSC injector/spark plug itself could be made to compensate for mixture problems with gasoline, however. One possible solution would be to use air assisted direct injection of slightly rich mixtures, for instance.

The lower heating value of natural gas is approximately 49,000 kJ/kg versus that of gasoline, which is around 43,000 kJ/kg; adjusting the flow rates to achieve the same energy release negates this, however. The lower and upper flammability limits for gasoline are approximately $\lambda = 1.7$ to $\lambda = 0.2$, versus $\lambda = 1.8$ and $\lambda = 0.6$ for natural gas.

The significantly greater rich flammability limit of gasoline could potentially result in better PSC combustion with very rich locally stratified mixtures provided, good atomization and vaporization of the fuel takes place. Under some conditions, laminar flame speeds for rich gasoline mixtures are greater than those for natural gas mixtures (Heywood, 1988). Furthermore, the ignition delay and minimum ignition energies in air are generally less for gasoline mixtures. Table 4.1 presents a list of important natural gas and gasoline properties.

Perhaps the most important thing to keep in mind with the test results presented here is that the total amount of fuel injected using the PSC system is less than 10 % of the total fuel flow. As a result, it is very unlikely that the use of natural gas rather than gasoline for the PSC system would significantly impact the overall engine performance in any way. The effect on emissions on the other hand may be more significant. A simple test was performed to see if the presence of an equivalent amount of natural gas in the main homogeneous lean mixture, approximate 50 g/h, produced any significant performance improvements. The tests revealed no extension of the LL or improvements in BMEP, (or any other performance indicators), when compared to homogeneous lean gasoline operation. There were also no significant changes in NOx or HC emissions with the addition of the natural gas into the main homogeneous mixture. The results of these tests are shown in Figures 4.32 through 4.36.

Table 4.1 : Fuel Properties

Property	Gasoline	Methane
Molecular Weight (g/mole)	≈ 110[2]	16.04[2]
Hydrogen to Carbon Ratio (mole/mole)	1.60 - 2.10[1]	4.00
Boiling Point[4] (K)	310 – 478[3]	111.6[3]
Diffusion Coefficient	0.05[3]	0.61[3]
Enthalpy of vaporisation (kJ/kg)	309[3]	na
Lower Heating Value (MJ/kg)	42– 44[1]	50[2]
Flammability Limits (% Volume in Air)	1.4 – 7.6[1,3]	5.3 - 15[3]
Minimum Ignition Energy in Air (mJ)	0.29[3]	0.24[3]
Flame Temperature in Air (K)	2470[3]	2148[3]
Octane Number (Research)	91 - 99[2]	120[2]
Octane Number (Motor)	82 - 89[2]	120[2]
Stoichiometric Air-Fuel Ratio (% Volume in Air)	1.76[3]	9.48[3]
Stoichiometric Air-Fuel Ratio (By Mass)	14.3 – 14.8[1]	17.23[2]

[1] SAE J312
[2] (Heywood, 1988)
[3] (Hord, 1978)
[4] Normal Boiling Point

Lean throttled operation shows a large improvement over throttled stoichiometric operation in virtually every important measurement of engine performance. Of particular importance is the improved fuel efficiency and lower exhaust emissions that accompany lean burn engine operation (Germane et al., 1983). The problem with lean burn engines has been, at least up until recently, the design and development of lean burn catalytic converters (although improved, engine emissions are still too high to avoid the use of a catalytic converter). Conventional 3-way catalytic converters operate around stoichiometric air-fuel ratios to maximize the oxidation of HC and CO as well as the reduction of NOx. Lean burn operation however, diminishes NO catalytic conversion due

to an excess of oxidizing species in the exhaust stream, thus potentially increasing NOx emissions relative to stoichiometric operation. One viable alternative is to control NOx by running the engine very lean and utilize a 2-way oxidation catalyst or thermal reactor to further reduce HC and CO emissions. This could save the costs of using a lean burn 3-way catalytic converter and provide the fuel efficiency benefits of lean operation. Regardless of whether a 2-way or 3-way catalyst is used, lean burn operation will reduce emissions at the source and thus lower overall emissions levels may be expected with proper engine development.

The throttled PSC tests indicate that the advantages of the PSC system are the improvements in NOx emissions and perhaps some improvements in efficiency over the current lean burn strategy. The improvements in NOx emissions are a result of burning leaner mixtures. The improvements in combustion are most likely realized as higher average in-cylinder temperatures, but lower peak temperatures. (NOx emissions are highly dependent on the peak in-cylinder combustion temperatures). As with nearly every other stratified technology, increased HC emissions with PSC operation have proved to be a problem, though perhaps not to the same extent, due to the greatly reduced stratified volume. The increase in HC emissions is most likely a result of rich combustion of the locally stratified-charge, a leaner main charge, and quenching of the flame in the PSC plug. Furthermore, low pressure, unburned fuel from the PSC injection may leak out during the expansion and exhaust strokes.

4.3 Gasoline PSC Results

Initial studies of the gasoline partially stratified-charge system indicated reduced engine performance under lean conditions. This contradicted earlier studies with the natural gas PSC system and an attempt was made to optimize the PSC injection parameters to see if any performance improvements could be realized. Tests examining the effects of the PSC flow rate, injection pressure and spark plug location were performed at 2000 rpm and wide-open throttle conditions. These tests were done by fixing the relative air-fuel ratio near the homogeneous lean limit ($\lambda = 1.3 +/- 0.01$) and varying the above injection parameters over a range of spark timings. The injection timing was adjusted to achieve maximum torque in all cases.

Even with optimization of the PSC system, no significant improvements were observed over homogeneous lean operation. All major performance indicators showed a reduction in engine performance and were supported by an equivalent deterioration in in-cylinder combustion measurements. A variety of important trends were observed however, and with qualitative observations of the systems' operation, provided great insight into the problems with the system and where improvements needed to be made. For the gasoline PSC series, the following nomenclature is used in the accompanying plots, PSC – x g/h – y bar. Where x is the PSC flow rate and y is the PSC injection pressure.

The BMEP, BSFC and COV of GIMEP results of the homogeneous lean baseline tests are given in Figure 4.37 through 4.39. These results are similar to those obtained during the natural gas studies and are presented for reference. The slight deviations in

these performance parameters, compared to the natural gas baseline tests, are a result of a change in spark plug type. For instance, the location of the lean limit for this set of tests is $\lambda = 1.35$ rather than $\lambda = 1.3$ for the natural gas studies. In addition, the BMEP and BSFC results are slightly better than those recorded during the natural gas PSC studies. This change in baseline performance is a direct result of a change in spark plug type. The results from two different spark plug positions are also shown in Figure 4.37 through 4.39. The recessed plug is the identical plug that is used for all other gasoline PSC tests, but utilizes a 1.5 mm washer to reduce penetration into the combustion chamber. The use of the recessed plug results in a noticeable reduction of performance at lean air-fuel ratios compared to the original spark plug configuration.

4.3.1 Injection Pressure

In Figures 4.40 through 4.42, there is trend towards poorer performance with increased injection pressures and in almost all cases the performance is worse than under homogeneous condition. (Note that the injection flow rates could be maintained with in +/- 2 g/h and that the range of injection pressure was limited by system components). There is a definite shift towards earlier ignition timings, some 6 to 10 degrees earlier, for best performance when using PSC. The performance of PSC falls off rapidly with retarded timings and indicates the importance of locating the minimum advanced for best torque (MBT). As shown in Figure 4.43, better CO emissions are apparent with retarded timings for PSC operation. The opposite is true for HC emissions, (see Figures 4.44). In the region of the best PSC performance, i.e. best BMEP and BSFC, CO and HC emissions are as much as 50% higher than homogeneous operation and stay higher even with dramatic changes in spark timing. Higher injection pressure also has a negative

effect on CO emissions and the effect becomes more pronounced as ignition timings are retarded. In general, CO emissions are reduced with earlier ignition timing as peak temperatures are higher and oxidation occurs more readily. Increased oxidation of hydrocarbon emissions during the expansion and exhaust strokes are known to occur for retarded spark timings. This is due to a decrease in work transfer from the combustion gases causing higher exhaust temperatures and thus more favorable conditions for oxidation of HC emissions (Heywood, 1988).

The results of the combustion analysis are illustrated by Figures 4.45 through 4.47. The effect of injection pressure, at fixed ignition timing, appears to be minimal even though engine performance changed. Ignition timing, however, did have a more significant effect. Retarded ignition timings resulted in reduced ignition delay, increased burn duration and lower peak pressure. This is expected as initial pressure and temperatures are higher for more retarded ignition timings. However, the later ignition timing means that increasing amounts of heat release occur when pressure and temperatures are falling during the expansion stroke. What is important is that, in all cases, the burn duration and ignition delay was longer for PSC than for homogeneous operation.

4.3.2 Injection Flow Rate

Of the PSC parameters investigated, injection flow rate had the most significant impact on performance. The injection flow rate tests were undertaken at 21 bar as this pressure showed the best performance from the injection pressure tests. Figures 4.48 through 4.50 reveal that the best PSC performance was achieved with the lowest PSC

flow rate, 50 g/h, and that PSC performance approached homogeneous lean performance as flow rates were reduced. Once again, more advanced ignition timings, in the range of 6 to 10 degrees, produced the best PSC results. Hydrocarbon and carbon monoxide emissions were shown to have a strong dependence on PSC flow rates, with higher flow rates resulting in higher emission levels in both cases, (refer to Figures 4.51 and 4.52). At an ignition timing of 51 degrees before top dead center, the region of optimum PSC ignition timing based on BMEP and BSFC, HC and CO emissions increased by roughly 40% with a flow rate increase from 50 g/h to 90 g/h. These emission values were approximately 50% higher than those achieved with homogeneous operation at MBT timing. Emission trends as a function of spark timing, were similar to that observed with the injection pressure tests.

The effect of injection flow rate on combustion parameters was also clearer than the injection pressure tests, (see Figures 4.53, 4.54 and 4.55). In nearly every case, lower PSC flow rates resulted in higher combustion pressures, as well as shorter ignition delays and burn durations. The peak pressure, burn duration and ignition delay for PSC operation, about the baseline MBT timing, appeared to approach that of homogeneous lean operation with lower flow rates. As in the injection pressure tests, retarded ignition timings resulted in reduced ignition delay, increased burn duration and lower peak pressure.

4.3.3 Spark Plug Position

There was a strong indication after the injection pressure and flow rate tests that the bulk of the local charge stratification was not occurring in the region of the ignition

source. A recessed spark plug was thus implemented on the premise that it would be less likely to encounter the local charge stratification, and thus have a larger effect on PSC operation than it would on homogeneous lean operation. The results of these tests, shown in Figures 4.37 through 4.39, indicated that the use of the recessed plug resulted in a slight performance decrease for homogeneous lean operation. This was realized as deterioration in BSFC and BMEP, as well as a richer lean limit.

The effect of using the recessed plug on the PSC results was dramatic, especially for more advanced timings, (refer to Figures 4.56, 4.57 and 4.58). As would be expected, more advanced timings result in lower pressures and temperatures during ignition, thus a greater amount of spark energy is required for proper ignition to occur and ignition is less reliable (i.e. COV of GIMEP goes up). The best performance was realized for ignition timings in the range of 39 to 43 degrees before top dead center. Compared to the normal plug at its best spark timing, BMEP dropped by roughly 5% with a similar increase in BSFC. The changes in homogeneous lean operation were much less pronounced with only a slight decrease in BMEP and increase in BSFC.

The results of the combustion analysis, presented in Figures 4.59 through 4.61, supported the performance loss when using the recessed plug. PSC ignition delay and peak pressures are worse for the recessed plug with advanced timings, however, the difference is negated with retarded timings. The 5 – 95% burn duration remains similar for both plug configurations under PSC operation. Comparing the best performance cases for the normal and recessed plug under PSC operation there is at least a 10 % reduction in maximum pressure and a 8 degree increase in ignition delay. Overall, the effects of the

recessed plug on lean homogeneous performance and in-cylinder combustion properties did not appear quite as significant as they were for PSC.

4.3.4 Discussion

Poor engine performance suggests that the current gasoline PSC system is unable to achieve local charge stratification in the region of the spark plug. This conclusion is supported by a number of observations.

Firstly, when the PSC system is run at the homogeneous lean limit and the system is turned off the engine begins to misfire frequently or not run at all. This suggests that fuel is getting into the engine at roughly the right time. A wide range of injection timings and pressures were attempted regardless and observations of injector response indicated that the actual injector timing agreed well with control settings. Furthermore, with the PSC system activated there is an increase in HC and CO emissions, which is a good indication that not only is the fuel entering the combustion chamber, but that a rich region may exist in the combustion chamber. Higher PSC flow rates caused higher HC and CO emissions, most likely due to the excess fuel concentration, increased wall wetting and limited oxygen availability in the fuel rich region. If this rich region or pocket is not in the vicinity of the ignition source, combustion will initiate utilizing the lean homogeneous mixture, which fills the rest of the combustion chamber.

Because some fuel is injected through the PSC system, the lean homogeneous mixture that remains is actually leaner than that during normal homogeneous lean operation. Longer ignition delays and burn durations result from this leaner mixture, as

previously shown. Higher flow rates also compound this problem and result in a corresponding deterioration in performance. Improved performance with low injection pressures, on the other hand, may be a result of better mixing. This may be due to greater distribution of the rich pocket from longer injection pulse widths.

The results of the tests with the recessed spark plug were inconclusive. The performance of the recessed plug was similar to the original plug for retarded timings but not for more advanced timings when using PSC. Generally for the optimum cases, the effect of the recessed spark plug on PSC performance was greater than it was on homogeneous charge performance.

Perhaps the most interesting evidence came upon disassembly of the engine during which observations of the combustion chamber were made. Figures 4.62 through 4.64 show the piston crown, PSC plate and cylinder head after disassembly. Although extensive testing was performed under homogeneous lean conditions, there was a significant build up of carbon deposits around the outlet of the PSC injector port and on a section of the piston top. In contrast, the remaining surface area of the combustion chamber, including the cylinder head and spark plug, remained light brown or white indicating extensive lean combustion. These deposits are believed to be a result of locally rich combustion and wetting of the nearby surfaces by the liquid fuel spray, (which could lead to higher CO and HC emissions).

While not representative of the complicated flow conditions inside a working engine, observations of the injector spray pattern and penetration were made with the engine disassembled. With differential pressures similar to in-cylinder conditions, it

quickly became apparent that only a small portion of the injected fuel could reach the spark plug electrodes. The bulk of the spray cloud appeared to be approximately 1 - 1.5 cm away from the spark plug with a noticeable re-circulation, which resulted in wall wetting around the injector port. This wall wetting coincided quite well with the deposits mentioned earlier.

With the cause of the poor performance of the gasoline PSC system identified, the next questions are 1) what can be done to improve it, and 2) what sort of performance benefits would be seen? The second question can be partially answered by the positive results of the natural gas PSC tests and certainly with refinement, further improvements would be realized. As far as the first question is concerned, the first step, perhaps obviously, will be to ensure that the local charge stratification reaches the ignition source at the correct time.

Unlike gaseous fuels, gasoline must be first atomized, vaporized and mixed with air before proper combustion can occur. This puts some limitations on how gasoline is injected into the combustion chamber. The simplest solution to the first question posed above is to retrofit the current PSC plate so that the outlet of the injector is closer to the spark plug. Another option would be to design the gasoline direct injector into the spark plug itself, as originally proposed. This would result in a spark plug-injector similar to that currently used in the natural gas PSC system. A spark plug-injector design would ensure that at least some fuel was available in the region of the spark, but careful attention would have to be paid to make sure proper atomization, vaporization and mixing occurred. Perhaps the best solution in the foreseeable future would be to integrate

an air assisted direct injector with the spark plug. This technology exists, at least in a prototype stage, in Saabs' Spark Plug Injector (SPI^{TM}), which is based on Orbital Engine Corporations' Combustion Process (OCP^{TM}) technology. This technology has been implemented into a gasoline direct injection engine, but there is no evidence that it has bee used for local charge stratification. Should such a technology be integrated into the PSC system it would provide a well-atomized and well-mixed spray cloud for local charge stratification.

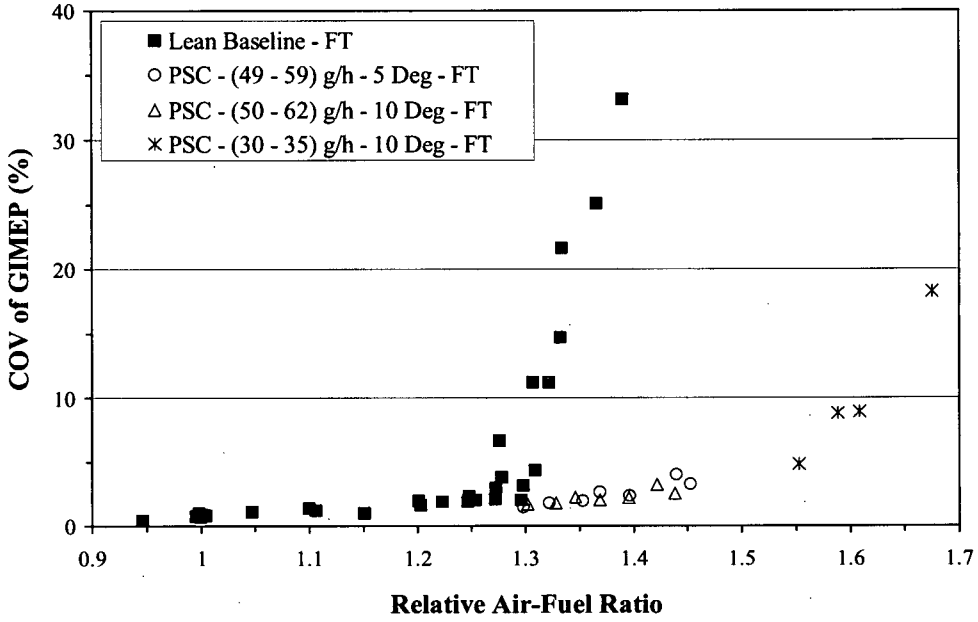

Figure 4.1: Coefficient of Variation of Indicated Mean Effective Pressure, Full Throttle

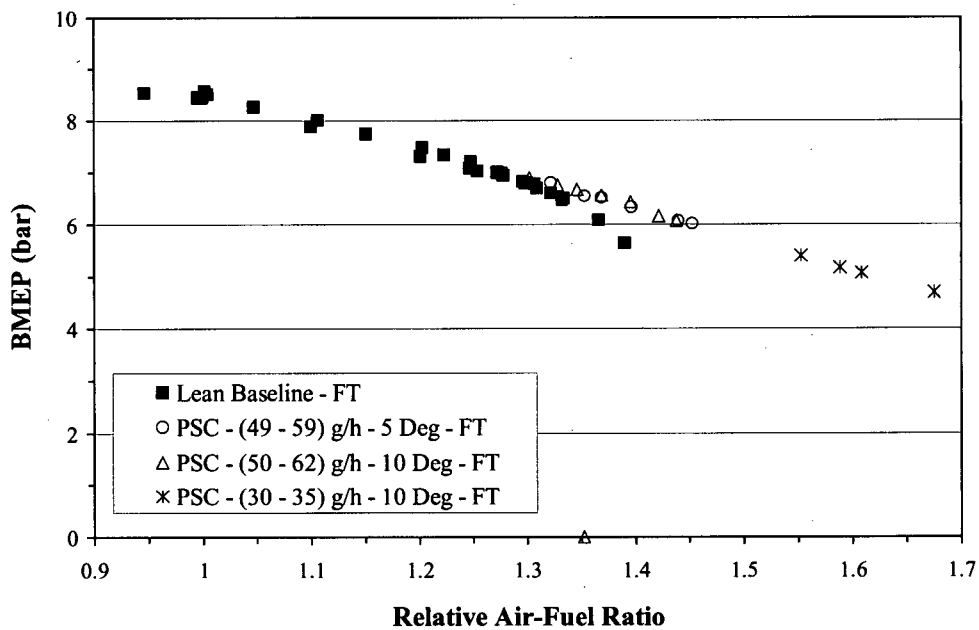

Figure 4.2: Brake Mean Effective Pressure, Full Throttle

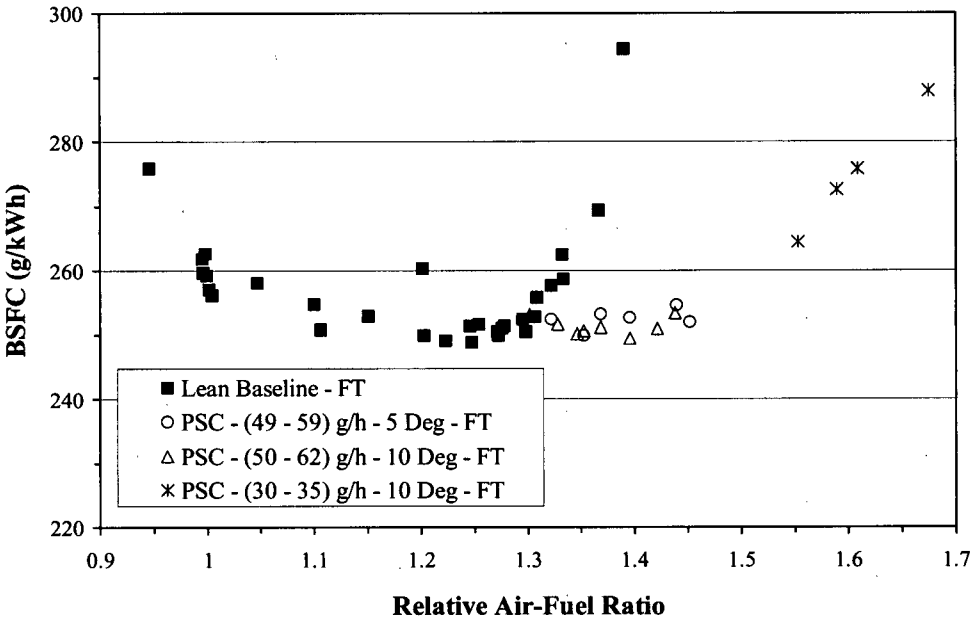

Figure 4.3: Brake Specific Fuel Consumption, Full Throttle

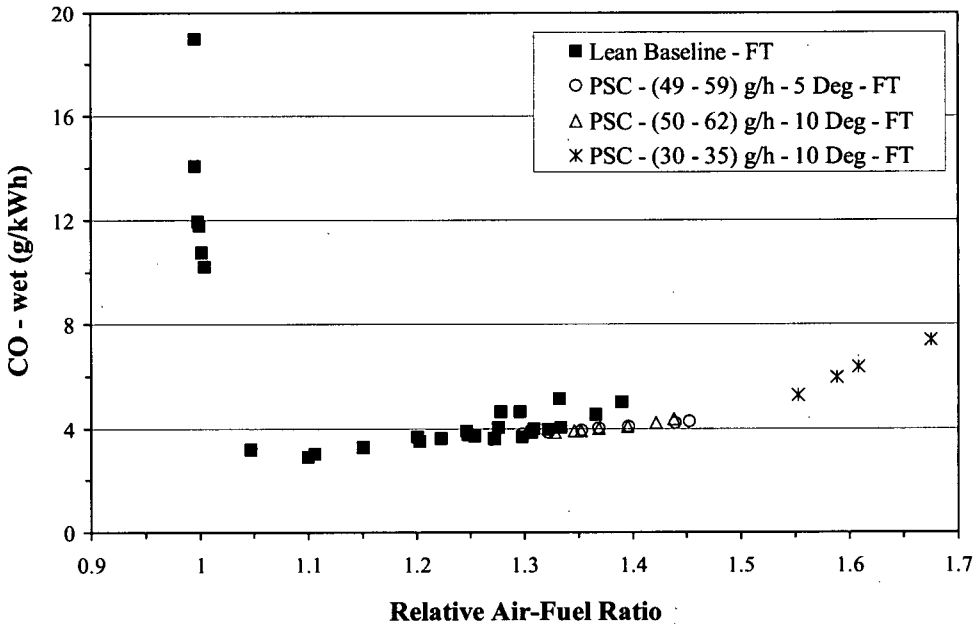

Figure 4.4: Brake Specific Carbon Monoxide Emissions, Full Throttle

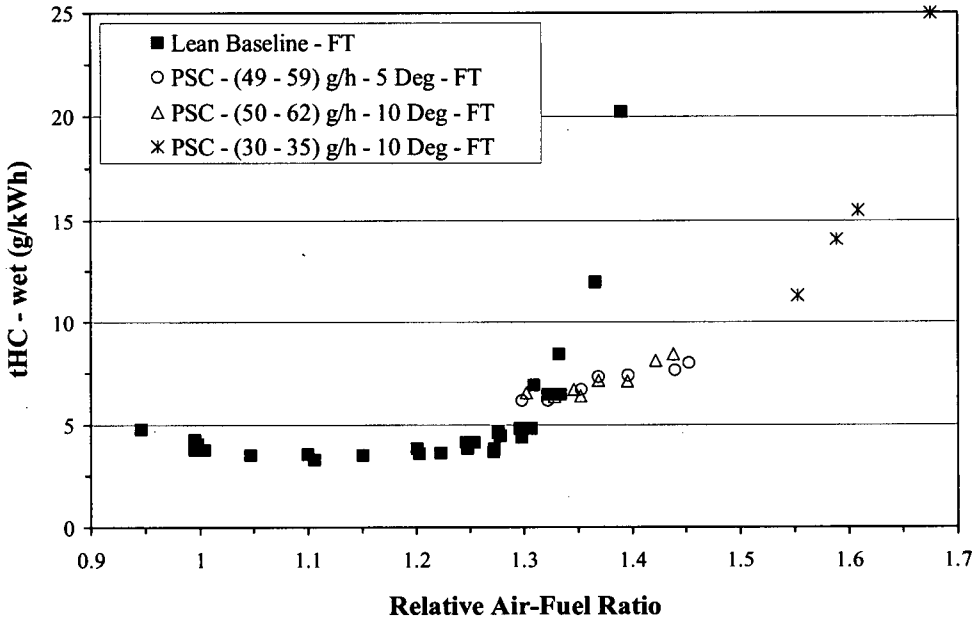

Figure 4.5: Brake Specific Hydrocarbon Emissions, Full Throttle

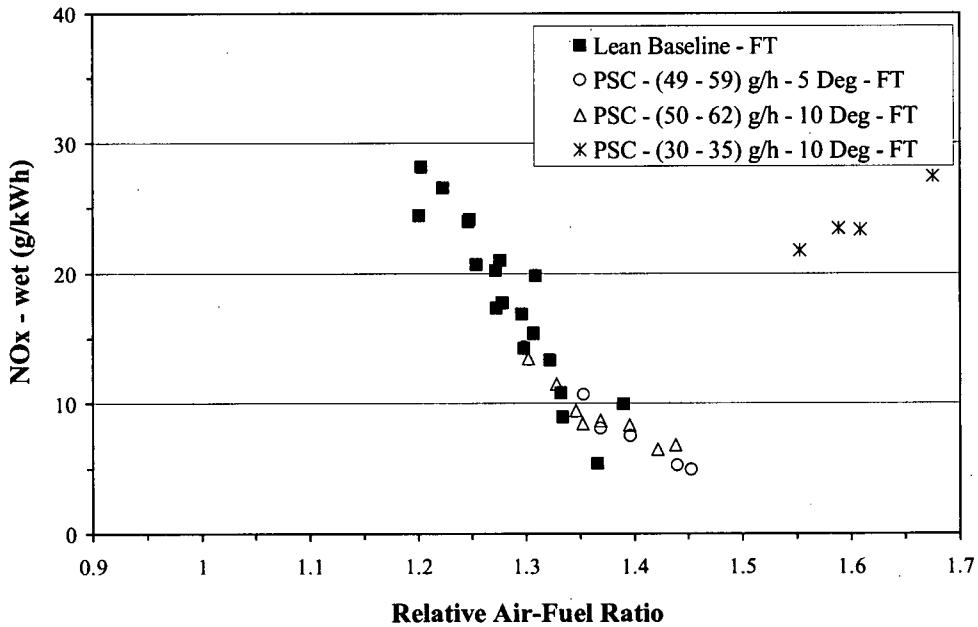

Figure 4.6: Brake Specific Nitrogen Oxide Emissions, Full Throttle

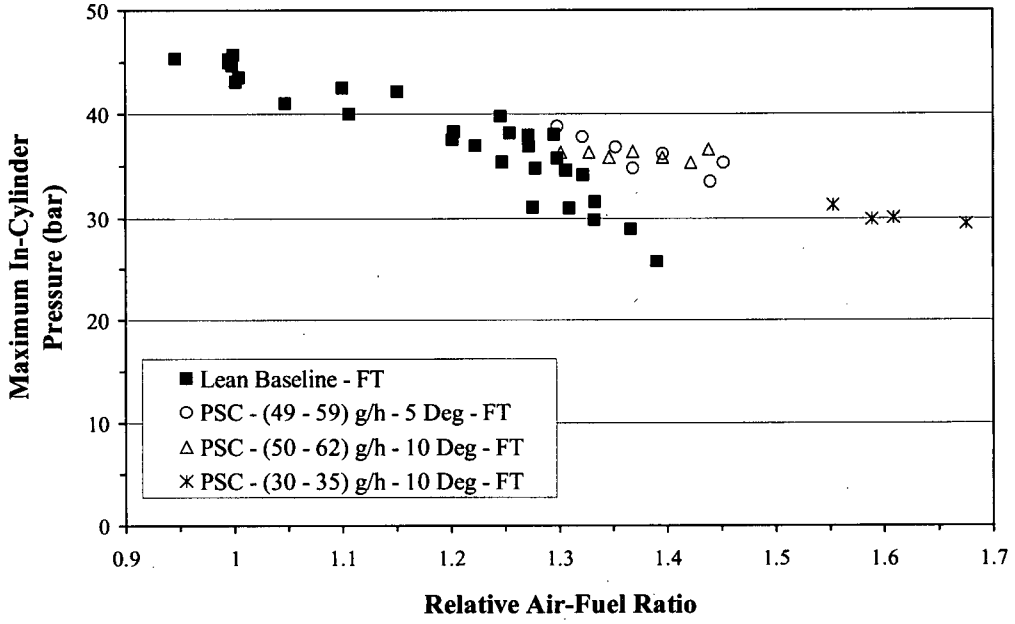

Figure 4.7: Maximum In-Cylinder Pressure, Full Throttle

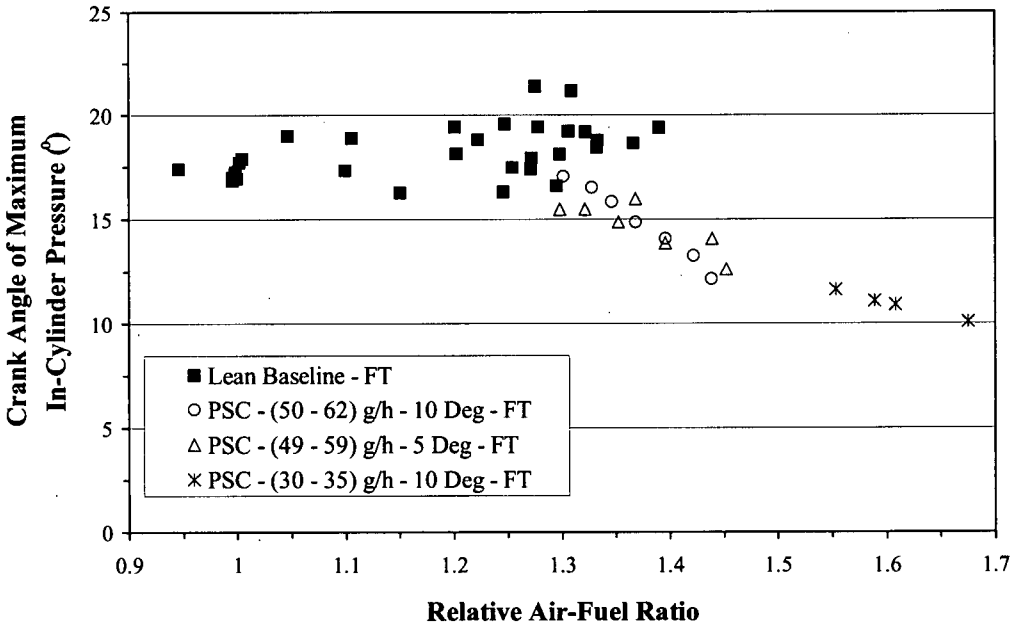

Figure 4.8: Crank Angle of Maximum In-Cylinder Pressure, Full Throttle

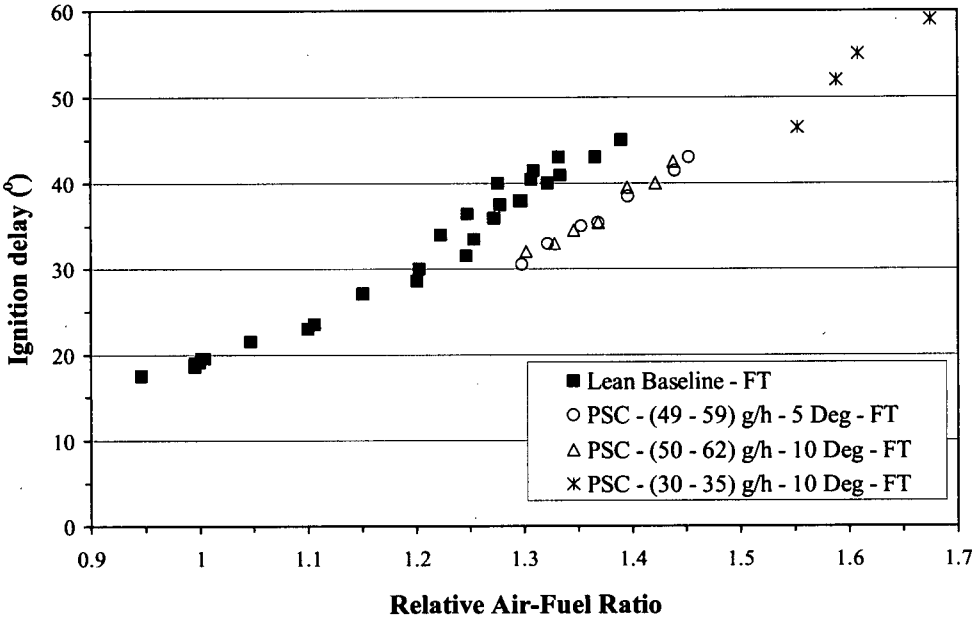

Figure 4.9: Ignition Delay, 0% - 5% Heat Release, Full Throttle

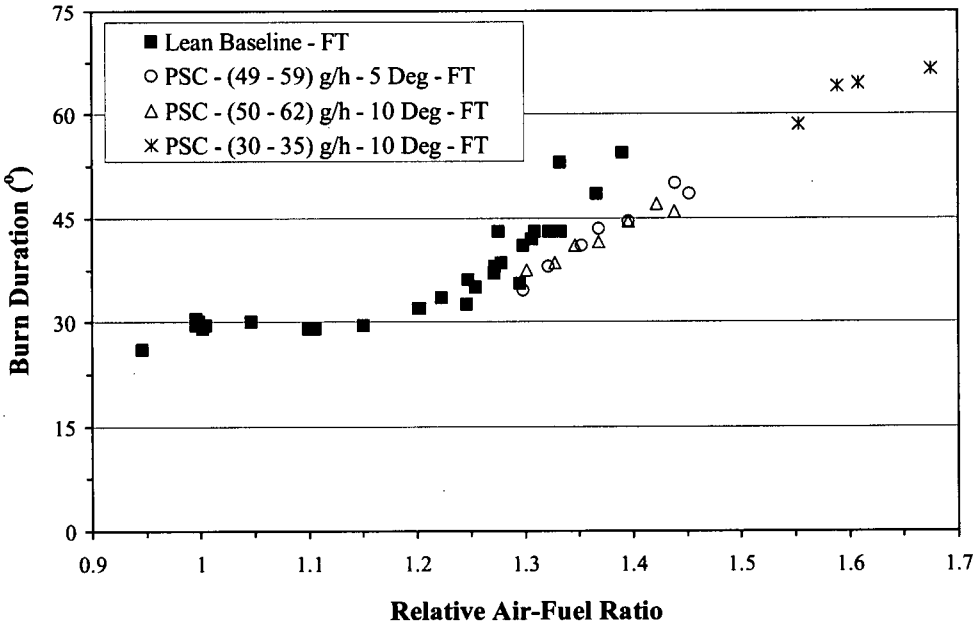

Figure 4.10: Burn Duration, 5% - 95% Heat Release, Full Throttle

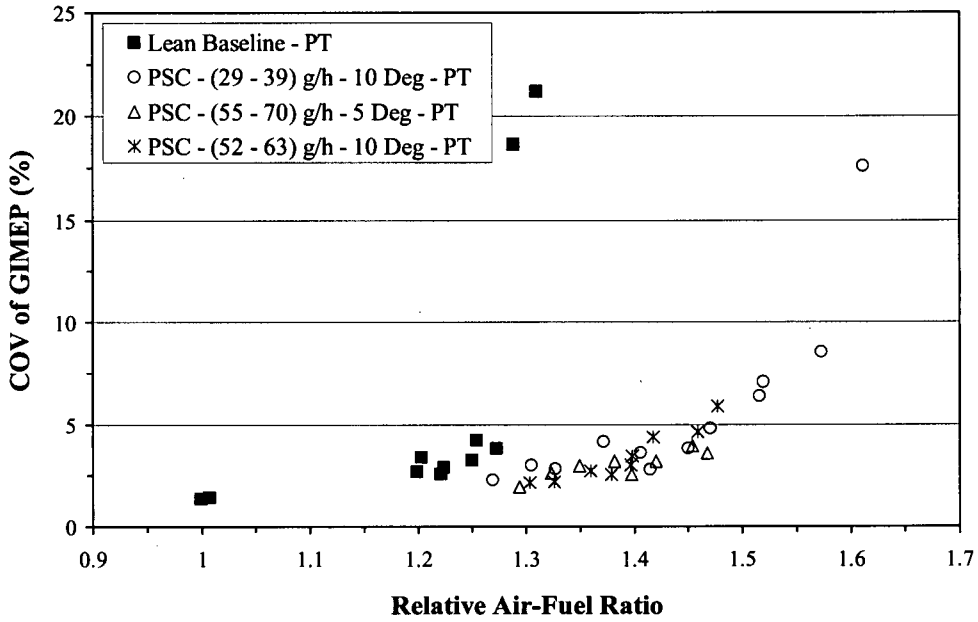

Figure 4.11: Coefficient of Variation of Indicated Mean Effective Pressure, Part Throttle

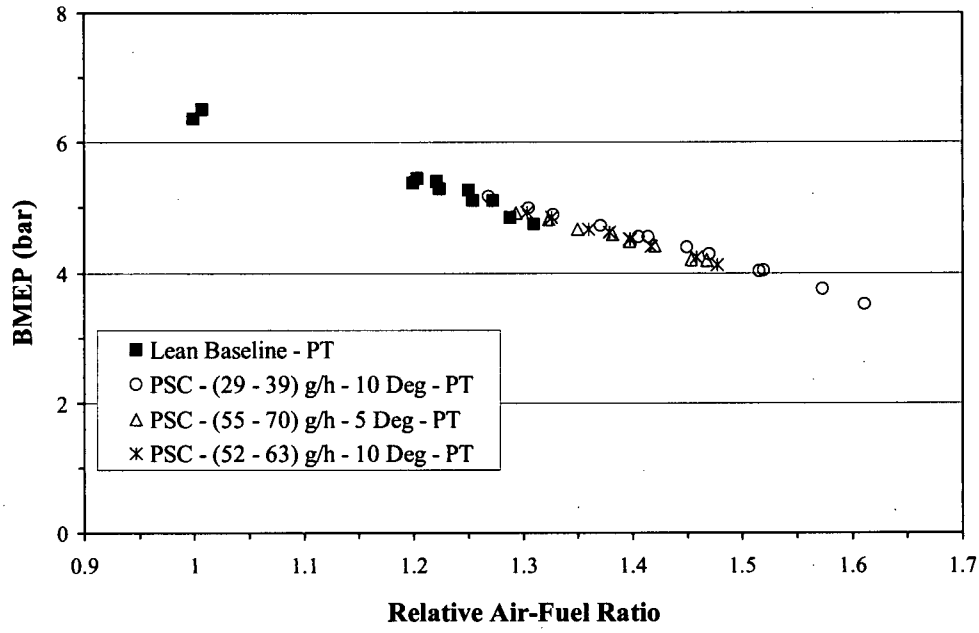

Figure 4.12: Brake Mean Effective Pressure, Part Throttle

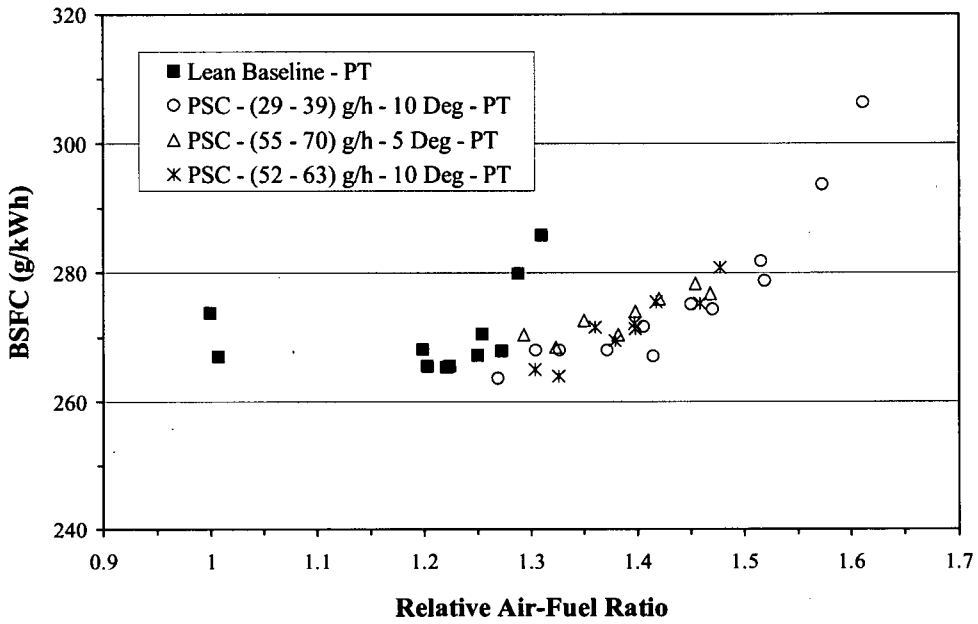

Figure 4.13: Brake Specific Fuel Consumption, Part Throttle

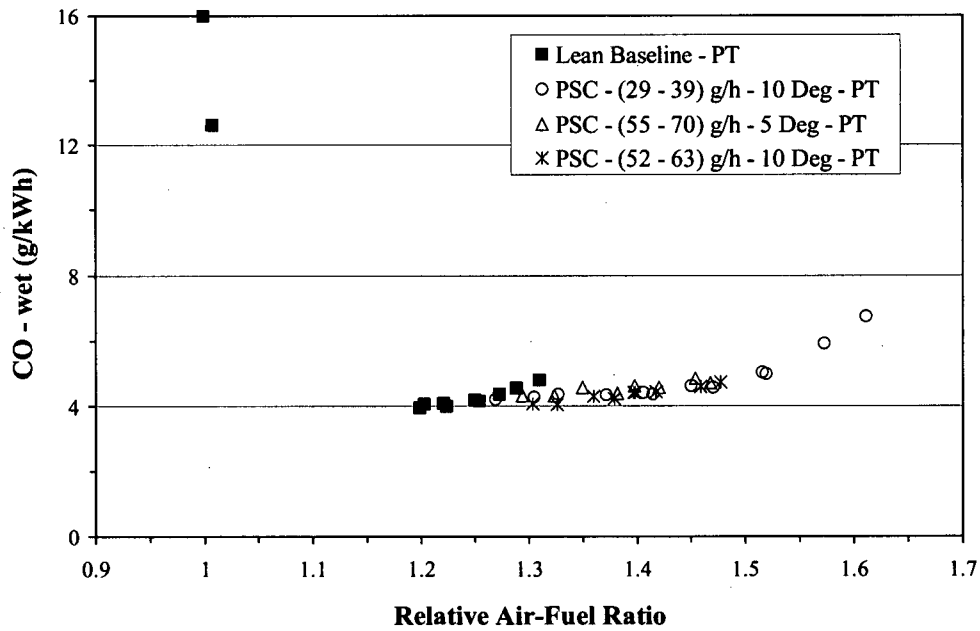

Figure 4.14: Brake Specific Carbon Monoxide Emissions, Part Throttle

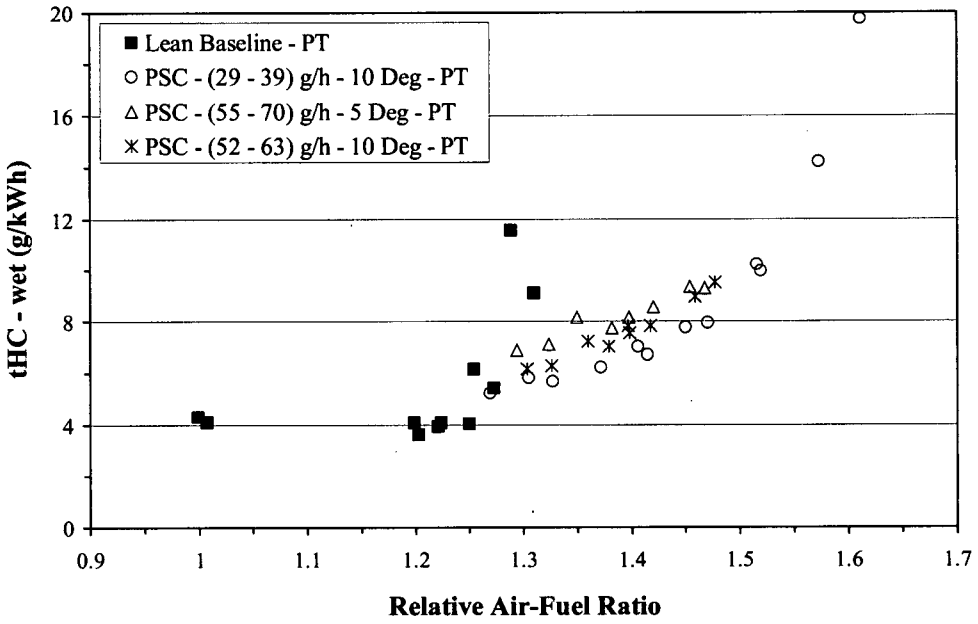

Figure 4.15: Brake Specific Hydrocarbon Emissions, Part Throttle

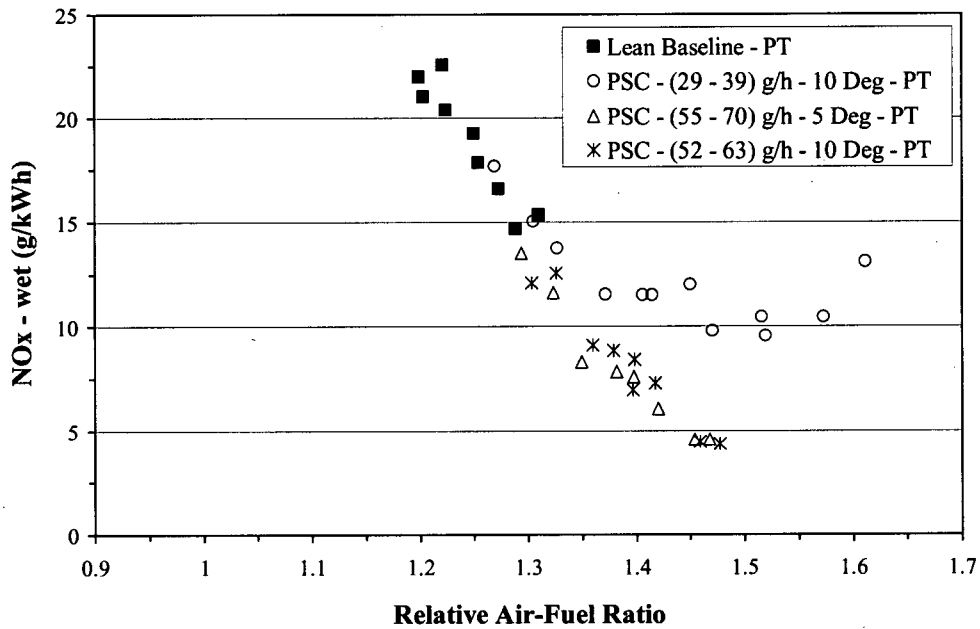

Figure 4.16: Brake Specific Nitrogen Oxide Emissions, Part Throttle

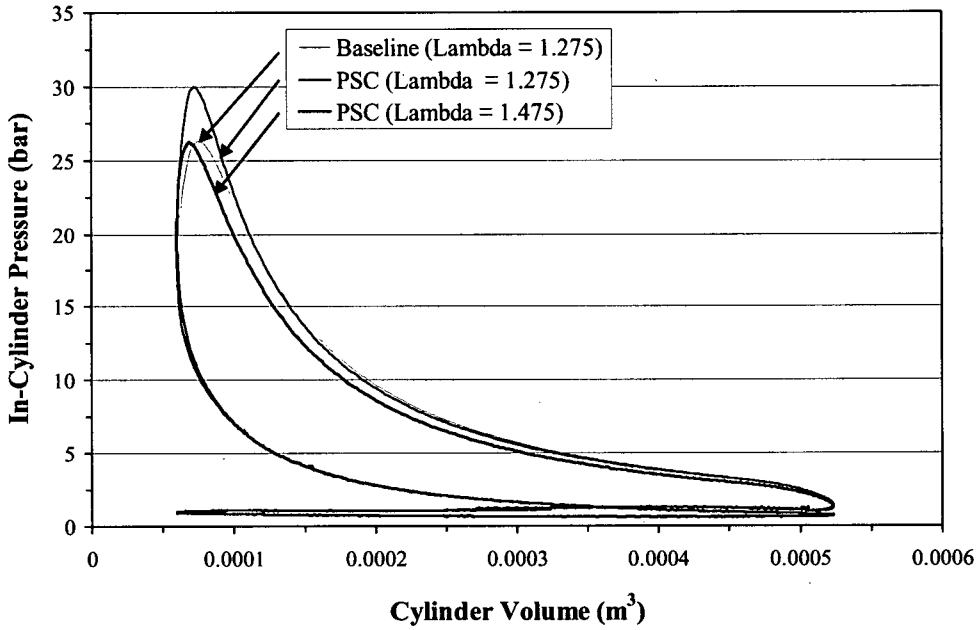

Figure 4.17: P - V Diagram, Part Throttle

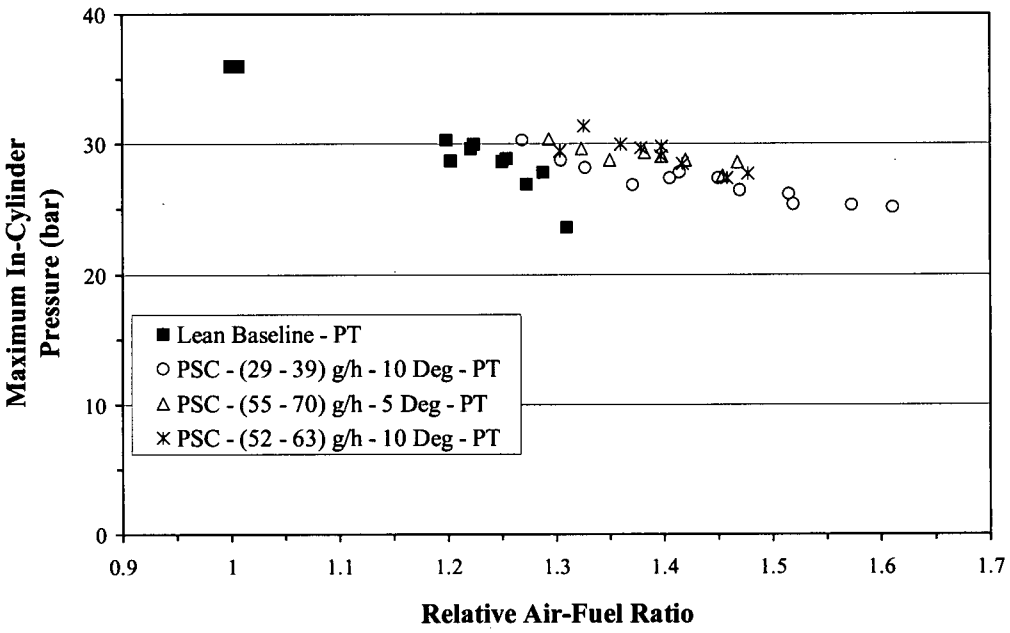

Figure 4.18: Maximum In-Cylinder Pressure, Part Throttle

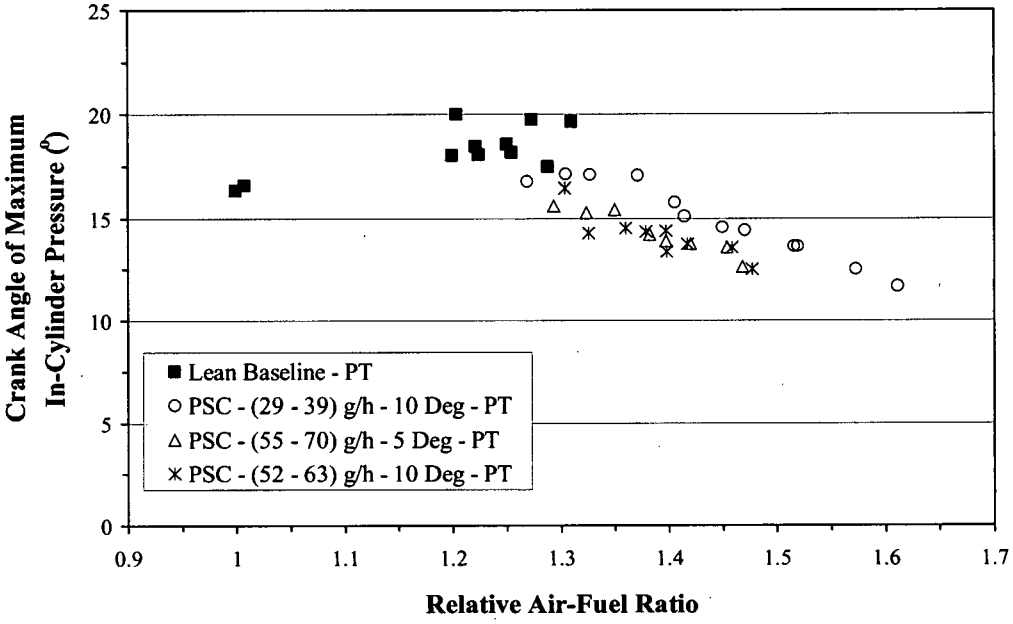

Figure 4.19: Crank Angle of Maximum In-Cylinder Pressure, Part Throttle

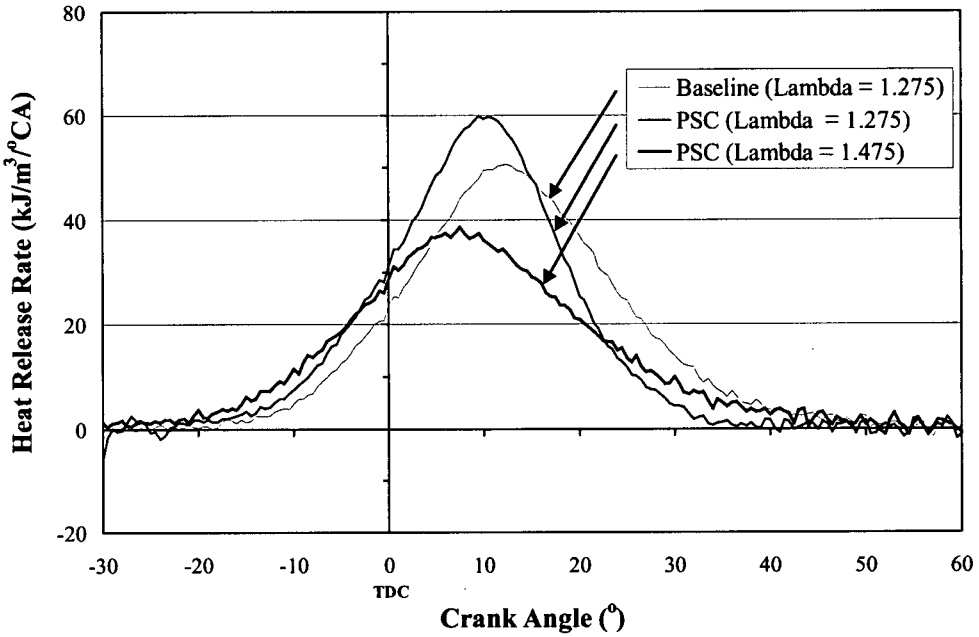

Figure 4.20: Heat Release Rate, Part Throttle

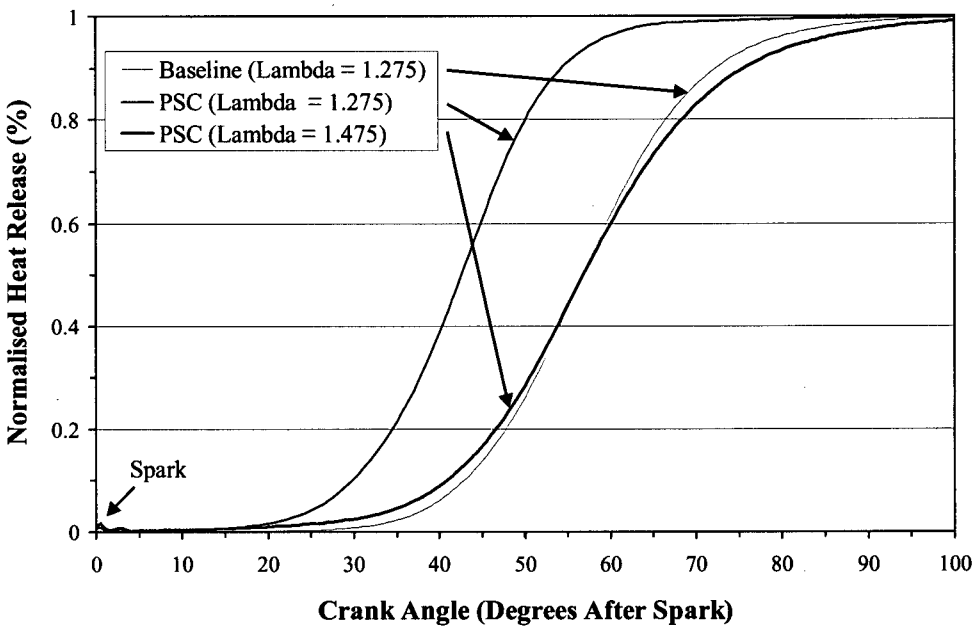

Figure 4.21: Integrated Heat Release Rate, Part Throttle

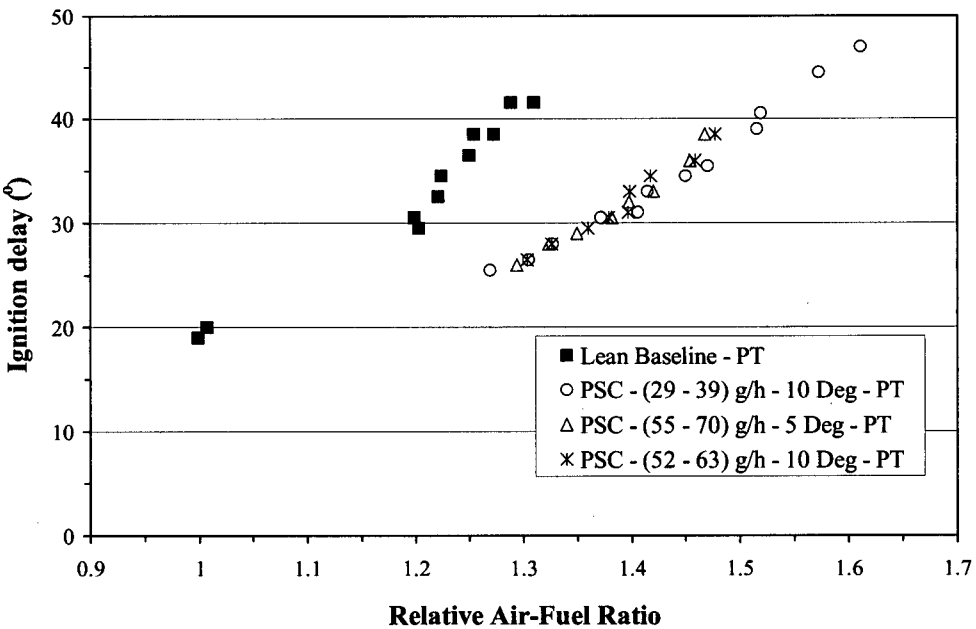

Figure 4.22: Ignition Delay, 0% - 5% Heat Release, Part Throttle

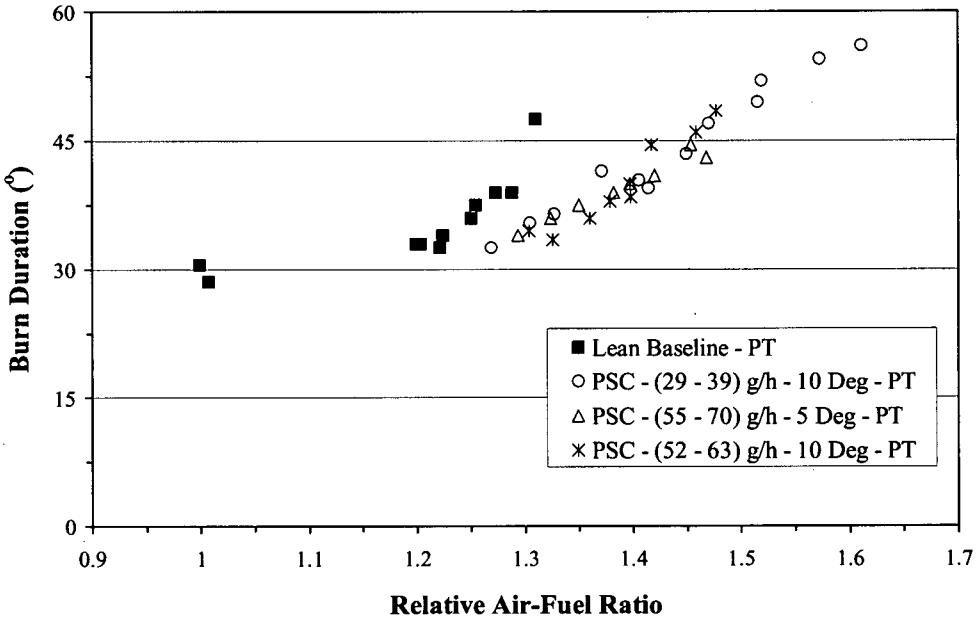

Figure 4.23: Burn Duration, 5% - 95% Heat Release, Part Throttle

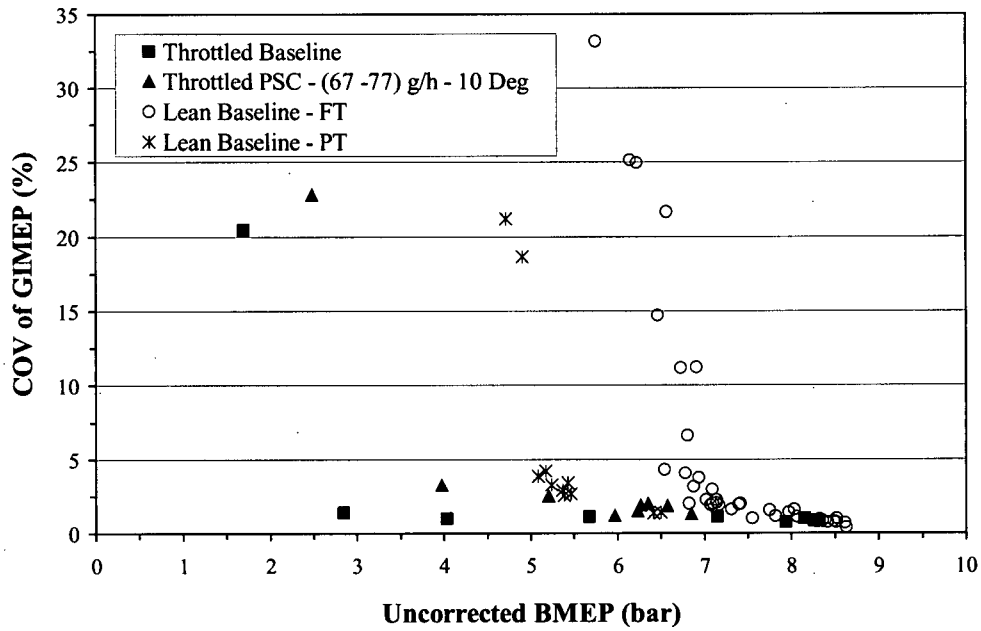

Figure 4.24: Coefficient of Variation of Indicated Mean Effective Pressure, Throttled

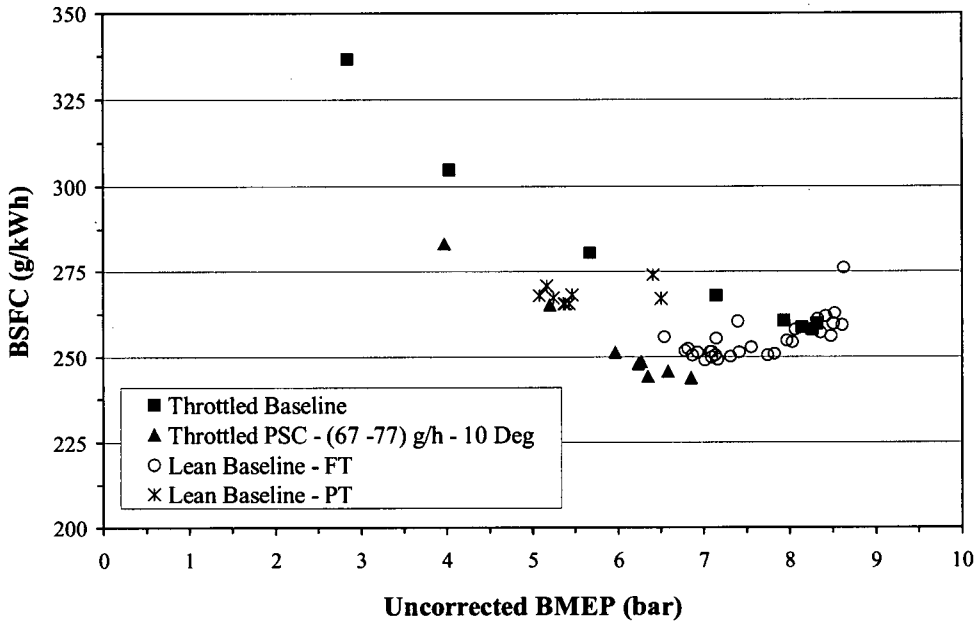

Figure 4.25: Brake Specific Fuel Consumption, Throttled

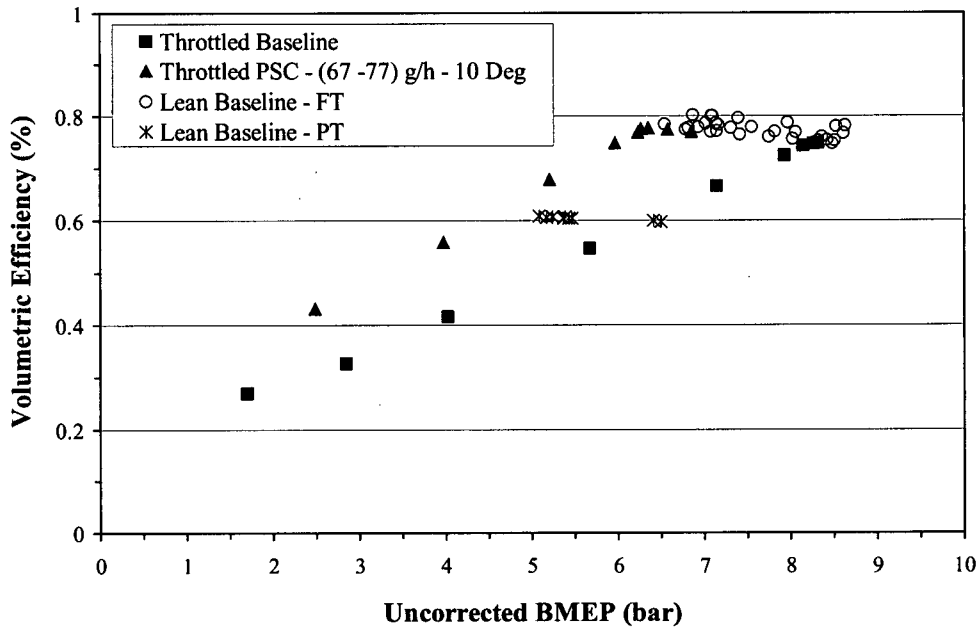

Figure 4.26: Volumetric Efficiency, Throttled

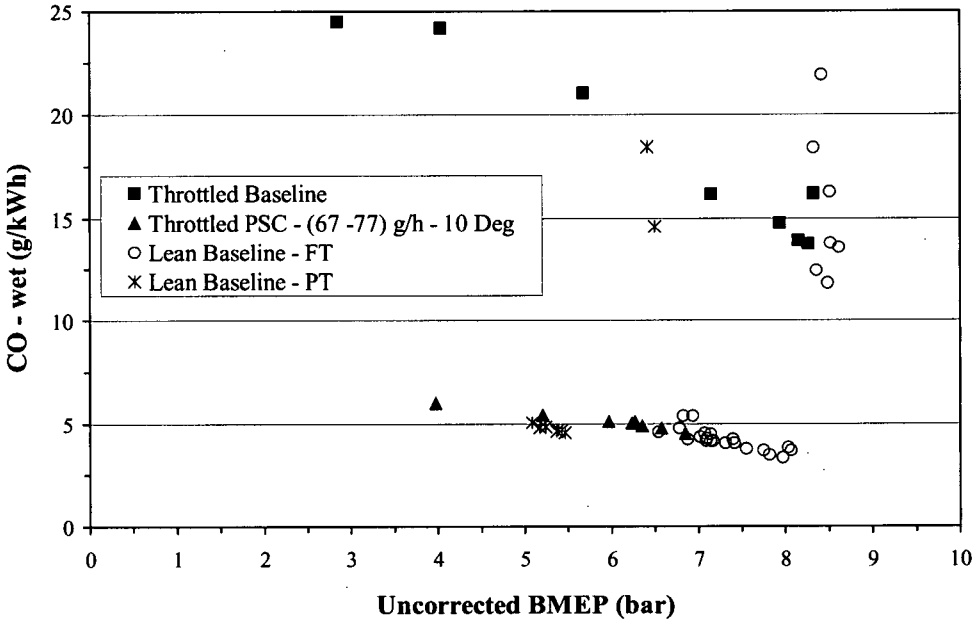

Figure 4.27: Brake Specific Carbon Monoxide Emissions, Throttled

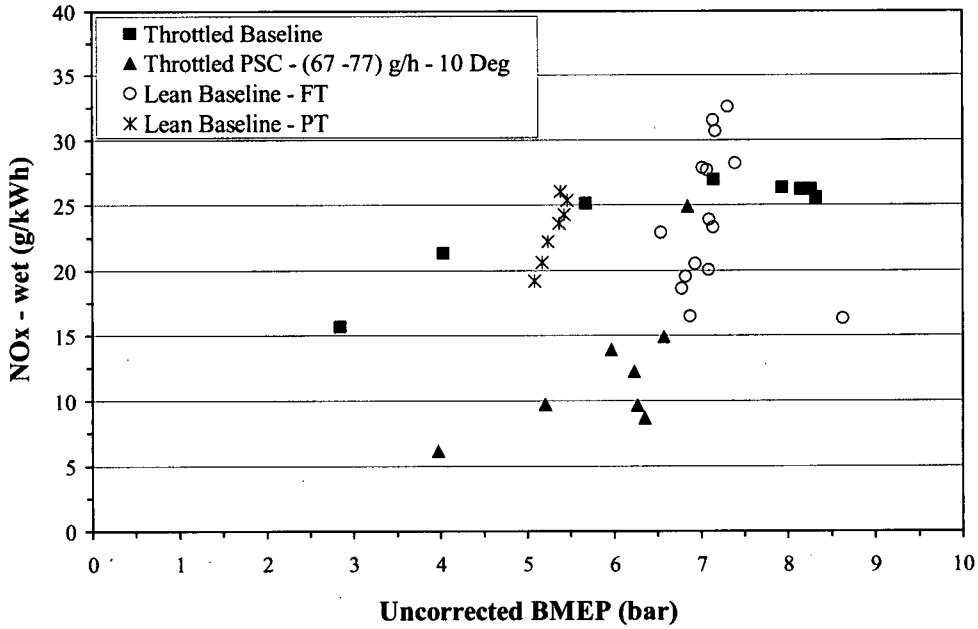

Figure 4.28: Brake Specific Nitrogen Oxide Emissions, Throttled

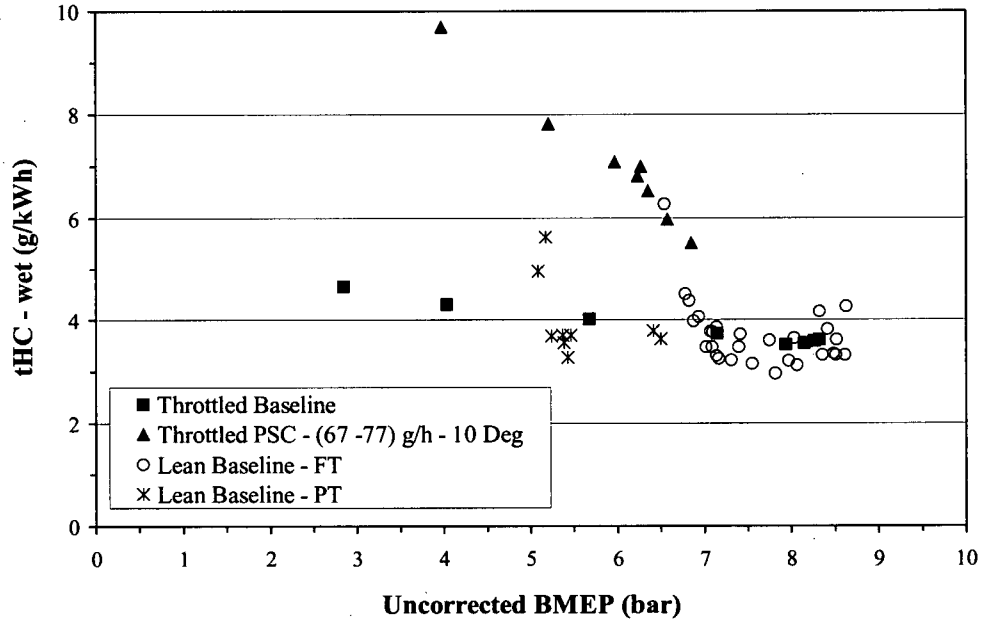

Figure 4.29: Brake Specific Hydrocarbon Emissions, Throttled

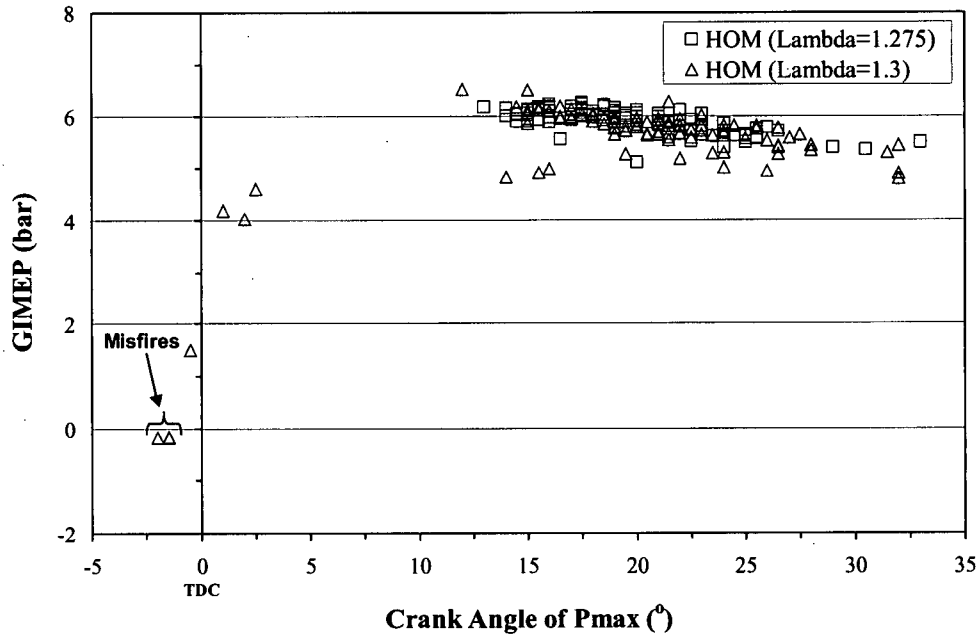

Figure 4.30: Indicated Mean Effective Pressure for 100 Cycles, Homogenous

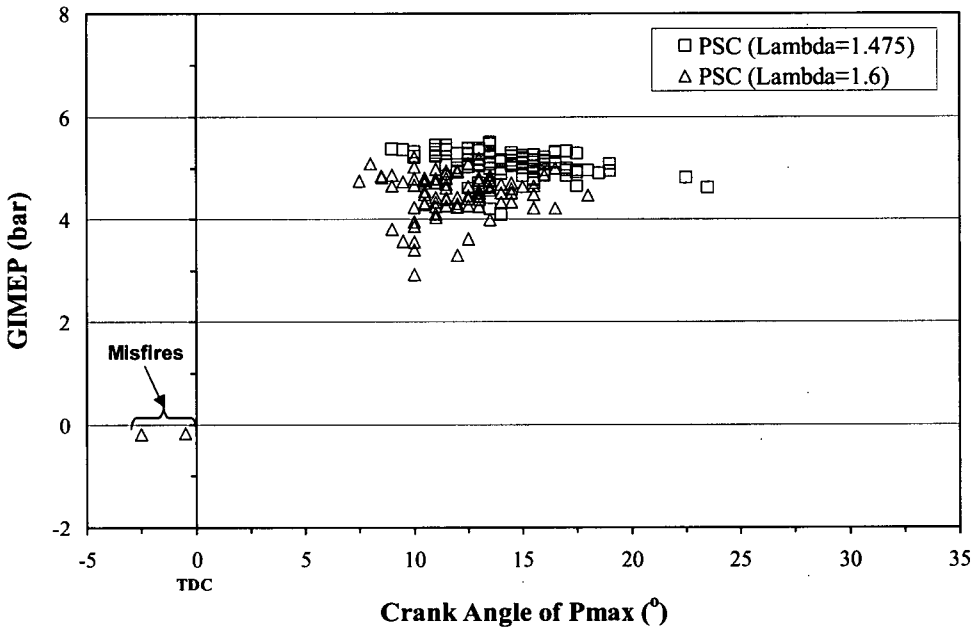

Figure 4.31: Indicated Mean Effective Pressure Pressure for 100 Cycles, PSC

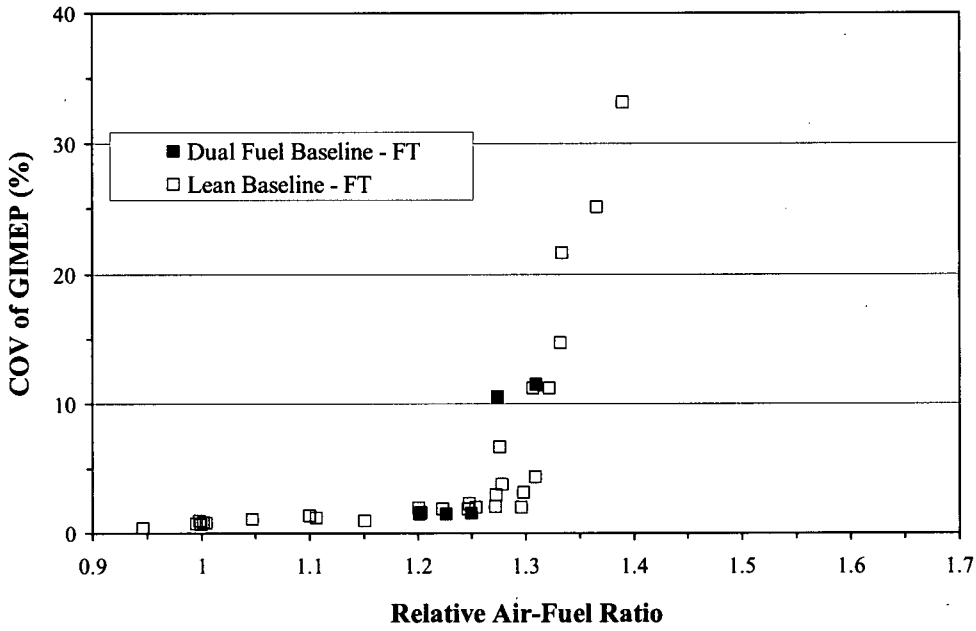

Figure 4.32: Coefficient of Variation of Indicated Mean Effective Pressure, Homogeneous Lean Operation

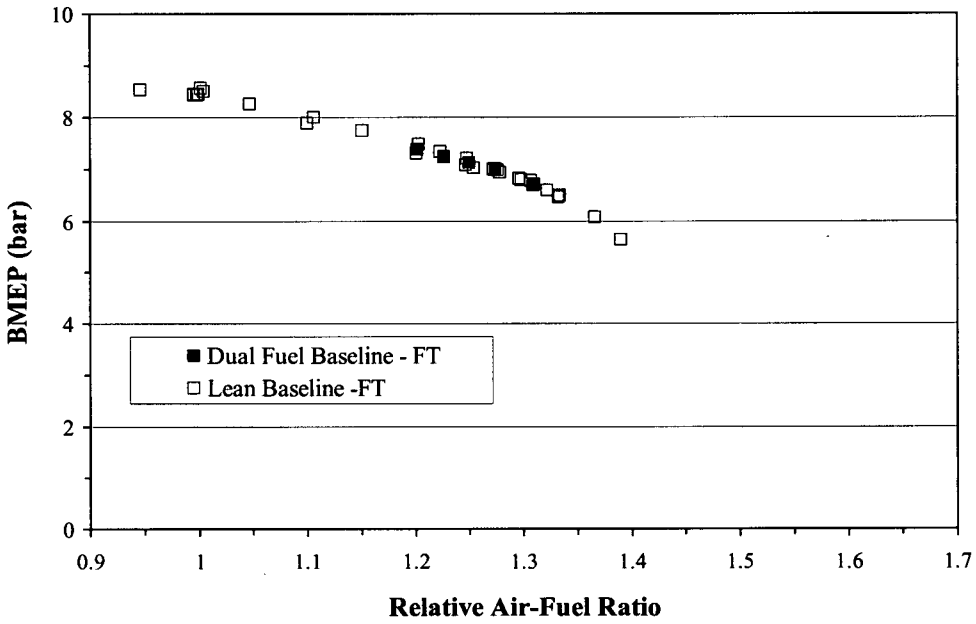

Figure 4.33: Brake Mean Effective Pressure, Homogeneous Lean Operation

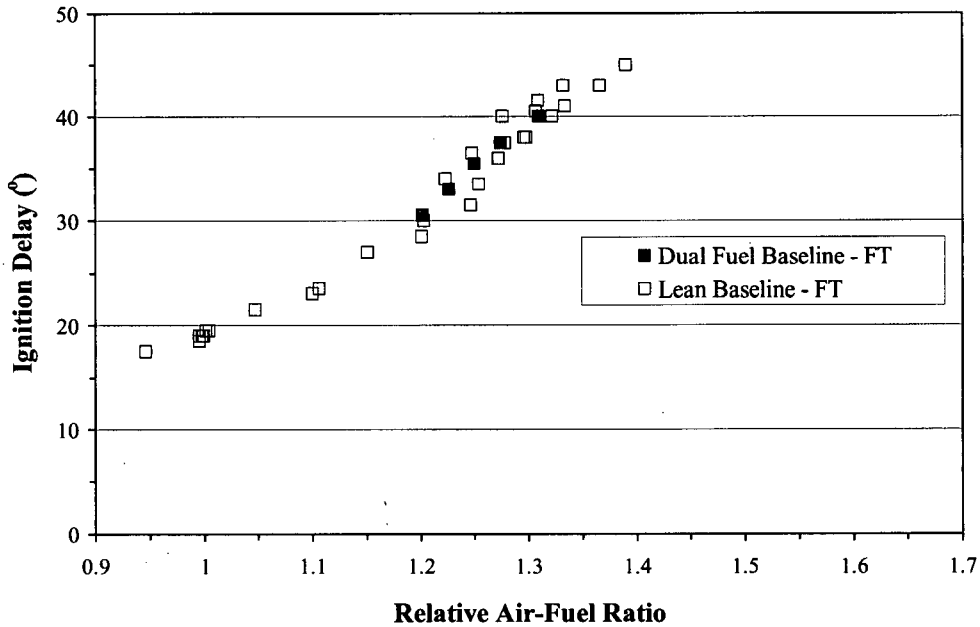

Figure 4.34: Ignition Delay, Homogeneous Lean Operation

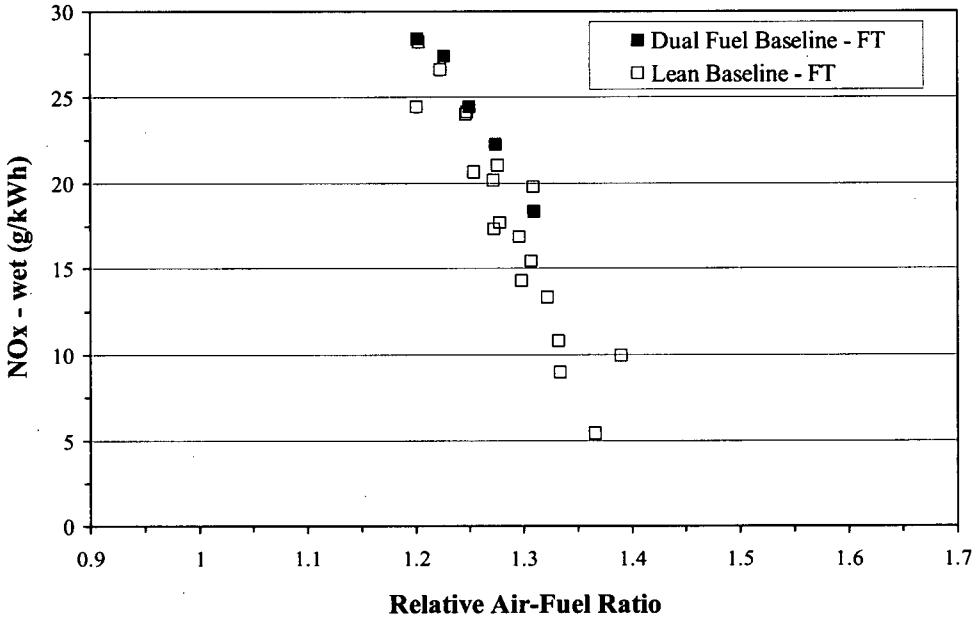

Figure 4.35: Nitrogen Oxide Emissions, Homogeneous Lean Operation

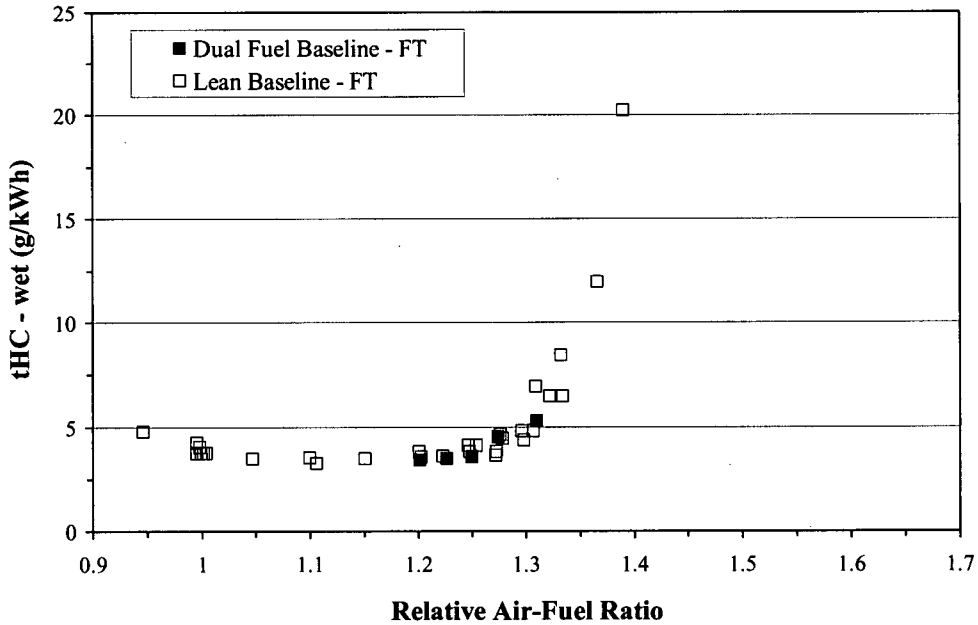

Figure 4.36: Hydrocarbon Emissions, Homogeneous Lean Operation

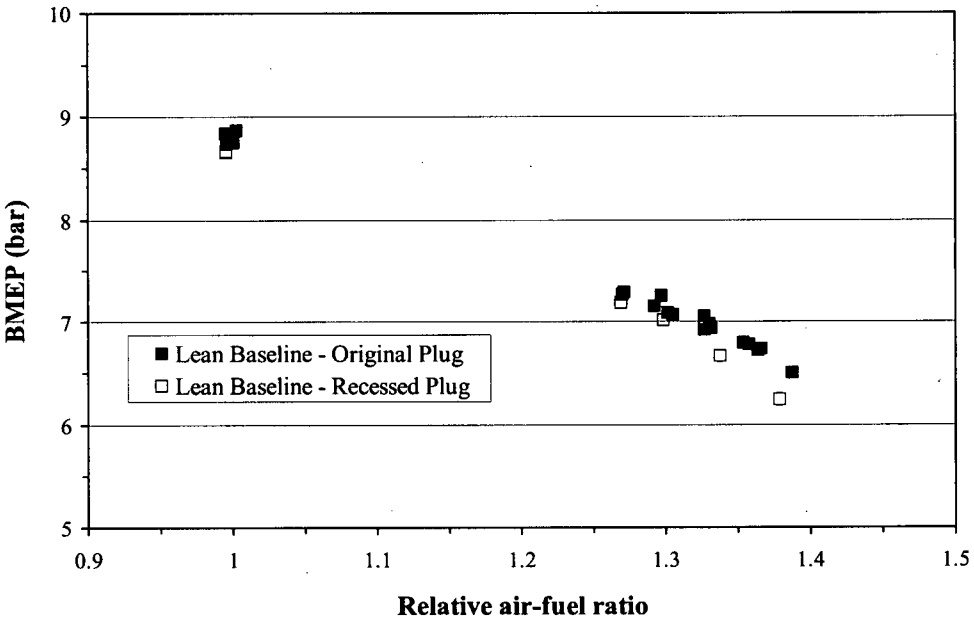

Figure 4.37: Brake Mean Effective Pressure, Gasoline Baseline

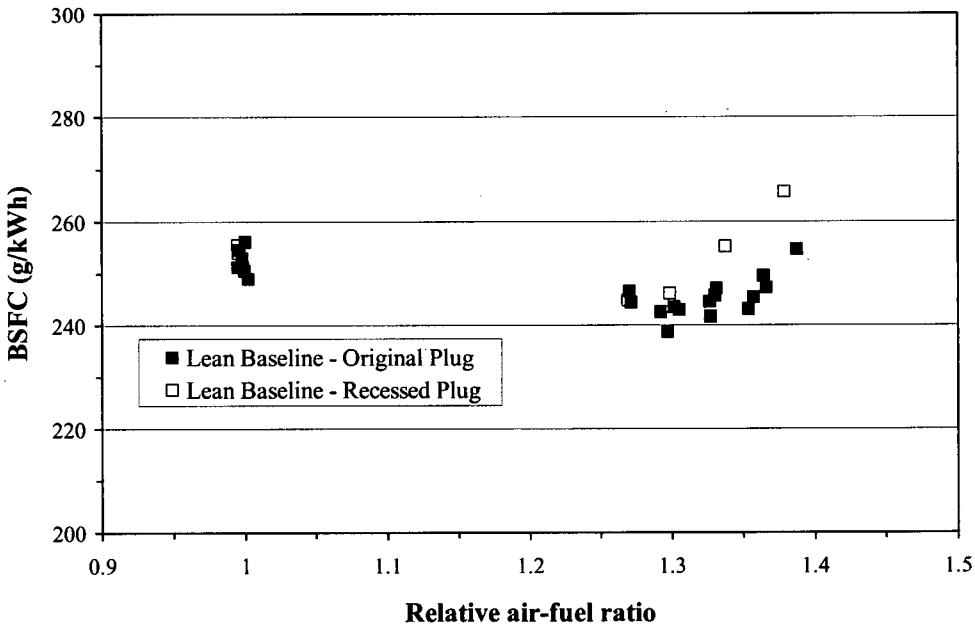

Figure 4.38: Brake Specific Fuel Consumption, Gasoline Baseline

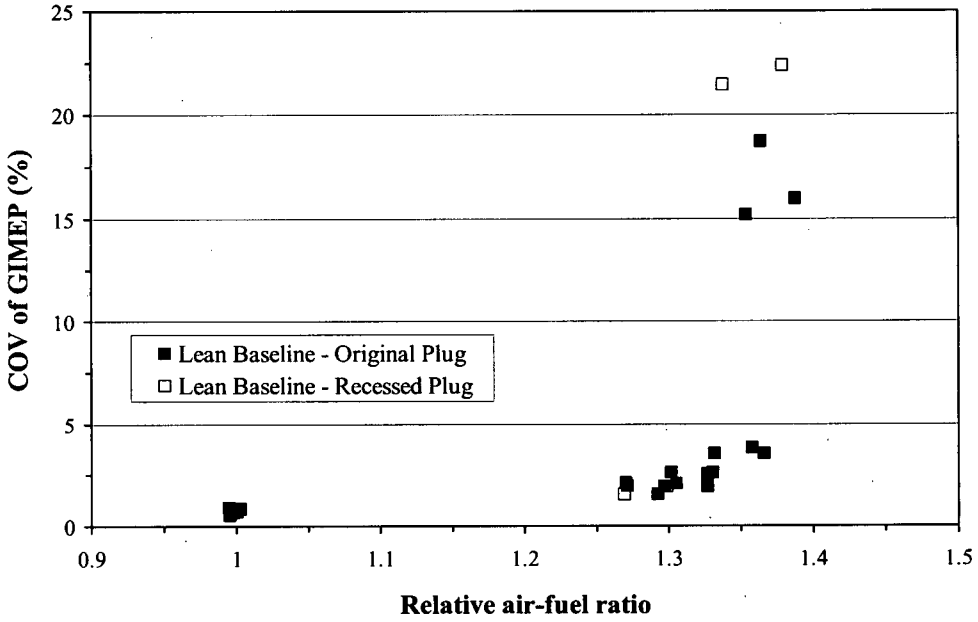

Figure 4.39: Coefficient of Variation of Indicated Mean Effective Pressure, Gasoline Baseline

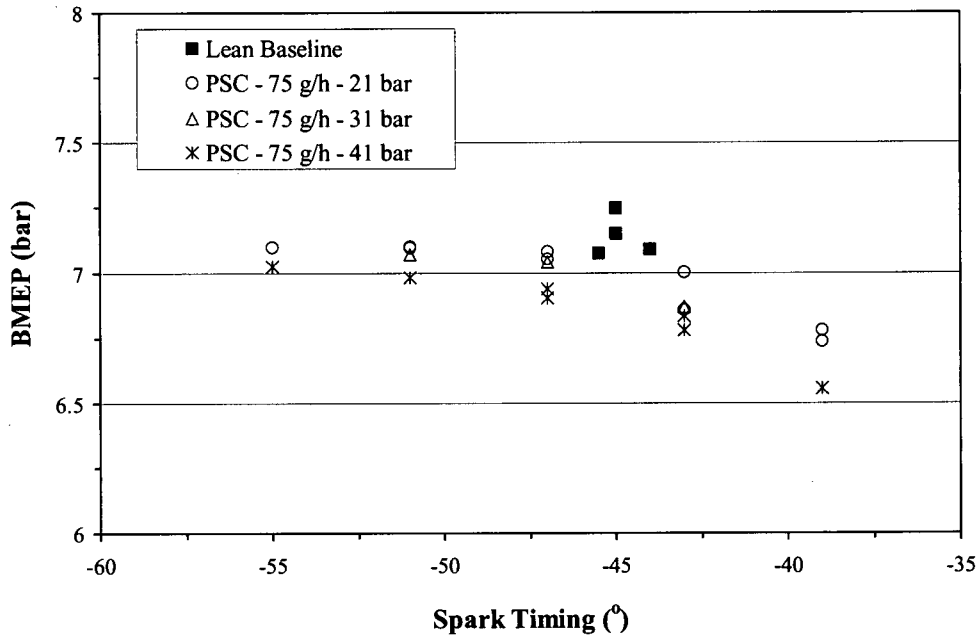

Figure 4.40: Brake Mean Effective Pressure, Varying Injection Pressure, Gasoline PSC

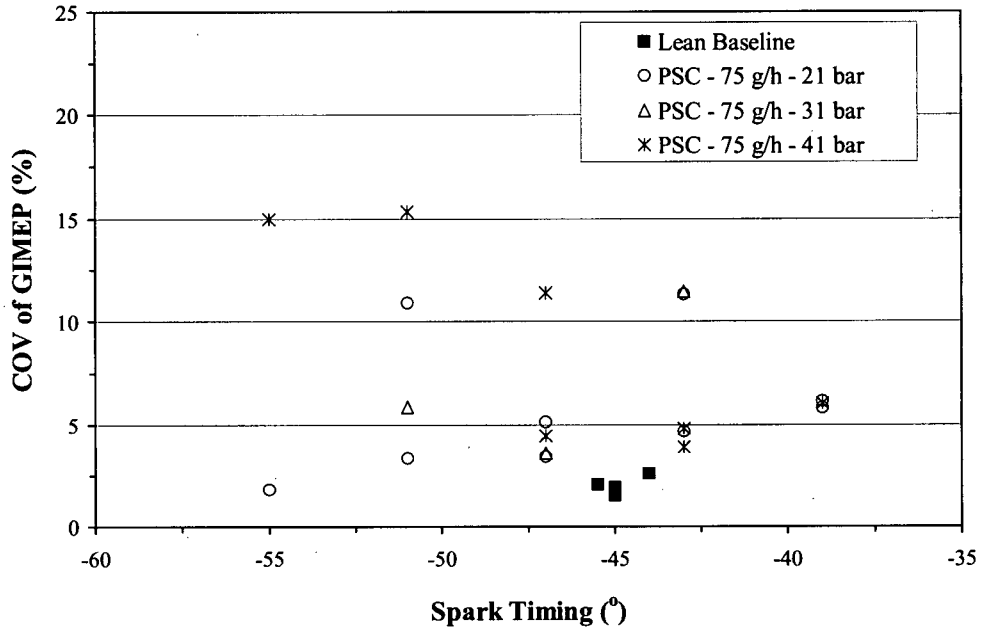

Figure 4.41: Coefficient of Variation of Indicated Mean Effective Pressure, Varying Injection Pressure, Gasoline PSC

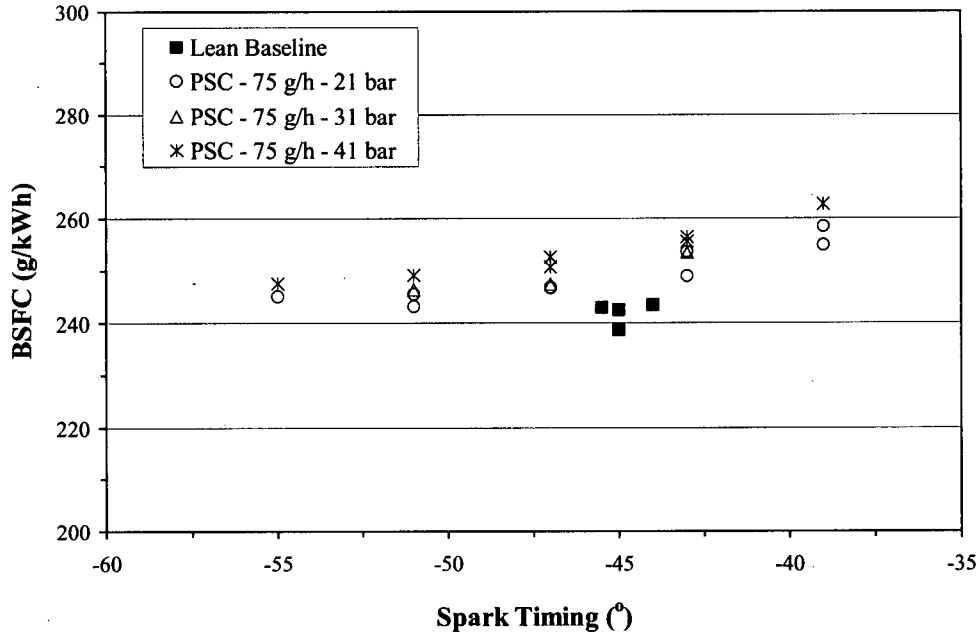

Figure 4.42: Brake Specific Fuel Consumption, Varying Injection Pressure, Gasoline PSC

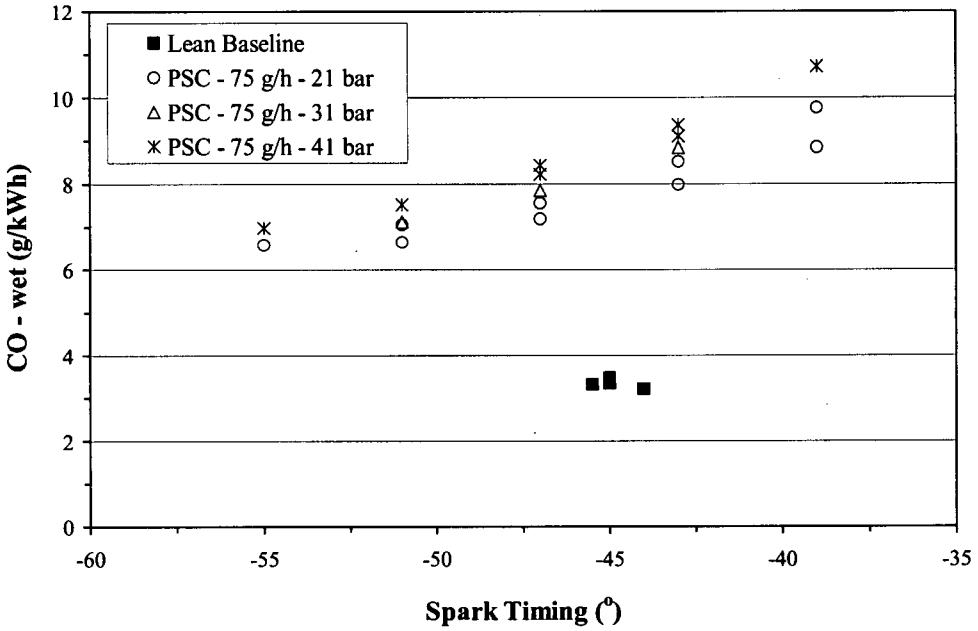

Figure 4.43: Brake Specific Carbon Monoxide Emissions, Varying Injection Pressure, Gasoline PSC

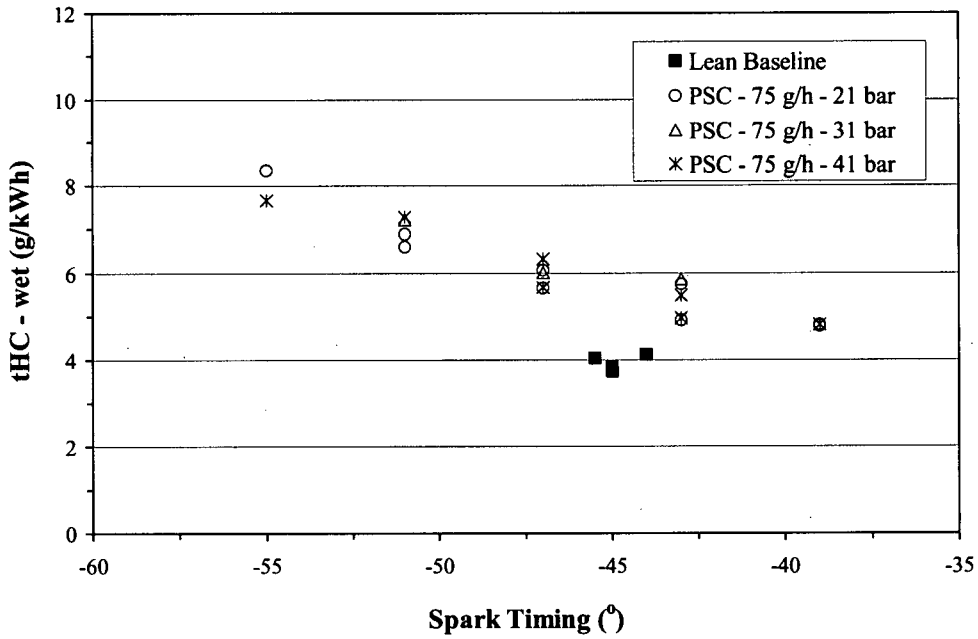

Figure 4.44: Brake Specific Hydrocarbon Emissions, Varying Injection Pressure, Gasoline PSC

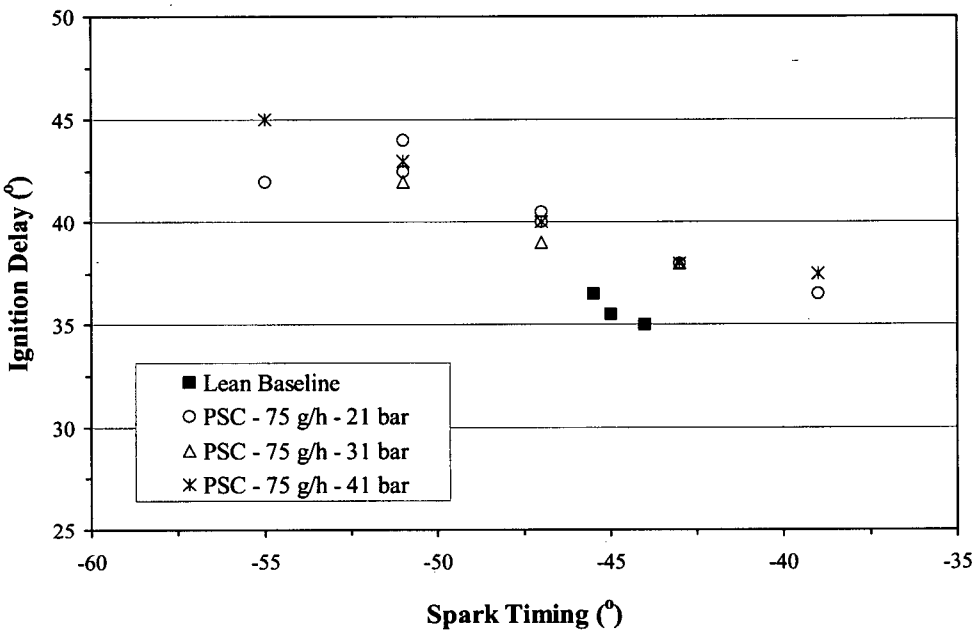

Figure 4.45: Ignition Delay, 0% - 5%, Varying Injection Pressure, Gasoline PSC

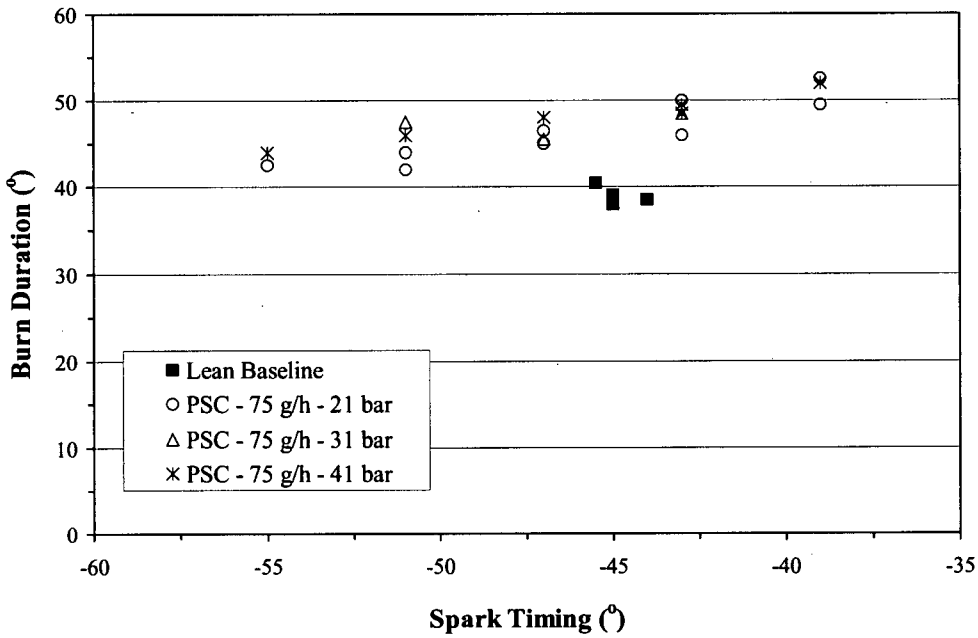

Figure 4.46: Burn Duration, 5% - 95%, Varying Injection Pressure, Gasoline PSC

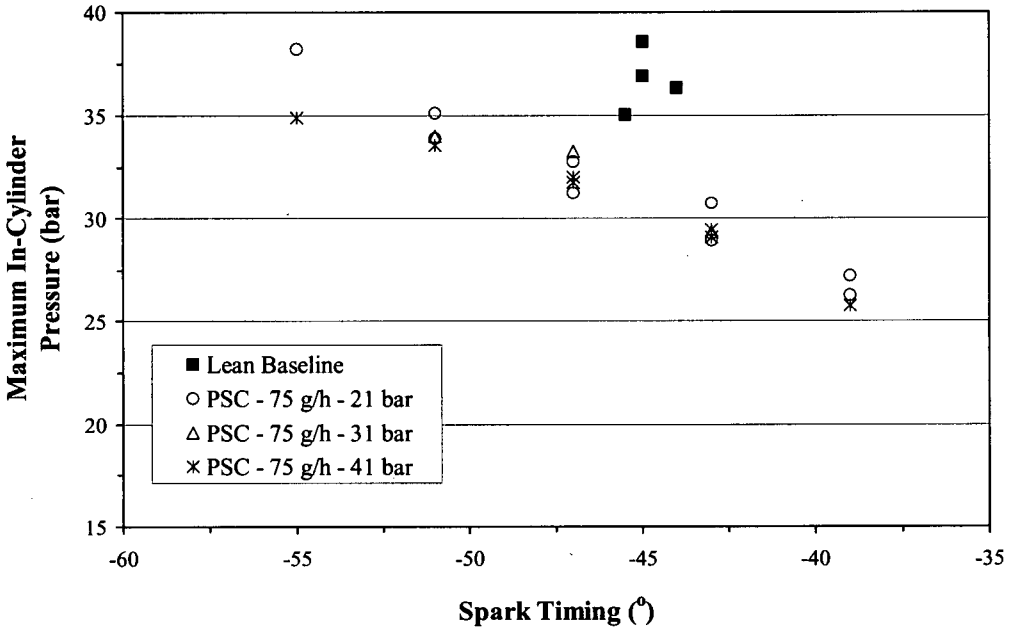

Figure 4.47: Maximum In-Cylinder Pressure, Varying Injection Pressure, Gasoline PSC

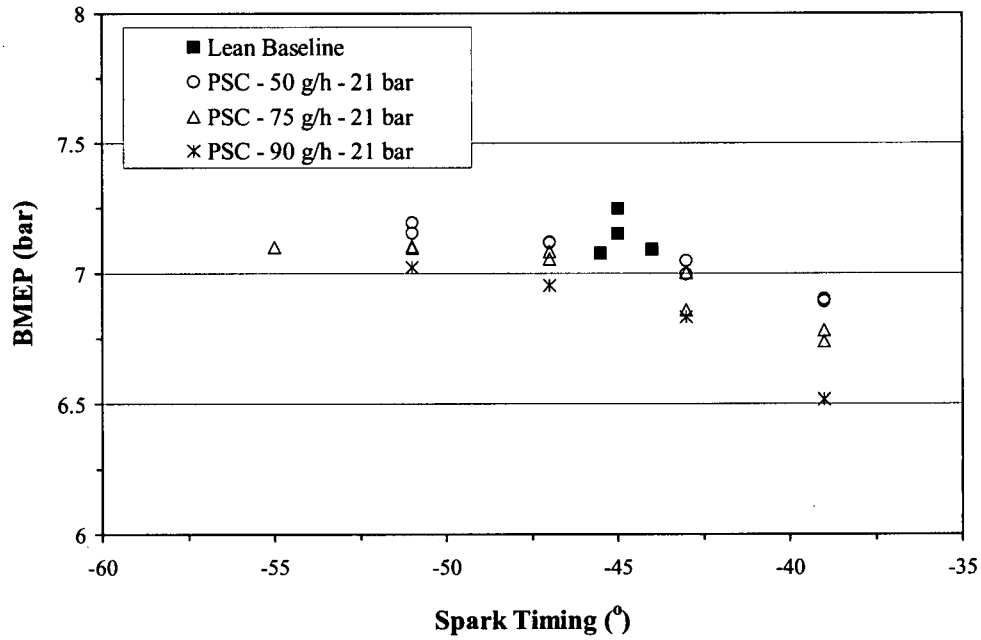

Figure 4.48: Brake Mean Effective Pressure, Varying Injection Flow Rate, Gasoline PSC

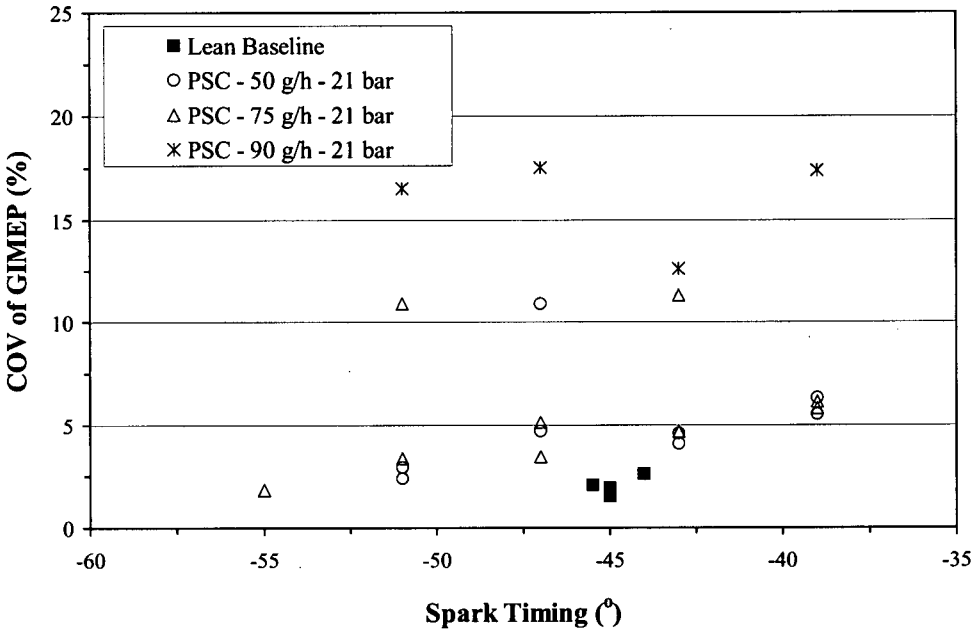

Figure 4.49: Coefficient of Variation of Indicated Mean Effective Pressure, Varying Injection Flow Rate, Gasoline PSC

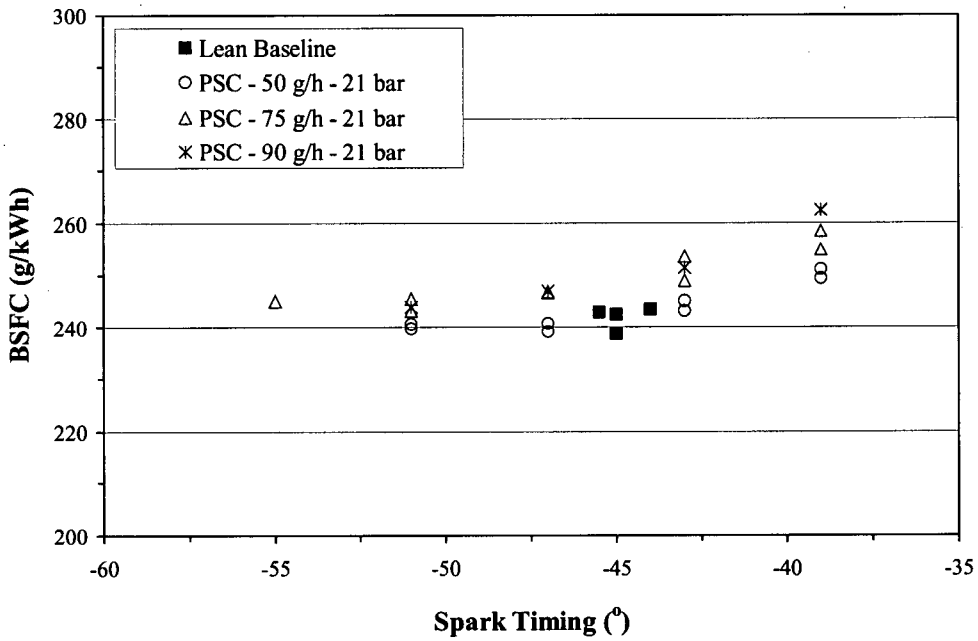

Figure 4.50: Brake Specific Fuel Consumption, Varying Injection Flow Rate, Gasoline PSC

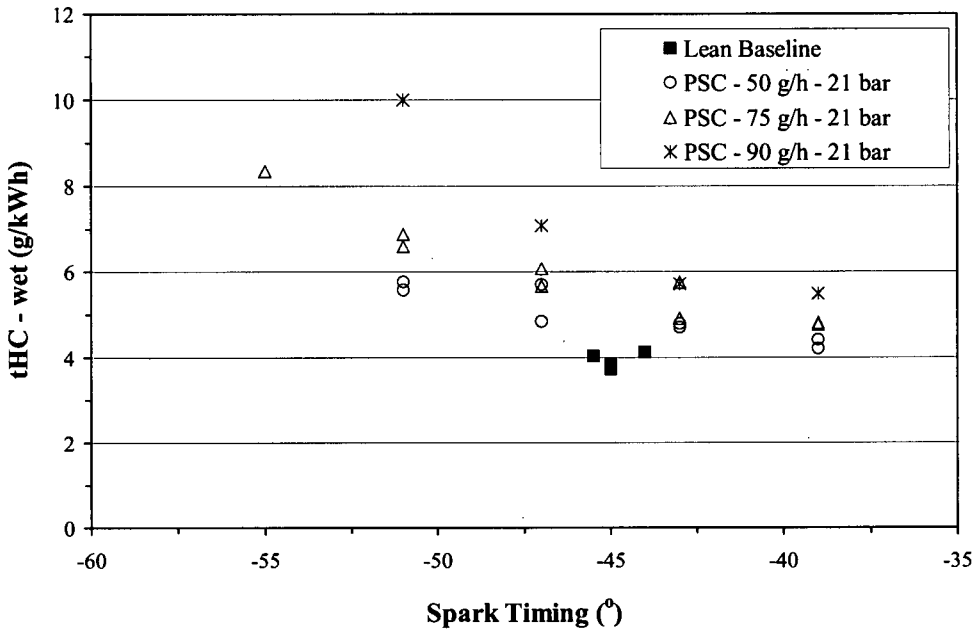

Figure 4.51: Brake Specific Hydrocarbon Emissions, Varying Injection Flow Rate, Gasoline PSC

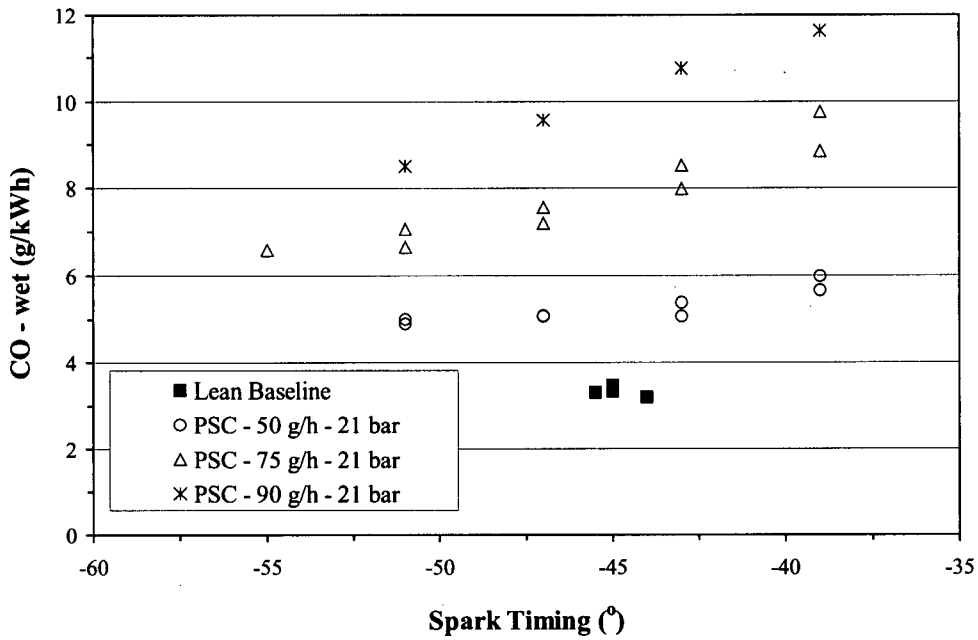

Figure 4.52: Brake Specific Carbon Monoxide Emissions, Varying Injection Flow Rate, Gasoline PSC

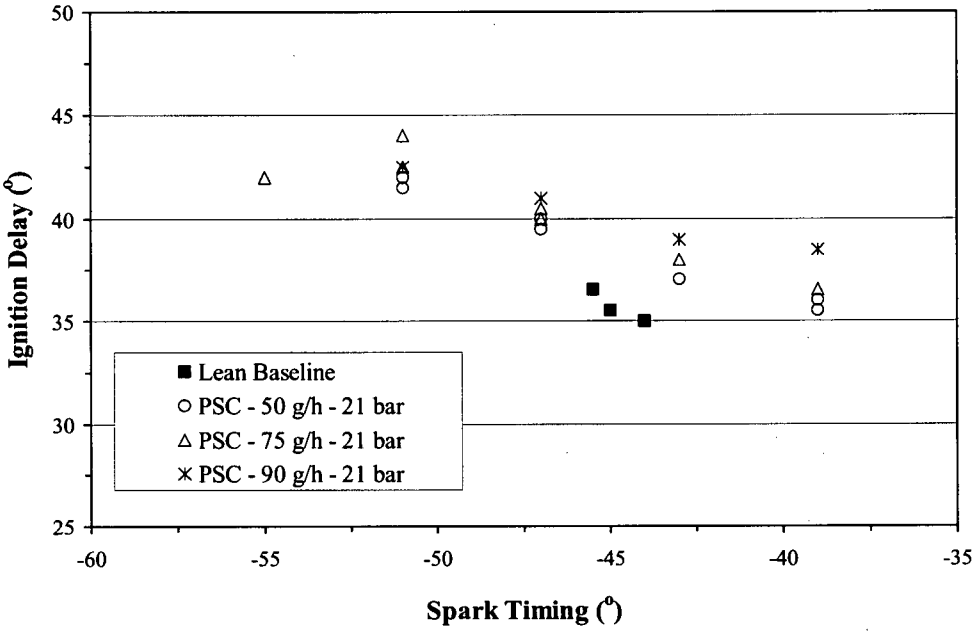

Figure 4.53: Ignition Delay, 0% - 5%, Varying Injection Flow Rate, Gasoline PSC

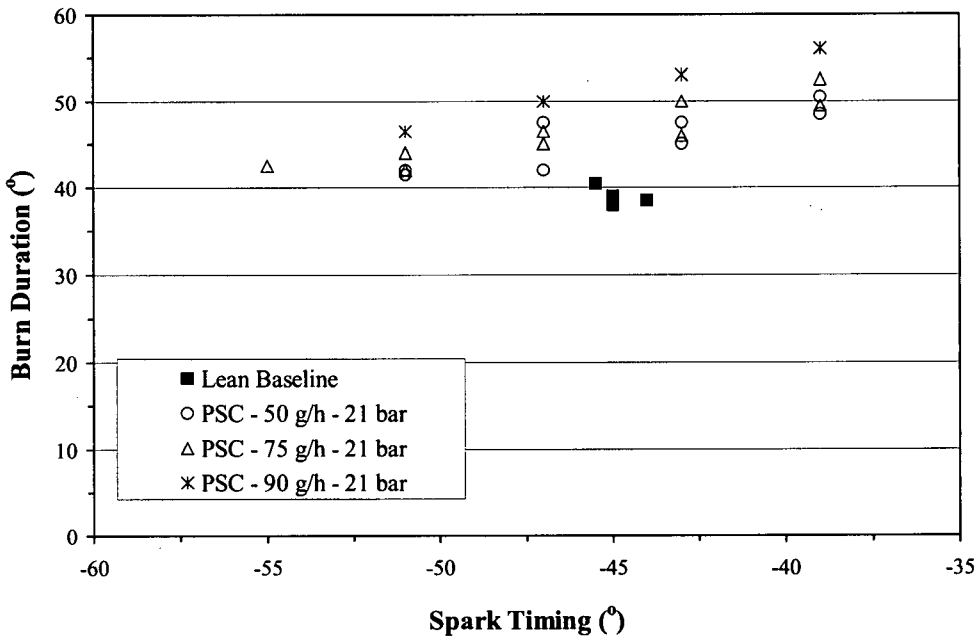

Figure 4.54: Burn Duration, 5% - 95%, Varying Injection Flow Rate, Gasoline PSC

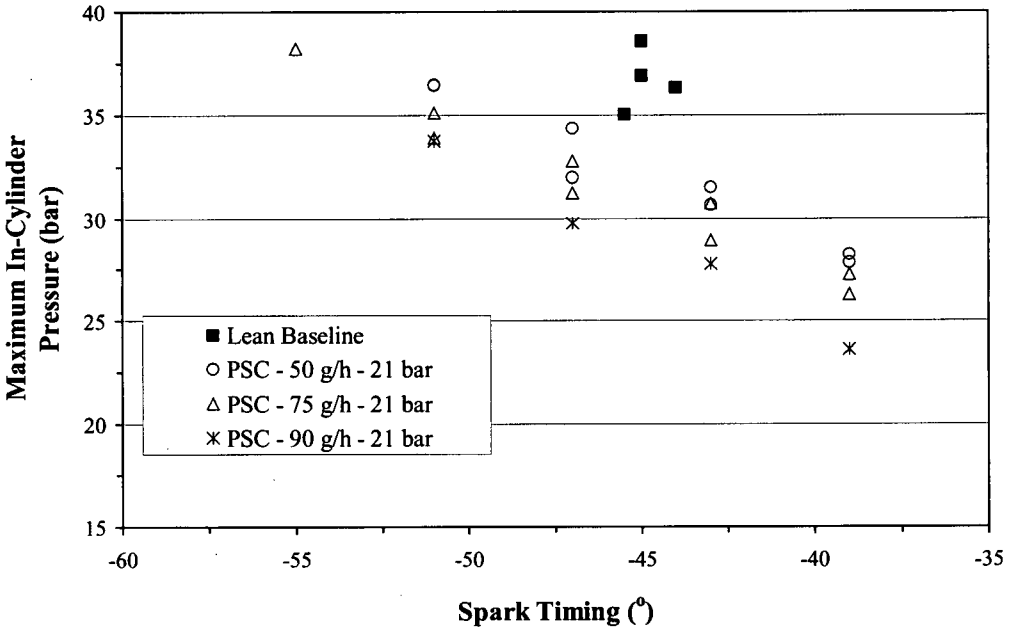

Figure 4.55: Maximum In-Cylinder Pressure, Varying Injection Flow Rate, Gasoline PSC

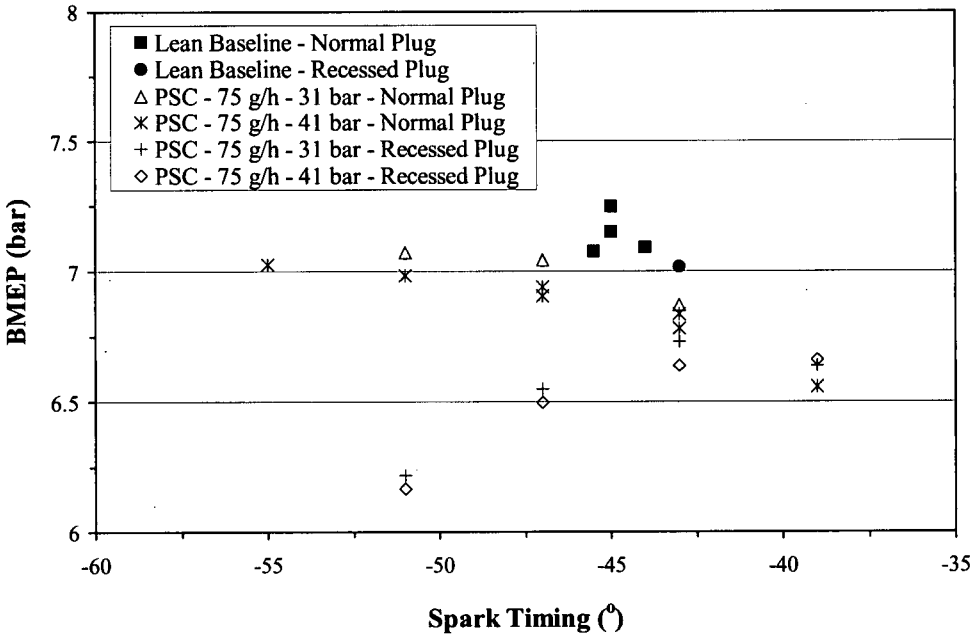

Figure 4.56: Brake Mean Effective Pressure, Varying Plug Position, Gasoline PSC

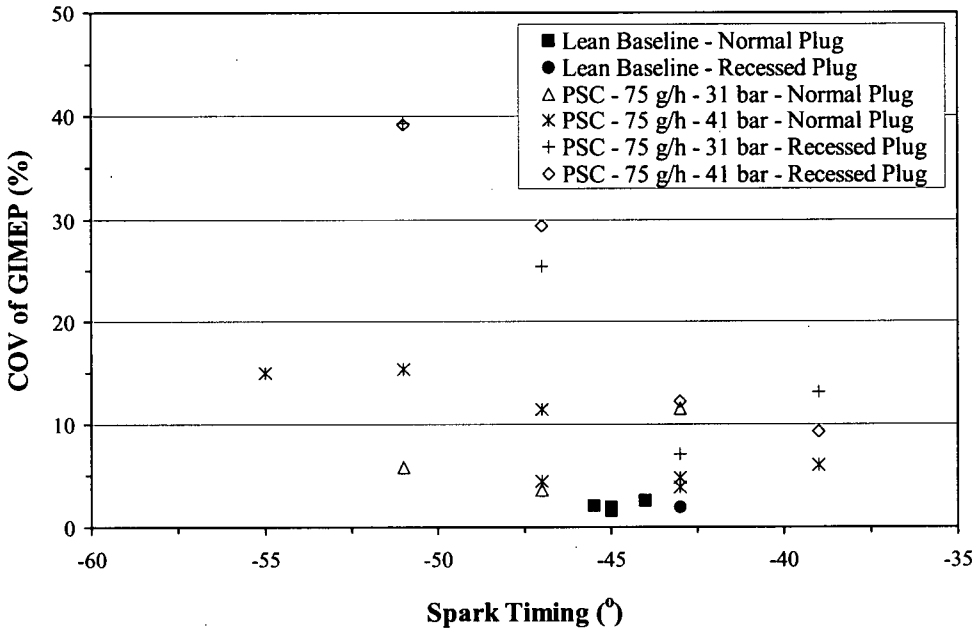

Figure 4.57: Coefficient of Variation of Indicated Mean Effective Pressure, Varying Plug Position, Gasoline PSC

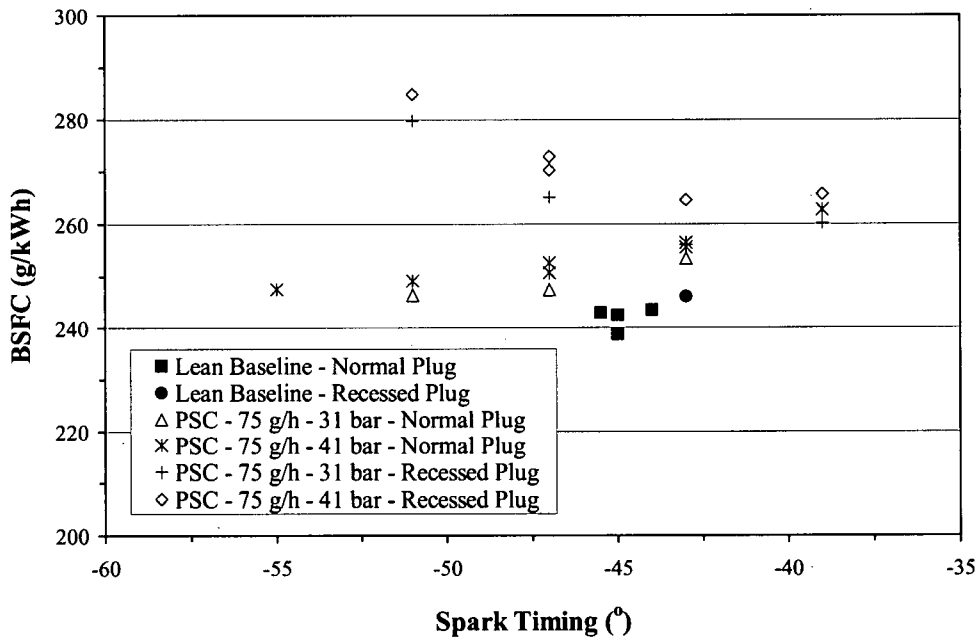

Figure 4.58: Brake Specific Fuel Consumption, Varying Plug Position, Gasoline PSC

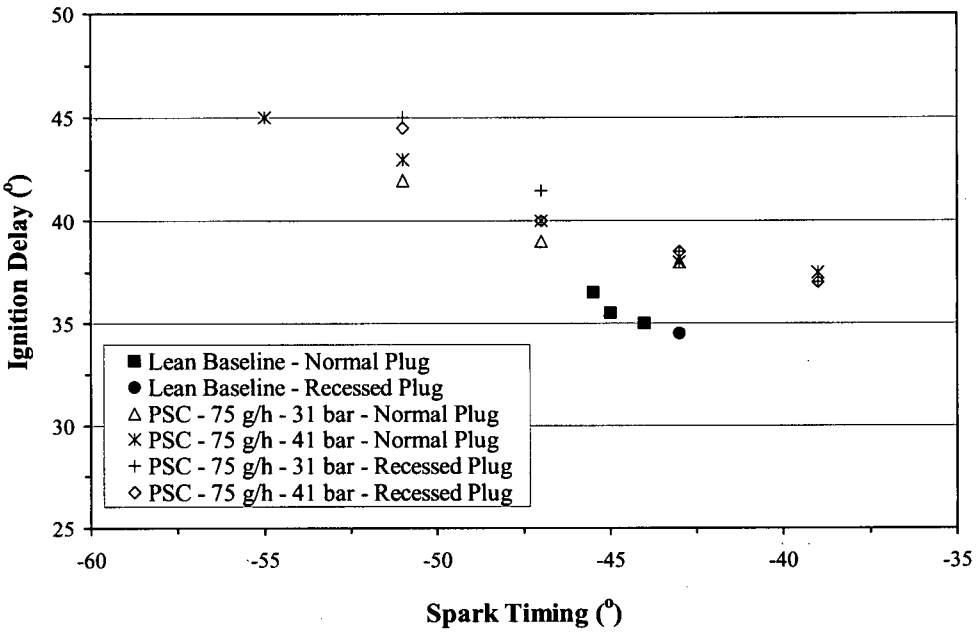

Figure 4.59: Ignition Delay, 0% - 5%, Varying Plug Position, Gasoline PSC

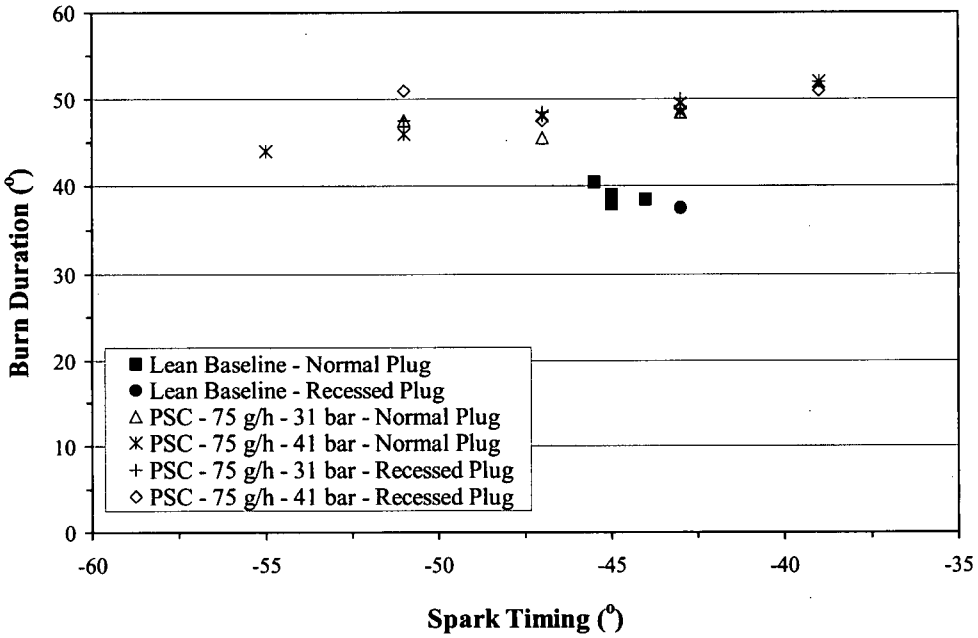

Figure 4.60: Burn Duration, 5% - 95%, Varying Plug Position, Gasoline PSC

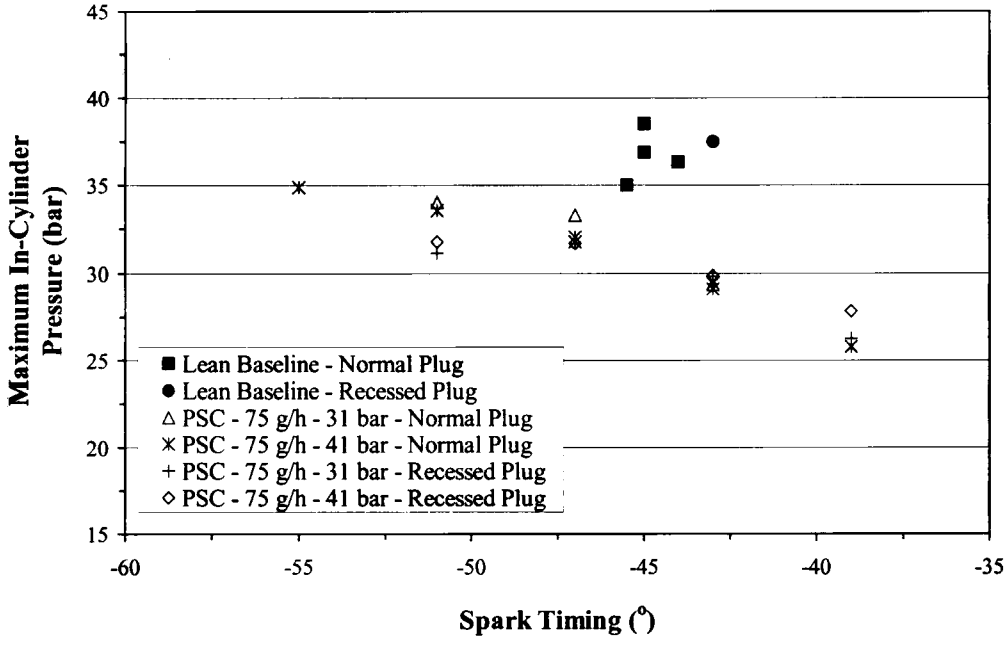

Figure 4.61: Maximum In-Cylinder Pressure, Varying Plug Position, Gasoline PSC

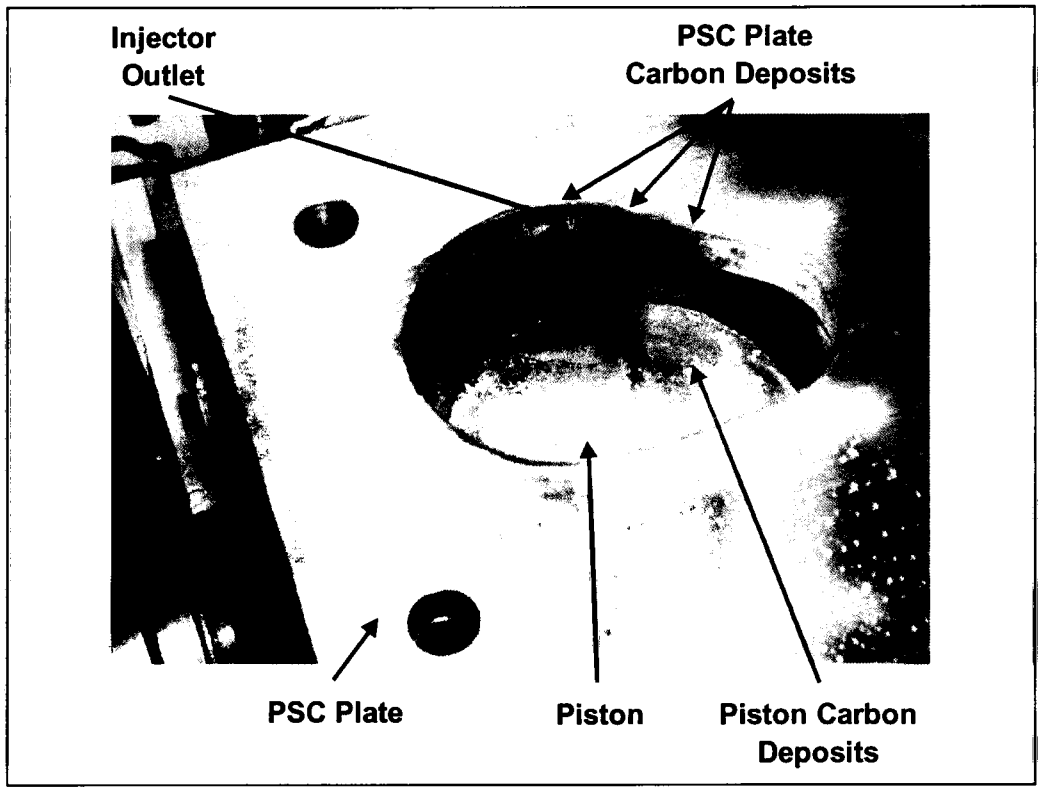

Figure 4.62: PSC Plate and Piston Crown after Disassembly

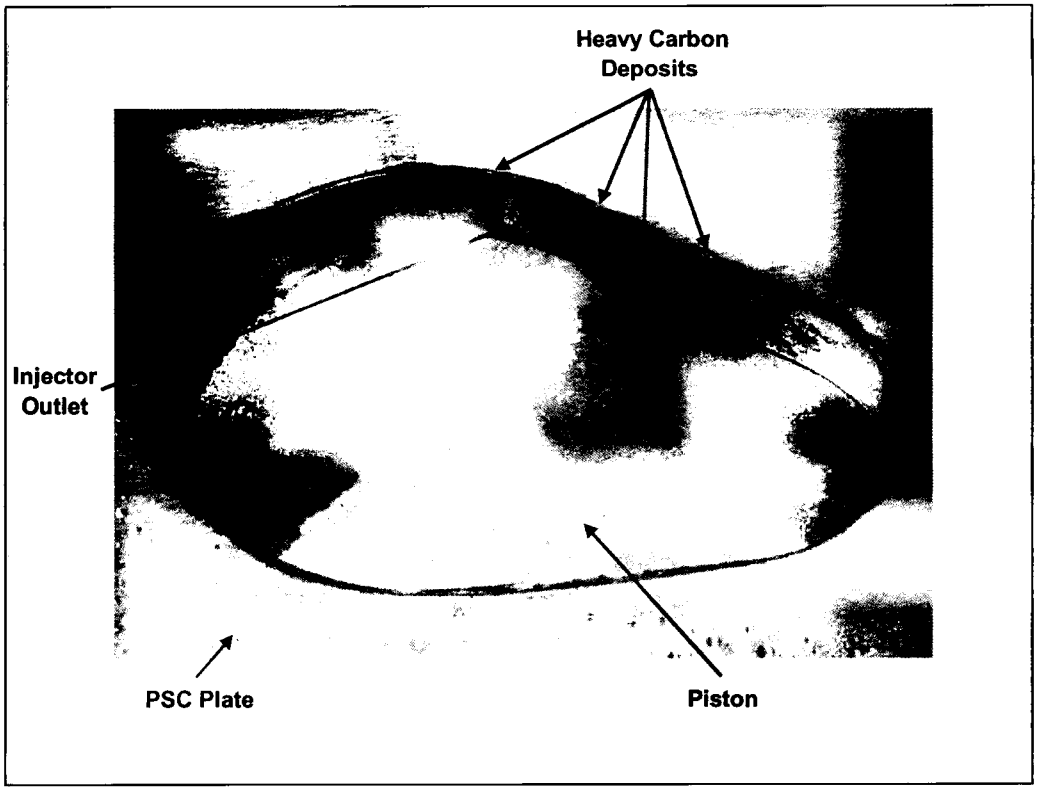

Figure 4.63: Close Up of PSC Plate and Piston Crown after Disassembly

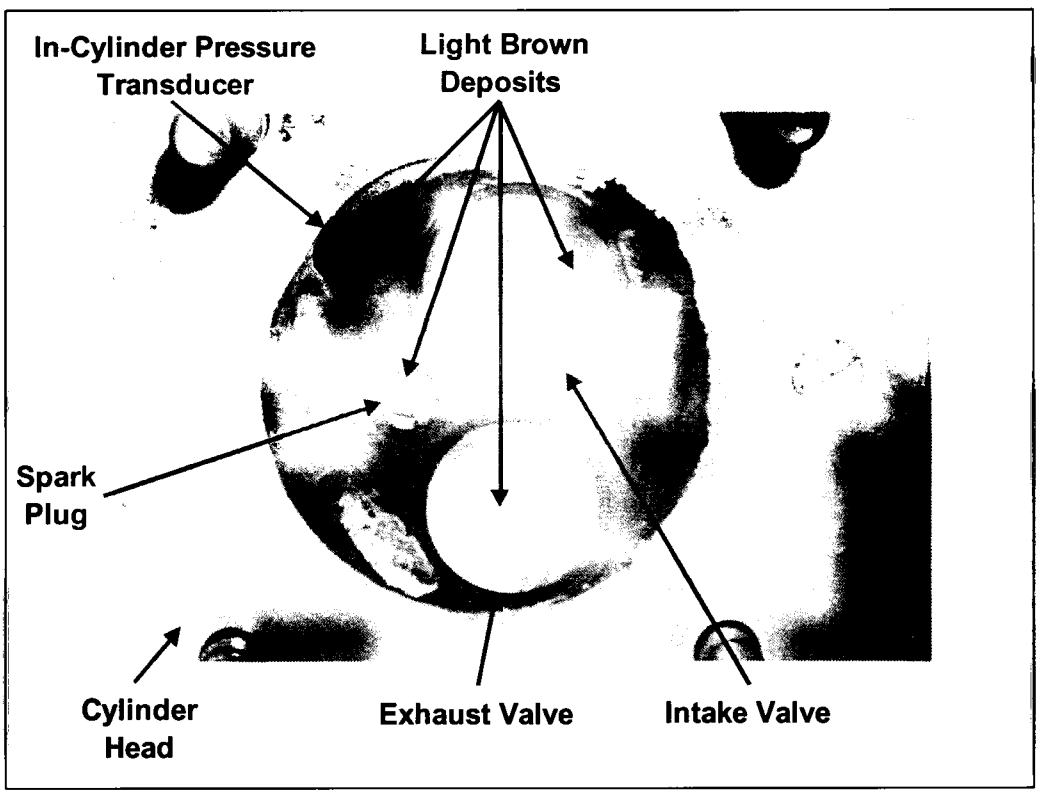

Figure 4.64: Close Up of Cylinder Head after Disassembly

Chapter 5
Conclusions and Future Work

5 Conclusions

A local charge stratification process, based on the Partially Stratified-Charge (PSC) concept, has been implemented on a gasoline-fuelled engine at the University of British Columbia. The primary objective of this work was to explore the performance of a PSC engine using gasoline as the primary fuel for lean burn applications. The research took place in two stages with both the performance of natural gas PSC and gasoline based PSC systems being explored.

5.1.1 Natural Gas PSC

The effectiveness of the natural gas PSC system was investigated compare to homogeneous gasoline fuelling under lean operation at fixed throttle settings. Tests were carried out at 2000 rpm, at part and full throttle, by gradually leaning out the air-fuel mixture with and without PSC system enabled. The following conclusions can be drawn from the data:

1) Natural gas PSC operation resulted in up to a 15% extension of the lean limit over homogeneous lean operation. Accompanying this extension of the lean limit was improved engine stability with the COV of GIMEP remaining below 5% for mixtures as lean as $\lambda = 1.475$.

2) Through extension of the lean limit, lower engine loads were achieved, i.e., PSC allowed a reduction in BMEP of up to 1 bar, without further throttling.

3) PSC maintained higher fuel conversion efficiencies over a greater range of lean mixtures. BSFC remained relatively constant at homogeneous lean limit levels for mixtures as lean as $\lambda = 1.325$ and $\lambda = 1.425$ at part and full throttle, respectively.

4) The use of the natural gas PSC system decreased nitrogen oxide emissions up to 50% through the extension of the lean limit. Lower nitrogen oxide emissions were achieved with higher PSC flow rates. Hydrocarbon emissions increased beyond the homogeneous lean limit. At the PSC lean limit hydrocarbon emissions were shown to increase by as much as 100%, with higher emissions occurring with higher PSC flow rates. Changes in carbon monoxide emissions were negligible with PSC operation under most operating conditions.

5) Higher peak in-cylinder pressures and shorter ignition delays were achieved with PSC. At the homogeneous lean limit peak pressure was increased by up to 5% and the ignition delay reduced by as much as 13 degrees. The crank angle at which the peak pressure occurred approached TDC as mixtures were made leaner when using PSC.

6) Results indicated that the homogeneous lean limit was a result of difficulties with flame initiation. The use of the natural gas PSC system led to significant improvements in the ignition of lean mixtures and resulted in the extensive

extension of the lean limit. With PSC operation, the lean limit also appeared to be a result of poor flame propagation rather than flame initiation.

The effectiveness of throttled PSC operation was also evaluated with respect to throttled stoichiometric and throttled lean homogeneous operation. For the PSC tests, the air-fuel ratio was leaned out from the homogeneous lean limit to $\lambda = 1.375$, after which the air-fuel ratio was fixed and the throttled closed. From these tests the following findings were apparent:

1) As a result of reduced throttling, the use of the PSC system led to improvements of up to 15% and 5% in volumetric efficiency versus throttled stoichiometric and throttled lean homogeneous operation, respectively.

2) Throttled lean burn operation improved BSFC by approximately 8% over stoichiometric throttled operation under most load conditions. There was also an indication that throttled PSC could further reduce BSFC over homogeneous lean operation at high loads.

3) Throttled lean burn operation offered at least a four-fold reduction in carbon monoxide emissions. With throttled PSC, nitrogen oxides were reduced by 25% over throttled lean homogeneous operation and by 50% over stoichiometric operation. Throttled PSC increased hydrocarbon emissions by 50% compared to homogeneous throttled operation.

5.1.2 Gasoline PSC

Tests were carried out at 2000 rpm under full throttle conditions with the gasoline PSC system and the results compared to homogeneous lean burn performance. The implementation of the gasoline PSC system, although expected, did not result in a performance improvement, however. The following conclusions may be drawn from the gasoline PSC tests:

1) The engine's power, efficiency and stability were impaired by operation with the gasoline PSC system. These effects were a direct result of reduced peak in-cylinder pressures and increased ignition delays. Earlier PSC injection timings, lower fuel flow rates and longer pulse widths, (i.e. a more homogeneous air-fuel mixture), resulted in better engine performance which approached that of homogeneous lean operation.

2) The quantitative results, coupled with qualitative observations of the combustion chamber, suggested that the gasoline PSC system was unable to achieve significant local charge stratification in the vicinity of the ignition source. This prevented the gasoline PSC system from achieving any significantly beneficial effects on lean burn engine performance.

5.2 Future Work

Preliminary results with a natural gas Partially Stratified-Charge system have demonstrated the potential for PSC to improve lean burn engine performance on a gasoline-fuelled engine. Although tests with a gasoline PSC system were unsuccessful,

the findings of this work have established a foundation for the redesign of the gasoline PSC system. During this next stage of PSC development, it will be critical for investigators to more closely examine the implementation details of the local charge stratification process. This will not only include the effects of PSC injection parameters but also how other engine systems affect its performance. Of particular interest will be the effects of combustion chamber design, ignition system design and the preparation of the lean homogeneous mixture. A more fundamental examination of how the local stratification process actually improves combustion will also be required before the PSC system can be fully optimized. This will most likely involve a more precise investigation of the local bulk flow, turbulence and mixture properties in the combustion chamber through optical means. Further along, the PSC system may be implemented on a commercial engine, perhaps with other newly developed engine technologies, and its performance will have to be proven over a real driving cycle. At this point, it will be essential to create a control system with the ability to seamlessly integrate PSC and non-PSC operation over the various regimes of engine operation. With further development, the PSC system could be a valuable contributor in maintaining current levels of engine performance as well as simultaneously reducing fuel consumption and exhaust emissions in future engine designs. Should this goal be achieved, it would be another important step towards reducing the burden that internal combustion engines place on our natural resources and the environment.

Appendix A
Schematics and Drawings

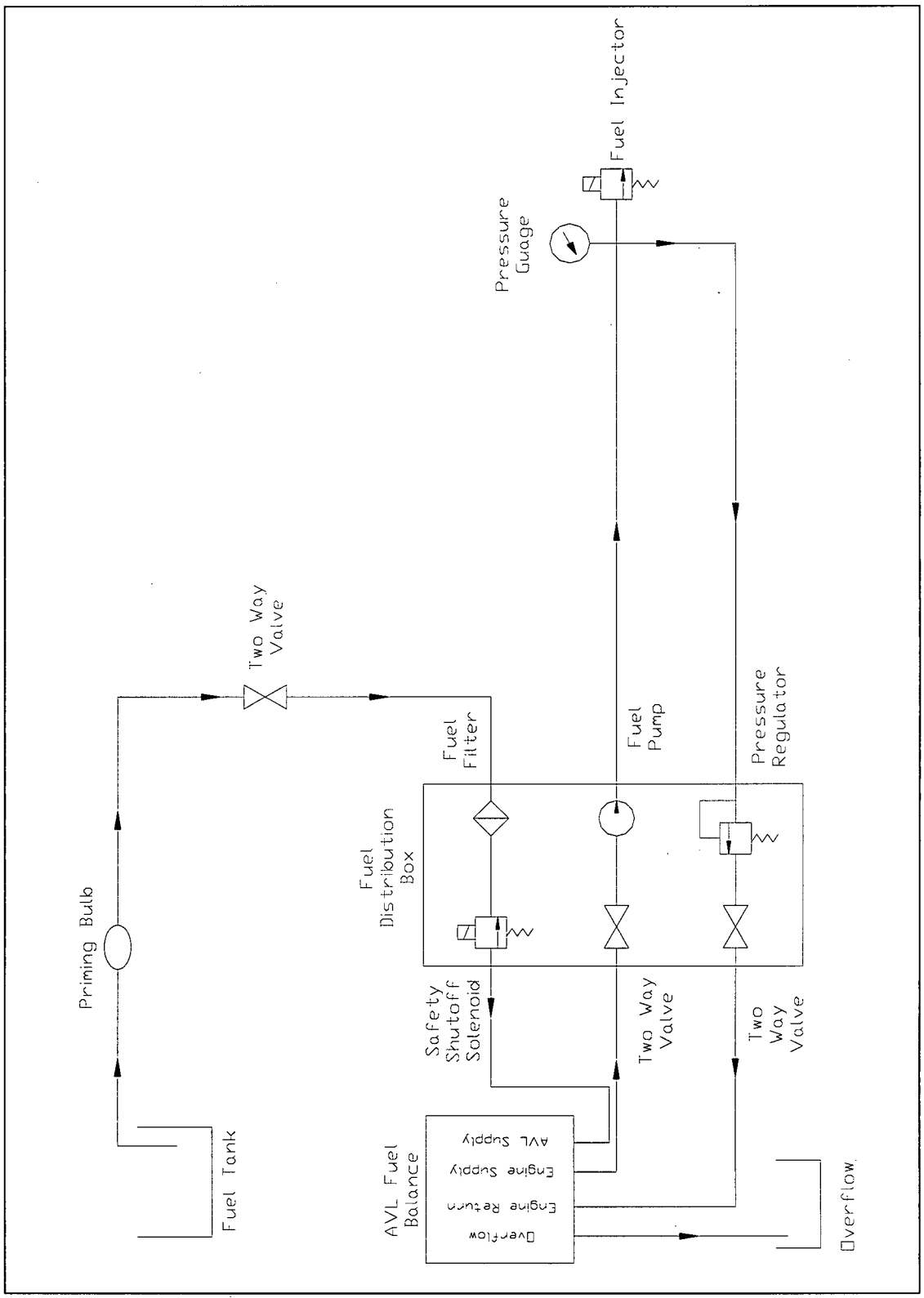

Figure A.1: Gasoline Port Injection System Schematic

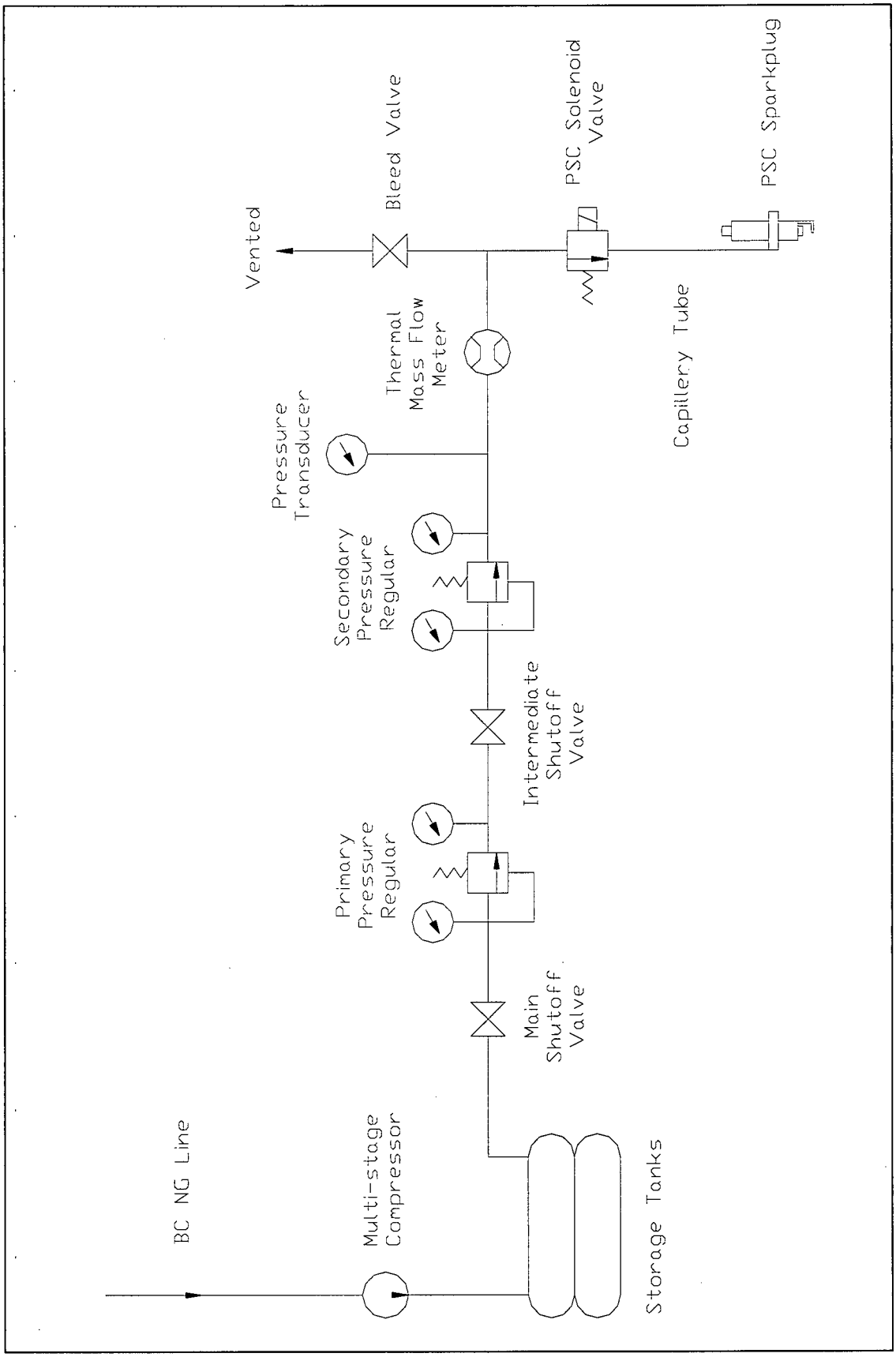

Figure A.2: Natural Gas PSC System Schematic

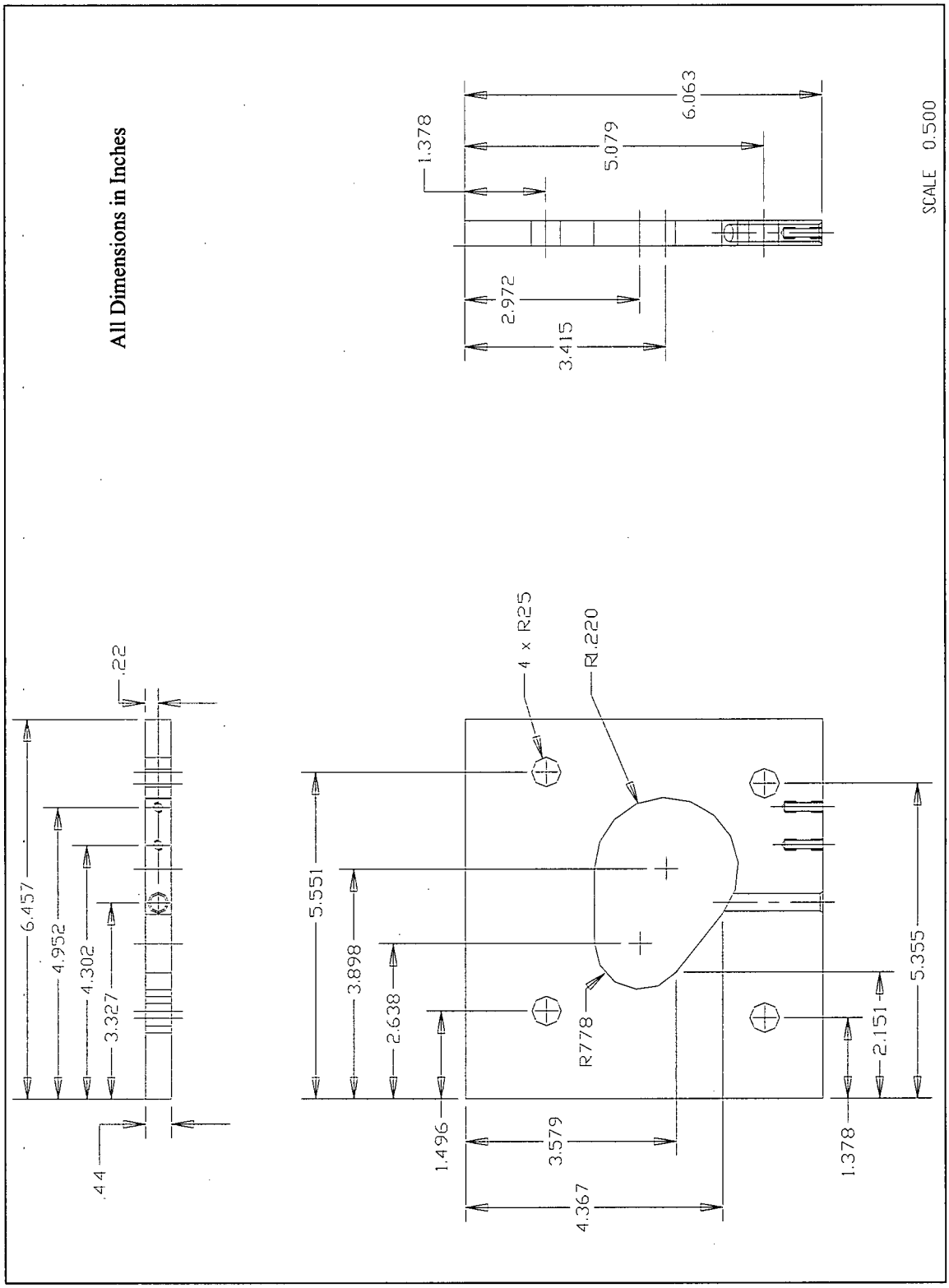

Figure A.3: Gasoline PSC Plate Drawing

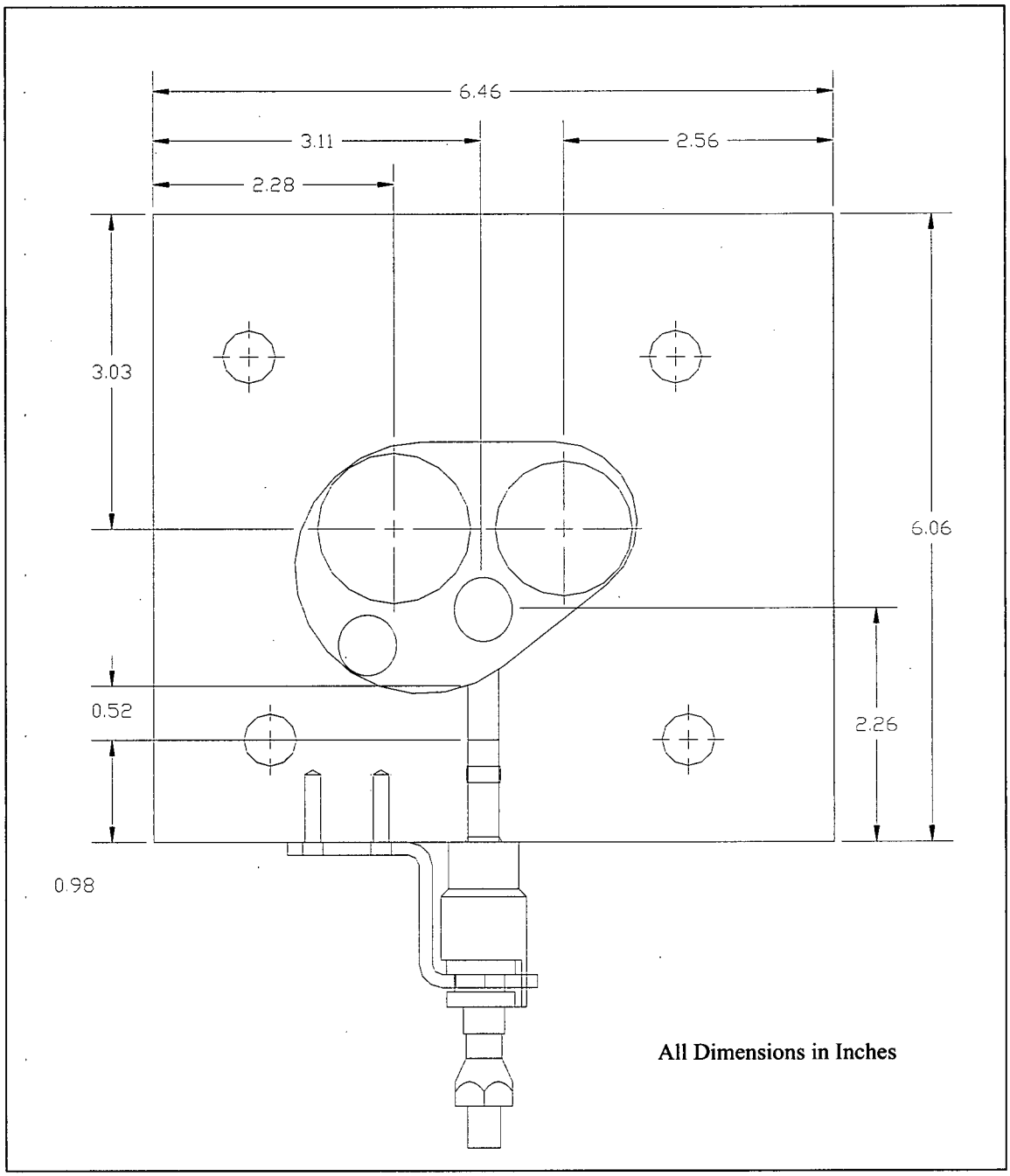

Figure A.4: Combustion Chamber Assembly Drawing

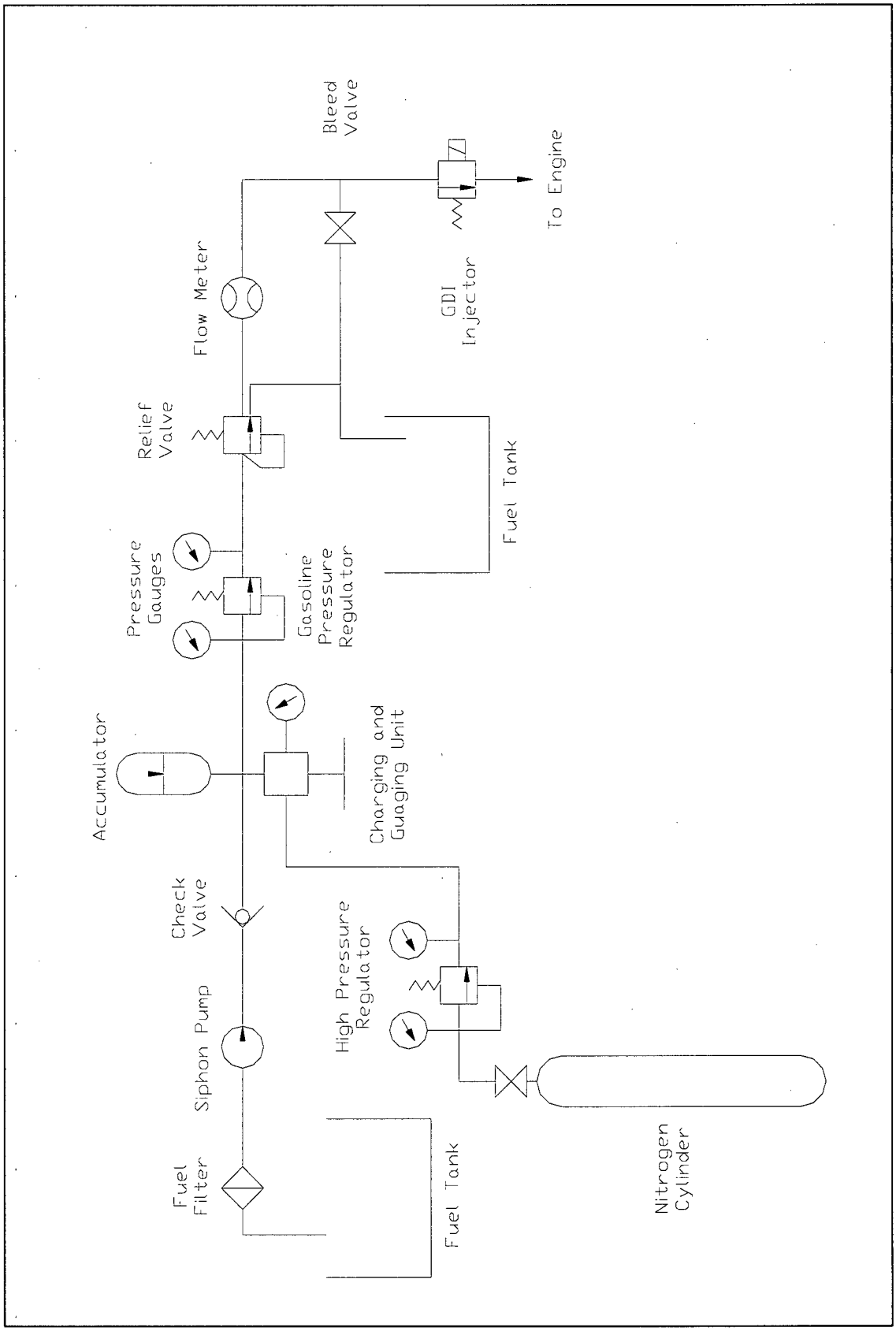

Figure A.5: Gasoline PSC System Schematic

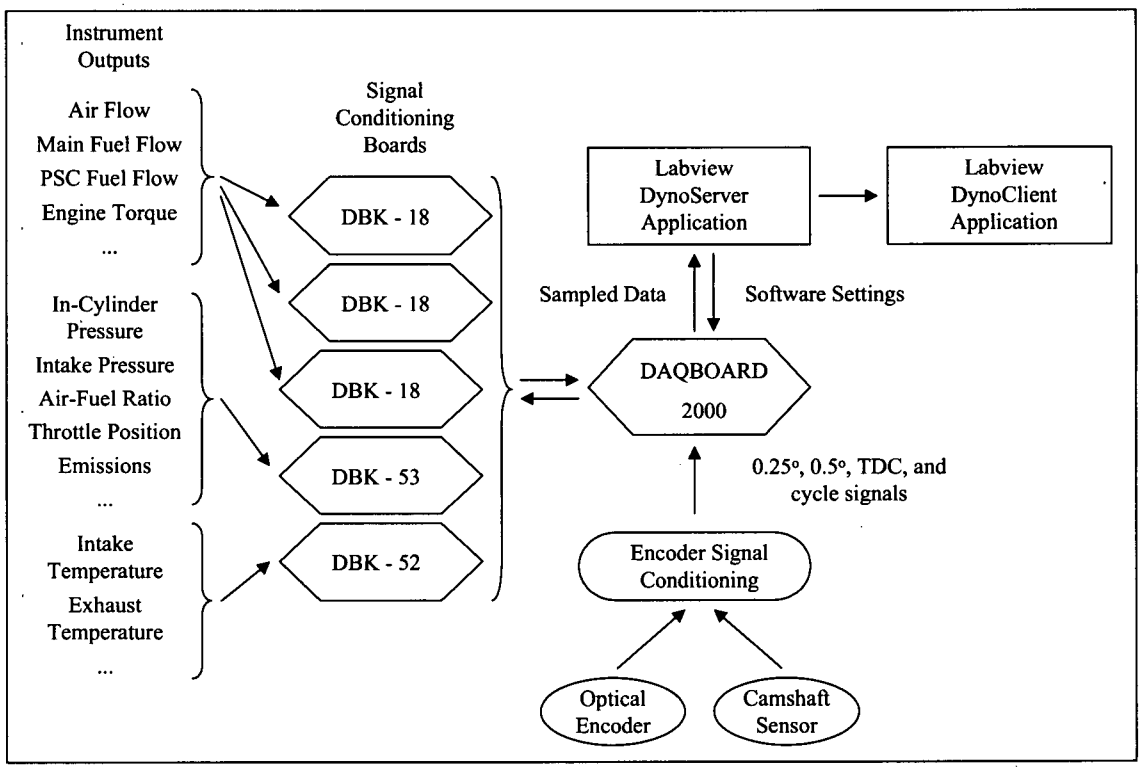

Figure A.6: Data Acquisition System Schematic

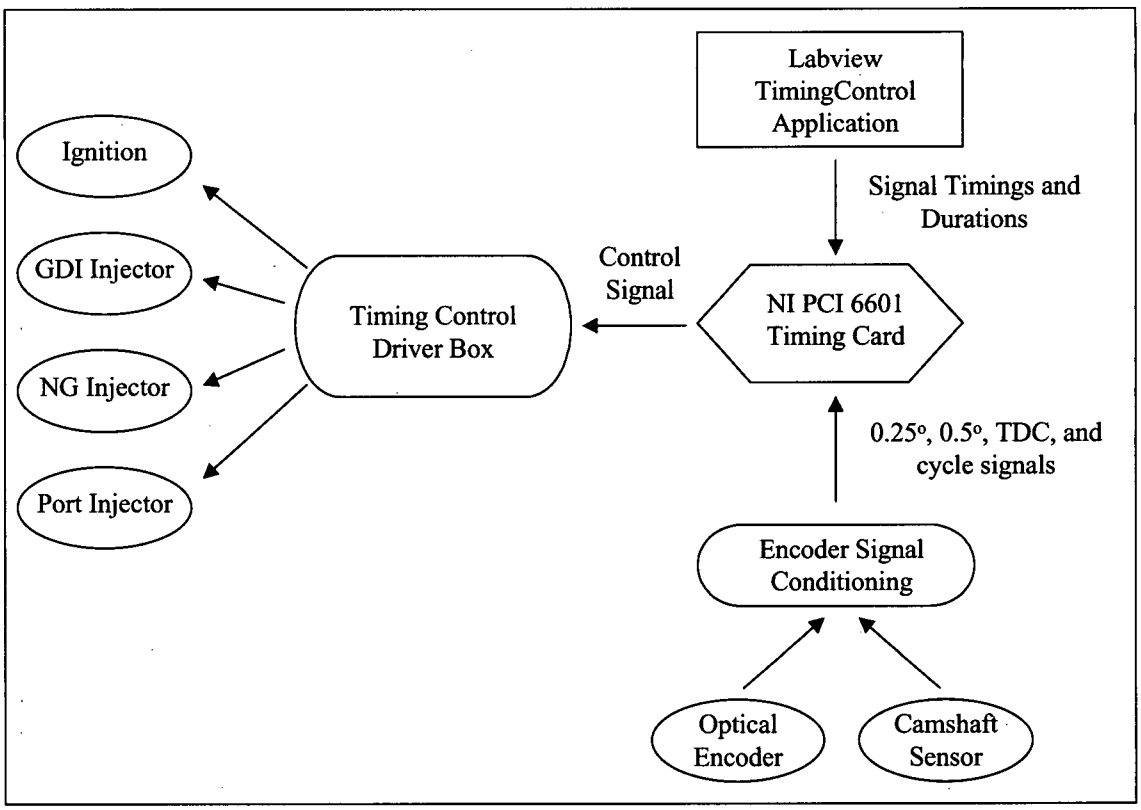

Figure A.7: Timing Control System Schematic

Appendix B
Engine Operating Procedures

Summary

The following document outline the various steps required to start and shutdown the Ricardo Hydra under gasoline fuelling. Please follow the steps carefully to avoid damaging the equipment or personal injury.

Pre-start

1. Ensure that the oil, anti-freeze and fuel levels are sufficient.
2. Open up the water drain for the exhaust system to ensure that no water has been collected. Close the water drain.
3. Check the engine for leaks and loose components. Fix accordingly.
4. Open up the main gasoline supply valve and the supply and return valves on the fuel distribution box.
5. Fully open the cooling water supply tap.
6. Turn on the main breaker in the test cell and the main switch for the dynamometer as well as plug in the main control panel.
7. Turn on the timing control box.
8. Reset the emergency stop button on the engine's ancillary tower and on the main control panel.
9. Turn on the test cell ventilation fans.
10. Turn on the two data acquisition computers and the AVL fuel balance computer.
11. Login to the control room computer and start the DynoClient, PressureClient, TimingControl applications.

General Startup

1. In the control room turn on the fuel, oil and water pumps as well as the oil and water heaters. Check to see that all pumps and heaters are in fact working.
2. Check the main control panel and see that the dynamometer control is set to "auto", the Ricardo ignition is set to "off" and the throttle is set to "run."
3. Wait for the oil temperature to reach 60oC. This is a good time to take note of the relative humidity, barometric pressure and engine hours.
4. Set the speed dial to 4.1 and the throttle to 100% on the main control panel.
5. Press the "reset" button on the acu and immediately press the green "start" button on the dynamometer control.
6. The engine should now increase to a motored speed of about 2000 rpm.
7. Turn the ignition switch on the main console to the on position
8. Set the ignition timing to 23o BTDC, 10o duration, and turn on the ignition through the TimingControl application.
9. Set the port fuel injection timing to 205o (155o BTDC), 140o duration and turn the main fuel on. The engine should now fire.

10. After the engine has been running for 1-minute enable the exhaust lambda sensor through the AFRecorder.
11. Wait for the "RDY" LED on the AVL fuel balance and press the start button on the fuel balance front panel to initiate the fuel measurement.
12. Check for leaks, sufficient crankcase ventilation and any unusual noises.

PSC Startup

1. For PSC pre-start procedures see the instructions given in the "Set-up Procedure for PSC Systems" document.
2. Using the TimingControl application, turn on the PSC system by pressing the on/off control button.
3. Adjust the injection timing and duration as required to meet test conditions. In some instances the injector will get stuck and will require abnormally high injection duration initially before they will open but will operate normally afterwards.

Testing

1. Run the engine for at least 30 minutes under full throttle and near stoichiometric conditions. The water and oil temperatures should be around 90 – 95 oC and 95 – 100 oC before tests commence.
2. Watch the engine oil and water temperatures and ensure they do not rise much above 100 oC. Adjust the water and oil thermostats located on the radiator if necessary. Also make sure that the oil pressure is greater than 5 bar.
3. Check the exhaust temperature periodically to make sure temperatures are not exceedingly high (> 700 oC).
4. Before sampling data allow for approximately 2 minutes to pass or for the emissions measurements to settle.
5. Acquire data by running the "save data to file" command in the DynoClient and PressureClient applications.

Shutdown

1. Turn off the port injector, PSC injectors and the ignition by pressing their respective on/off control buttons in the TimingControl application.
2. Continue to motor the engine until the measured exhaust temperature drops below 100oC, at which point the red stop button on the dynamometer control can be pressed to bring the engine to a halt. Note that this is also a good time to acquire motored pressure data.
3. Disable the exhaust lambda sensor after about 2 minutes of inactivity.
4. Turn off the oil and water heaters as well as the fuel pump at the control panel.
5. Turn off the timing control box and AVL fuel balance.
6. Lock off the main gasoline supply valve and the supply and return valves on the fuel distribution box.

7. Depress both emergency stop buttons.
8. After allowing the engine to cool for at least 15 minutes shut of the oil and water pumps and the cooling water supply to the engine.
9. Turn off the main breaker in the test cell and the main switch for the dynamometer.
10. Turn off the ventilation fans and shut down the data acquisition computers.

Appendix C
PSC Operating Procedures

Summary

The following document outline the various steps required to startup and shutdown the PSC natural gas and gasoline systems. Please follow the steps carefully to avoid damaging the equipment or personal injury.

Natural Gas System

Startup

1. Ensure all valves on the main natural gas distribution panel are in the "closed" or "off" position.
2. Ensure that the PSC bleed valve, which is located in between the radiator and the data acquisition system, is closed.
3. Check to see that all PSC connections are secure by tracing the lines back from the engine.
4. Turn the emergency shutoff valve on the main natural gas distribution panel to the "on" position.
5. Starting on the left-hand side of the distribution panel select the intermediate pressure storage tanks by turning the appropriate valve.
6. Working from left to right, follow the schematic provided on the distribution panel and route the natural gas stream to the engines. (This will involve turning two valves in sequence).
7. Open the intermediate shutoff valve for the Ricardo Hydra, which is located above the distribution panel and is just prior to the PSC pressure regulator.
8. If necessary adjust the PSC pressure regulator to the required setting. This may require opening the PSC bleed valve briefly to release residual pressure in the lines.
9. The system is now ready for operation.

Shutdown

1. Close all valves on the main natural gas distribution panel leaving the emergency shutoff valve for last.
2. Close the intermediate shutoff valve for the Ricardo Hydra.
3. If work is to be performed on the PSC system ensure that the lines are purged first, by opening the PSC bleed valve.

Gasoline System

Startup

1. Fill up a jerry can with 1.25L of gasoline and attach the siphon pump assembly.
2. Using the quick connects provided, attach the siphon pump assembly to the high-pressure system.
3. Open the nitrogen gas bleed valve, located on the accumulator's charging and gauging unit, and ensure that all the nitrogen has been purged from the accumulator.
4. Locate the main gasoline bleed valve, located beside the GDI Injector, and relieve any pressure remaining the high-pressure lines.
5. With the main gasoline valve open, start pumping gasoline into the high-pressure system using the siphon pump.
6. Once gasoline starts draining into the overflow tank, close the main gasoline bleed valve and continue to pump the remaining gasoline into the high-pressure system.
7. Close the nitrogen gas bleed valve.
8. With the charging and gauging unit handle backed off completely turn the handle 3 times in the clockwise direction to open the shrader valve on the gas side of the accumulator.
9. Open the valve on the nitrogen bottle ensuring that the nitrogen pressure regulator is backed off completely.
10. Making sure that the pressure down stream of the gasoline pressure regulator does not rise above 50 bar. Slowly increase the pressure on the gas side of the accumulator, using the pressure regulator attached to the nitrogen bottle, to 80 bar utilizing the pressure gauge on the charging and gauging unit for reference.
11. Closed the valve on the nitrogen bottle and back off the nitrogen pressure regulator completely.
12. Back off charging and gauging unit handle completely to close the accumulator's shrader valve.
13. Adjust the gasoline pressure regulator to achieve the required injection pressure (21 – 41 bar). The main gasoline bleed valve may have to be opened and closed briefly before the pressure settles in some cases.
14. The system is now ready for operation.

Shutdown

1. Open the nitrogen gas bleed valve, located on the accumulator's charging and gauging unit, and ensure that all the nitrogen has been purged from the accumulator. (In the case of system maintenance see Step 4)
2. Locate the main gasoline bleed valve, located beside the GDI Injector, and relieve any pressure remaining the high-pressure lines.

3. Locate the secondary bleed valve, located beside the nitrogen bottle, and drain any remaining gasoline in the high-pressure lines.
4. If work is to be performed on the PSC system do not completely purge all the nitrogen from the gas side of the accumulator. A small amount of pressure will help to remove gasoline that remains in the accumulator and the lines preceding the gasoline pressure regulator.

Appendix D
Fuel Properties

Table E.1 : Natural Gas Composition[1]

Compound	Mole % in Fuel	Molecular Mass (kg/kmol)	Upper Heating Value (kJ/kg)	Lower Heating Value (kJ/kg)
Methane	95.945	16.043	55517	50030
Ethane	1.9549	30.070	51903	47511
Propane	0.5547	44.097	50325	46333
i-Butane	0.0689	58.123	49347	45560
n-Butane	0.1116	58.123	49505	45719
i-Pentane	0.0252	72.150	48909	45249
n-Pentane	0.0201	72.150	49006	45345
neo-Pentane	0	72.150	48712	45052
Hexane	0	86.177	48678	45103
Heptane	0.0248	100.204	48435	44921
Octane	0	114.231	48251	44783
Carbon Dioxide	0.4248	44.010	0	0
Nitrogen	0.87	28.013	0	0

[1] Based on BC Natural Gas results from Tilbury GC Stream 21 October 02, 16.05

Table E.2: Natural Gas Specifications

Property	Value
Molecular Mass of Fuel (kg/(kmol*C1))	16.63
Fuel Density[1] (kg/m^3)	0.713
Hydrogen/Carbon Ratio (mol/mol):	3.907
Oxygen/Carbon Ratio (mol/mol):	0.008
Nitrogen/Carbon Ratio (mol/mol):	0.017
Upper Heat Value (kJ/kg):	54437
Lower Heating Value (kJ/kg):	49109
Stoichiometric Air-Fuel Ratio[2] (kg/kg):	16.8
Stoichiometric Air-Fuel Ratio[2] H/C Only (kg/kg):	17.1

[1] @ 1 atm
[2] Based on SAE J1829 recommended practice

Table E.3: Gasoline Specifications

Property	Value
Manufacturer	Chevron
Type	Premium
Nominal (R+M)/2 Octane Rating (Octane)	92
Nominal Density[1] (kg/m^3)	700 – 800
Hydrogen/Carbon Ratio (mol/mol):	1.824
Molecular Mass of Fuel H/C Only (kg/(kmol*C1))	13.85
Stoichiometric Air-Fuel Ratio H/C Only (kg/kg):	14.5

[1] @ 15.6°C